The University of Jordan

Authorization Form

I, Murad Musa Mahmoud, authorize the University of Jordan to supply copies of my Thesis/ Dissertation to libraries or establishments or individuals on request, according to the University of Jordan regulations.

Signature:

Date: 24/5/2011

الجامعة الأردنيـــة
كلية الدراسات العليا

التاريـــخ: / /

نموذج رقم (١٨)
اقرار والتزام بالمعايير الأخلاقية والأمانة العلمية
وقوانين الجامعة الأردنية وأنظمتها وتعليماتها
لطلبة الماجستير

أنا الطالب: مراد موسى محمد محمود الرقم الجامعي: (8080763)
تخصص: الهندسة الميكانيكية الكليـــــــة: الهندسة والتكنولوجيا

عنوان الرسالة:
Analysis of a hybrid PV-Solar thermal collector with built-in water desalination system

اعلن بأنني قد التزمت بقوانين الجامعة الأردنية وأنظمتها وتعليماتها وقراراتها السارية المفعول المتعلقة باعداد رسائل الماجستير عندما قمت شخصيا" باعداد رسالتي وذلك بما ينسجم مع الأمانة العلمية وكافة المعايير الأخلاقية المتعارف عليها في كتابة الرسائل العلمية. كما أنني أعلن بأن رسالتي هذه غير منقولة أو مستلة من رسائل أو كتب أو أبحاث أو أي منشورات علمية تم نشرها أو تخزينها في أي وسيلة اعلامية، وتأسيسا" على ما تقدم فانني أتحمل المسؤولية بأنواعها كافة فيما لو تبين غير ذلك بما فيه حق مجلس العمداء في الجامعة الأردنية بالغاء قرار منحي الدرجة العلمية التي حصلت عليها وسحب شهادة التخرج مني بعد صدورها دون أن يكون لي أي حق في التظلم أو الاعتراض أو الطعن بأي صورة كانت في القرار الصادر عن مجلس العمداء بهذا الصدد.

توقيع الطالب: .... التاريخ: ٢٤ / ٥ / ٢٠١١

تعتمد كلية الدراسات العليا
هذه النسخة من الرسالة
التوقيع .... التاريخ ....

ANALYSIS OF A HYBRID PV-SOLAR THERMAL COLLECTOR WITH BUILT-IN WATER DESALINATION SYSTEM

By:

Murad Mahmoud

Supervisor:

Dr. Ali Badran, Prof.

This Thesis was Submitted in Partial Fullfillment of the Requirements for the Master's Degree in Mechanical Engineering

Faculty of Graduate Studies

University of Jordan

May 2011

II

COMMITTEE DECISION

This Thesis (Analysis of a Hybrid PV- Solar Thermal Collector with Built-in Water Desalination System) was successfully defended and approved on 12/5/2011

Examination Committee	**Signature**
Dr. Ali A. Badran, (Supervisor) Prof. of Mechanical Engineering	A. Badran
Dr. Ahmad Al-Salaymeh, (Member) Prof. of Mechanical Engineering	
Dr. Mahmoud Hammad, (Member) Prof. of Mechanical Engineering	Prof. M. Hammad
Dr. Esma'eel Al-Hinty, (Member) Associate Prof. of Mechanical Engineering (German-Jordanian University)	

Acknowledgement

I would like to send my thanks to Prof. Ali Badran for his guidance, patience and encouragement, and to all the people who helped or supported me to finish this work. The support of the Deanship of Scientific Research, The University of Jordan in executing this research is appreciated.

Table Of Contents:

List of Figures:

List of Tables:

Nomenclature:

Notation	Description	Units
A	The surface area of the heat exchanger	m^2
A_s	Still area	m^2
AST	Apparent solar time	Hour
B_s	The atmospheric extinction coefficient	m^{-1}
C_{pw}	Specific heat of water	kJ/kg °C
D	The mean diameter of the pipe of the heat exchanger	M
E	The equation of time	Minute
$\dot{E}_{PV}$	The electrical power output	W/m^2
F_{ss}	The view factor between the surface and the sky	
G	The incident solar radiation on the surface	W/m^2
h_{fg}	Latent heat of evaporation at vapor's temperature	kJ/kg
h_i	The inside heat transfer coefficient of the pipe	W/m^2 °C
h_o	Outside film heat transfer coefficient	W/m^2 °C
h_n	Natural convection heat transfer coefficient	W/m^2 °C
$h_{r,PV-a}$	Radiation heat transfer coefficient from the PV module to the ambient	W/m^2 °C
h_w	Wind heat transfer coefficient	W/m^2 °C
H	The hour angle	Degrees
I	Irradiation on the surface in one hour	MJ/m^2
k	Thermal conductivity	W/m °C
L	Plate length	M
$\dot{m}_c$	Condensate productivity of the still	ml/hr
$\dot{m}_I$	Mass flow rate of unevaporated intermediate water	ml/hr
$\dot{m}_s$	Mass flow rate of unevaporated saline water	ml/hr
$\dot{m}_{s,i}$	Mass flow rate of inletet saline water	g/s
MST	Mean solar time	Hour
n	Day of the year	Day
N	Number of glass covers	
Nu	Nusselt number	
PF	The packing factor	
Pr	Prandtle's number	
q_b	Heat loss through the bottom	W/m^2
q_{c-a}	Heat loss through glass cover to the ambient	W/m^2
q_{cond}	Heat of condensation	W/m^2
q_e	Heat used to evaporate the inlet water	W/m^2
q_{ex}	Heat recovered by the heat exchanger	W/m^2
q_{loss}	Heat loss through the edges of the still	W/m^2
q_{nc}	Heat used to heat the air for the natural convection process	W/m^2
q_{pv-c}	Heat loss from the PV module to the cover via convection and radiation	W/m^2
q_{unevap}	Heat used to heat the unevaporated water	W/m^2
Ra	Rayleigh's number	
Re	Reynold's number	
r_1	Inner radius of heat exchanger pipe	m
r_2	Outer radius of heat exchanger pipe	m

S	The spacing between plates	m
T_a	Ambient temperature	°C
T_b	Insulation board temperature	°C
T_c	Glass cover temperature	°C
$T_{c,o}$	Outlet condensate header temperature	°C
$T_{ex,i}$	Heat exchanger inlet temperature	°C
$T_{ex,o}$	Heat exchanger outlet temperature	°C
$T_{I,o}$	Intermediate water outlet temperature	°C
T_{int}	Intermediate water temperature	°C
T_{pv}	Mean PV module temperature	°C
T_s	Saline water temperature	°C
$T_{s,i}$	Inlet water temperature	°C
$T_{s,o}$	Saline water outlet temperature	°C
T_v	Vapor temperature	°C
T_w	Lower condenser plate temperature	°C
T_∞	Air temperature at the inlet of the absorbing part of the still	°C
U_{c-a}	Total heat transfer coefficient for the heat loss through the glass cover	W/m^2 °C
U_e	Total heat transfer coefficient for the heat loss through the edges	W/m^2 °C
U_{ov}	Overall heat transfer coefficient	W/m^2 °C
Greek Notations		
α	Solar azimuth	Degrees
α	Absorptance of PV Panel	
β	Volumetric thermal expansion coefficient	K^{-1}
β_1	The altitude angle of the sun	Degrees
β_2	Collector's tilt angle	Degrees
ΔT_{lm}	Mean log temperature	°C
δ	The declination angle	Degrees
ε_g	Emmitance of glass	
ε_{PV}	Emmitance of the PV module	
η_e	The electrical conversion efficiency	
η_h	Hourly efficiency of the still	
η_d	Daily efficiency of the still	
θ	The angle of incidence	
υ	Kinematic vsicosity	m^2/s
τ	Transmittance	
τ_g	Transmittance of glass	
$(\tau\alpha)_e$	Effective transmittance-absorbtance product	
φ_c	The temperature coefficient	% / °C

ANALYSIS OF A HYBRID PV-SOLAR THERMAL COLLECTOR WITH BUILT-IN WATER DESALINATION SYSTEM

By:
Murad Mahmoud

Supervisor:
Dr. Ali Badran, Prof.

Abstract

In this work, a hybrid photovoltaic (PV) - solar still device was designed, built and tested. The device has an effective area of 1.63 m^2. The aim of this work is to study the performance of the device as the losses from the PV module are used to heat up water and desalinate it in the same time. The device consists of a PV module that acts as an absorber plate. The backside of this plate is covered with porous material through which the saline raw water flows via capillary and gravity effects. Several measures were incorporated in the still including a heat exchanger of a suitable size, a wooden frame, and a polyurethane insulation board to minimize losses from the still to the ambient and to improve evaporation and condensation processes.

The size of the heat exchanger was studied to give optimum performance through utilizing the latent heat of condensation in heating the raw water entering the still. The wooden frame was designed in such a way to make the still easy to assemble and maintain and to separate the evaporation and condensation compartments. A high resistance insulation material made of polyurethane board sandwiched between two thin aluminum layers was installed between the two compartments to maximize the temperature difference between them.

The device was tested experimentally and a computer code was developed using MATLAB software to simulate the performance of the device. The experimental work focussed on measuring the performance of various components of the still, the salinity of inlet and outlet water, voltage, current and solar irradiation.

It was found that the productivity and efficiency of the still were significantly improved over previous work. The maximum productivity was 3.85 L/day of desalinated water at an average salinity of 40 PPM and the minimum salinity obtained was 7.5 PPM. The highest daily efficiency attained was 34%. The device was tested while the PV module wasn't covered with glazing and then while covered with glazing. It generated an average electrical power output of around 160 W and 130 W respectively, and a maximum power output of 215 W and 190 W respectively. The nominal power output of the PV module used is 250 W.

Chapter 1

Introduction

1.1 General:

Heating water and generating electricity is one of the applications in which solar energy could be utilized. It is possible to generate electricity and heat water or desalinate water by using a separate system for each. However, a more efficient method is to combine the photovoltaic cells with the solar still. Those systems utilize solar energy to generate both electricity and thermal energy via the so-called hybrid systems. Such combined systems usually take much less space, and utilize energy more efficiently.

1.2 Importance:

As time goes, the world approaches the point where there is no more fossil fuel, the population increases too much to sustain. The pollution levels continue to rise. This presents a challenge in the form of supplying electricity and drinkable water to increasing population. With those facts in mind, the importance of solar energy increases significantly, whether it is to generate electricity or to heat water for desalination purposes or otherwise.

1.3 Hybrid Systems:

Using hybrid systems is a very promising alternative for stand-alone PV panels and solar stills. One of the main reasons for that is the increased efficiency for the combined system over stand-alone systems. Combined systems also save space. For PV, the electricity conversion efficiency of a solar cell for commercial applications is about 14–17%. Around 85% of the incoming solar energy is either reflected or absorbed as heat energy. This causes the temperature of the PV panels to rise significantly, lowering its efficiency. Therefore, taking that energy to heat water will raise the PV cell efficiency while making use of that excess energy to produce desalinated water.

Usually, PV panels have low efficiency: around 4 to 7% for amorphous ones and around 14 to 17% for crystalline technology while the highest commercially available efficiency is 24.2% which is still new and isn’t widely spread (Press Releases, SunPower Announces New World Record Solar Cell Efficiency webpage 2011). However, some researchers in University of Delaware have set a new record achieving of 42.8% efficiency, but that is still a research and is not commercially available (UD-led team sets solar cell record, joins DuPont on $100 million project webpage 2011). Interestingly, most PV panels see their electric production decreasing as its temperature increases because of their negative temperature coefficient of around -0.5%/K. The PV module used in this work has a temperature coefficient of -0.38%/K.

1.4 The Scope of this Work:

This work is a theoretical and experimental investigation of the hybrid PV-Thermal water desalination system using a PV module and a solar trickle system. The study aims at establishing a mathematical model for a combined PV-Thermal water desalination system, and building an experimental rig to test its performance. This will be done by using the concepts behind the PV-Thermal model and applying them to a different design incorporating a water desalination system. This model was simulated to study the effect of various parameters on system performance.

The research methodologies followed in this work were theoretical and experimental. The components of both PV and thermal systems were modeled and a computer program was written on MATLAB software to simulate the performance of the combined system. The experimental part was composed of building an experimental rig of the hybrid PV-T collector, and data was collected to study system performance under varying conditions. Moreover, the PV-T solar desalination system model was compared with results from PV cells operating alone, a solar still operating alone, and the experimental results obtained through the experimental part.

Various parameters such as productivity, efficiency, power and overall efficiency were studied.

Chapter 2

Literature Survey

2.1 Introduction:

Using solar energy to generate heat or electricity is an old concept. However, the hybrid systems that combine PV cells with thermal systems are a new concept that is only a few decades old. The hybrid PV-Water desalination system under investigation in this work has not been studied before.

2.2 Previous Studies:

The concept of PV-T (Photovoltaic-Thermal) hybrid system was first developed by Wolf (1976) where the concept was applied as a combination of PV cells with a standard solar water heating system in one unit.

Garg and Agarwal (1995) established a mathematical model for the PV/T collector system and solved it using the finite difference method. It was found that a normal domestic solar water heater of about 2 m^2 area generates sufficient electrical energy to run two tube lights of 20 W each for five hours and a television set of 30 W for four hours in addition to heating 100 liters of water at 73°C every hour.

Zondag et al (2003) performed experimental and analytical study of a PV/T system. Analytically, they performed four different simulations with steady state 1D, 2D, and 3D

models, and a dynamical 3D model. It was found that all four models follow the experimental results within around 5% accuracy. Therefore, the 1D model was enough for a lot of calculations while being much simpler and much faster during simulations. However, the other models are more flexible and can easily adapt to more complicated configurations and provide more data as required for a further optimization of the collector.

Tripanagnostopoulos et al (2002) experimentally studied various PV/T variants including air and water systems with and without glazing, and with the use of a booster diffuse reflector. It was found that water-based systems generate a better efficiency than air systems especially during summer when water temperature from mains is lower than ambient air annual temperature. The additon of glazing increases the thermal efficiency but decreases the electrical efficiency. The addition of a booster diffuse reflector increases the electrical output by about 16% and the use of both a booster diffuse reflector and glazing increases the thermal efficiency considerably while balancing the negative effect that glazing has on the electrical efficiency.

Zondag et al (2003) analyzed various designs in the solar systems from stand-alone PV and thermal solar collector to nine PV/T variants under different conditions. The results showed that all PV/T variants give better overall energy efficiencies than PV or thermal collector alone. This makes the PV/T design flexible depending on the need of more thermal or electrical generation.

Saitoh et al (2003) performed experimental and analytical energy and exergy analysis of a hybrid solar collector. The experiments were conducted under constant supply temperature of brine water. The efficiency of the tested system was compared with a stand-alone PV system

and a collector system, and it was found out that the hybrid collector had an advantage in terms of exergy efficiency.

Zakharchenko et al (2004) studied the hybrid PV/T system with the PV panel being much smaller than the thermal collector as opposed to them being the same size in other studies. The performance of several types of panels was investigated including crystalline PV cells. The different materials and constructions of the thermal contact between the panel and the collector were studied. It was found that the PV panel used in a hybrid system needs special design to provide an efficient heat extraction from it for optimum cooling. The result was a 10% increase in efficiency for the PV panel when it was smaller than the collector and installed near the cold water entrance.

Badran et al (2005) studied an inverted trickle solar still. The study included experimental work and simulation. The test used brackish water at around 6000 ppm salinity. The results showed that the amount of water was 12% higher than when sea water at 35000 ppm salinity was used. It was also found that the optimum flow rate was low as 0.7 g/s.

Bakker et al (2005) studied the performance and costs of a roof-sized PV/T array combined with a ground coupled heat pump. The system was compared to a similar one with separate PV panels and solar thermal collectors. It was found that the PV/T system costs were almost the same, but takes around 25% less space and is more appealing visually while giving the same amount of electricity and heat energy.

Chow et al (2006) tested a PV/T system under various conditions, and developed a numerical model of the system. The results of the experimental work were compared with the numerical

model. The results were encouraging to use this system on a wider range of domestic solar systems.

Tiwari and Sodha (2006) developed a thermal model of a hybrid PV/T solar system that was experimented by previous researchers. The model was based on energy balance of each component of the system. The numerical computations and simulation using $\Delta T=18.18°C$ at peak solar irradiation of 852 W/m^2 predicted a daily thermal efficiency of around 58% which is in agreement with the experimental value of 61.3%.

Fraisse et al (2007) studied the integration of PV modules in buildings in conjunction with solar thermal systems in order to help cool the PV modules which would increase its efficiency. The PV panels used were mono-crystalline. It was found that the annual efficiency of PV was 6.8% when a glass cover is used compared to 10% without using a glass cover and 9.4% when it was a stand-alone PV system. The system was also used in conjunction with a Direct Solar Floor (DSF) and it was found that during summer for the glazed system the PV module temperature reaches over 100°C due to oversizing the collectors during the summer where hot water requirements are lower. As a result, using glazing in PV/T systems would decrease the lifetime of the PV module. Some variants of this PV/T system that can counter that problem were mentioned including not using glazing.

Zondag (2008) reviewed the research that was done on PV/T systems over the last 30 years. An overview of this research was presented in terms of the different variations, the results and the issues the various researchers encountered.

Chow et al (2009) studied the feasibility of using a glazed versus unglazed PV/T collector. The study was based on experimental work, and was validated numerically. It was found that

using a glass cover increases the amount of thermal heat gain, while using an unglazed version yields higher electrical efficiency.

The concept of combining PV and desalination was triggered by the introduction of the inverted trickle solar still because this type of still enabled the utilization of the back of the absorber plate for desalination while the front of the plate is capable of performing another task, desalination.

All previous works were about PV/T collector systems, and none of them incorporated desalination. This work tackles the problem of combined PV/T desalination systems.

Chapter 3

Theoretical Work and Simulation

3.1 Theoretical Analysis:

Theoretical analysis and simulation work follow in the general those of Badran et al (2005) for inverted trickle solar still with heat recovery and chow et al (2009) for hybrid PV/Collector. The only difference here is the introduction of the PV module into the analysis. An energy balance is performed on the still-PV hybrid system. In order to illustrate that, a schematic diagram of the still with all the respective temperatures, energy and mass flows is shown in Figure 3-1.

The energy balance considers the heat-exchanger installed in the condensation compartement. Water is pre-heated in the heat-exchanger before entering the system and flowing on the back of the PV panel.

Solar radiation falls on the system. That heat is either used in the PV module to generate electricity or to heat the saline water or is lost by radiation and convection heat transfer to the ambient. The energy that passes through the PV module to the inside of the system is divided into four parts. (i) Evaporation of a portion of the saline water. (ii) Heating up the saline water that continues going down and doesn't evaporate. (iii) Conduction through the insulation board or is lost through the edges and the lower condensating plate. (iv) Heating up the circulating air in the system. The heat that is used to evaporate the water and heat the circulating air is taken by the water entering the heat exchanger and the condensing compartement during the condensation process.

In this work, simulation and experimental, two cases where studied, one where the system was covered with a glazing and one without a glazing.

The following assumptions were considered during the theretical analysis and simulation:

1- Steady state operation. This is justified by the fact that the thermal mass of the system is relatively low, and thus there will be little thermal storage over the period of the simulation which is one-hour intervals. During this interval the temperature doesn't change much, and there is little thermal storage effect in various components.

2- Constant solar irradiation over the time period within which the energy balance is made. Solar irradiation changes over the course of the day, but within the same hour, the change can be considered small enough to warrant this assumption.

3- Low thermal resistance of the condenser plate of the still.

4- Clear sky model for solar radiation.

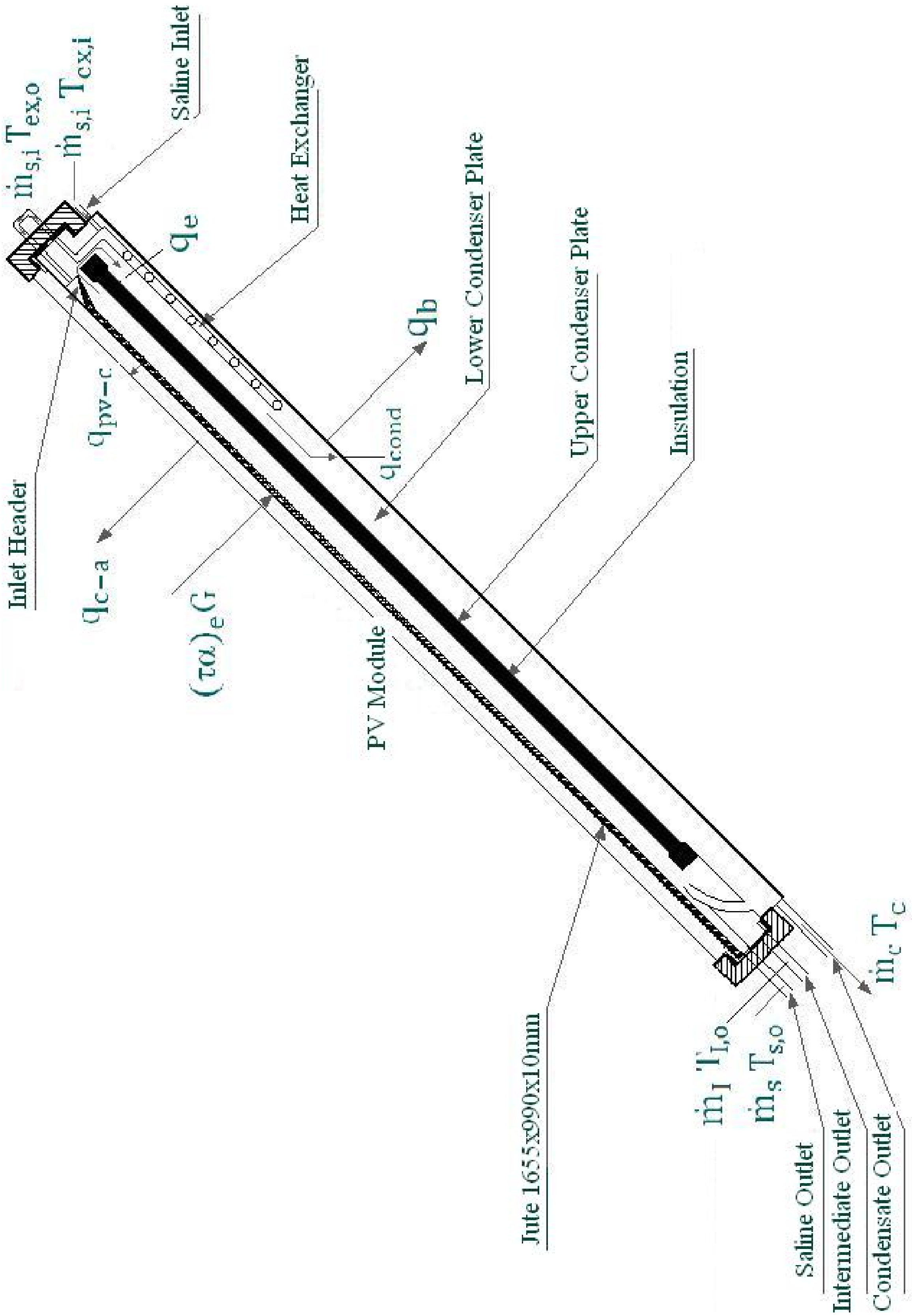


Fig 3-1, Temperature, energy and mass flows in the hybrid solar system.

3.1.1 System With Glass Cover Analysis:

Performing an energy balance on the system gives the following equation:

$$(\tau\alpha)_e G - \dot{E}_{PV} = q_e + q_{pv-c} + q_{unevap} + q_{loss} \quad \ldots\ldots(3.1)$$

Where:

$(\tau\alpha)_e$: Effective transmittance-absorptance product.

$(\tau\alpha)_e G$: Total heat absorbed by the PV (the useful heat input to the still).

$\dot{E}_{PV}$: The electrical power output.

q_e: Heat used to evaporate the inlet water.

q_{pv-c}: Heat loss from the PV to the glazing via convection and radiation.

q_{unevap} : Heat used to raise the temperature of the unevaporated saline water.

q_{loss} : Heat loss through the edges.

$\dot{E}_{PV}$ depends on the instantaneous operating temperature of the PV module (T_{pv}) and is a function of the packing factor PF, the effective transmissivity of the glazing τ_g, the electrical conversion efficiency η_e at the reference temperature of 25°C and the temperature coefficient φ_c of the PV panel. The packing factor represents the ratio of the PV panel's area to the area of the system. A packing factor of (1) means the system and the PV have the same area. $\dot{E}_{PV}$ can be given by the equation (Chow et al 2006):

$$\dot{E}_{PV} = G\tau_g PF\eta_e\left[1 - \varphi_c(T_{pv} - 25)\right] \quad \ldots\ldots(3.2)$$

$$q_{unevap} = \frac{Cp_W}{A_s}\left[\dot{m}_s\left(T_{s,o} - T_{s,i}\right) + \dot{m}_I\left(T_{I,o} - T_{s,i}\right)\right] \ldots\ldots\ldots(3.3)$$

Where:

Cp_W: Specific heat of water.

A_s: Still area.

$\dot{m}_s$: Mass flow rate of unevaporated saline water.

$T_{s,o}$: Saline water outlet temperature.

$T_{s,i}$: Saline water inlet temperature.

$\dot{m}_I$: Mass flow rate of unevaporated intermediate water.

$T_{I,o}$: Intermediate water outlet temperature.

Introducing heat balance for the glass cover results in:

$$q_{pv-c} = q_{c-a} \ldots\ldots\ldots(3.4)$$

Where:

q_{c-a}: Heal loss through glass cover to the ambient.

Heat balance on the heat exchanger and the lower condensing plate produces the following as seen in Figure 3-2:

$$q_e = q_b + q_{ex} + q_{con\,d} \ldots\ldots\ldots(3.5)$$

Where:

q_b: Heat lost through the bottom.

q_{ex}: Heat recovered by the heat exchanger.

q_{cond} : Heat of condensation.

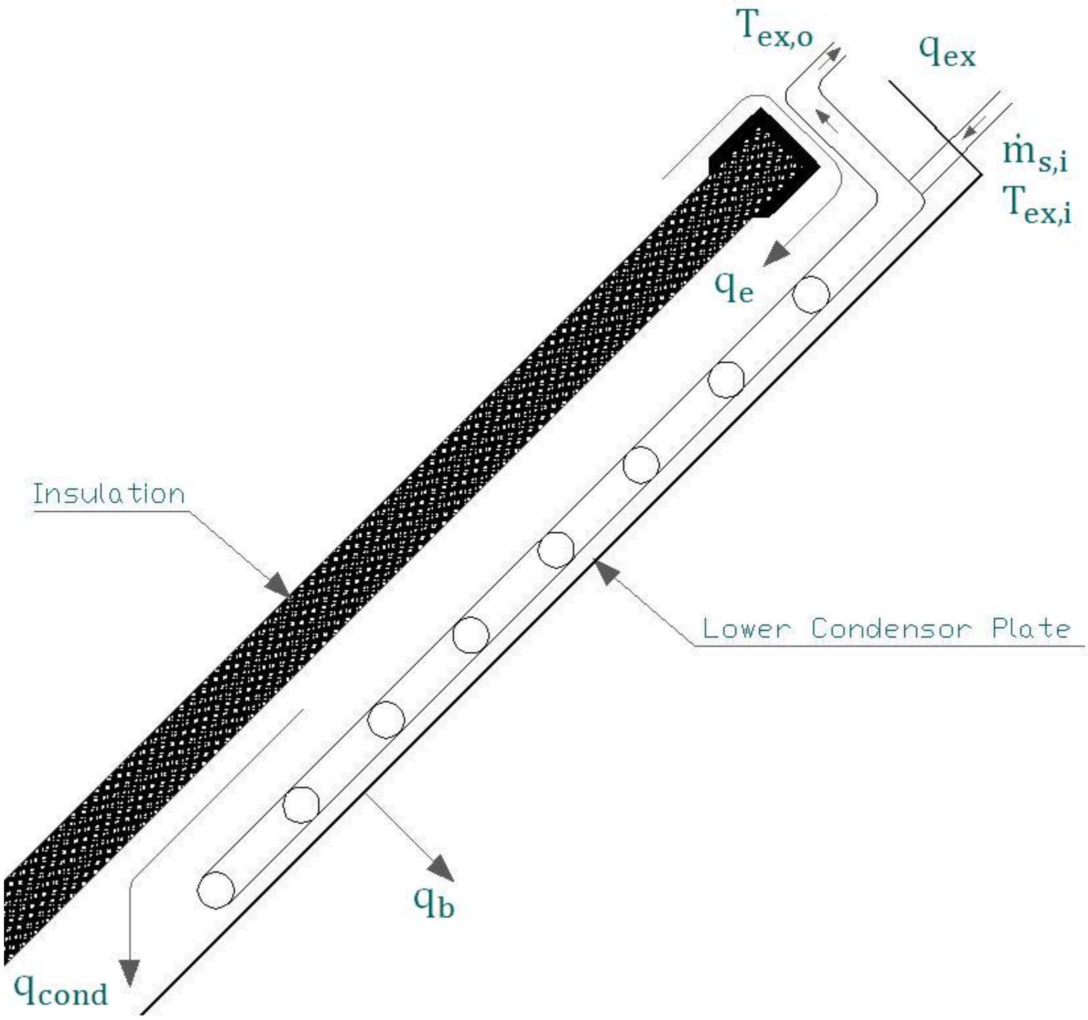


Fig 3-2, Heat balance on heat exchanger and lower condenser plate.

Introducing heat balance to the heat exchanger gives:

$$q_{ex} = \left(\frac{\dot{m}_{s,i}}{A_s}\right) Cp_W \left(T_{ex,o} - T_{ex,i}\right) \qquad (3.6)$$

Where:

$T_{ex,o}$: Heat exchanger saline water outlet temperature.

$T_{ex,i}$: Heat exchanger saline water inlet temperature.

From this, the total heat used to evaporate the saline water entering the still (q_e) in the presence of natural convection can be given by the equation:

$$q_e = q_{ex} + q_b + q_{nc} + q_{cond} \qquad (3.7)$$

Where:

q_{nc}: Heat used to raise the temperature of the air inside the system for the natural convection process.

The total related heat quantities may be evaluated as follows:

$$q_b = h_o(T_w - T_a) \qquad (3.8)$$

$$q_{nc} = h_n(T_{PVm} - T_\infty) \qquad (3.9)$$

$$q_{cond} = \dot{m}_c h_{fg}/A_s \qquad (3.10)$$

Where:

h_o: Outside film heat transfer coefficient. (To be calculated in a later section)

T_w: Bottom condenser plate wall temperature.

T_a: Ambient temperature

h_n: Natural convection heat transfer coefficient between the plates.

T_{PVm} : Mean PV panel temperature.

T_∞: Air temperature at the inlet of the absorbing part of the still (to be taken the same as the condensate tempertaure)

h_n is obtained with the help of the following equations (Incropera et al 2007):

$$Nu_s = 0.645\left[Ra_s\left(\frac{S}{L}\right)\right]^{\frac{1}{4}} \quad \text{.......(3.11)}$$

Where:

Nu_s: Nusselt Number and is given by the equation: $Nu_s = h_n\frac{S}{K}$

Ra_s: Rayleigh Number and is given by the equation: $Ra_s = (g\beta(T_s - T_\infty)S^3)/\alpha\upsilon$

Fluid properties where evaluated at the mean temperature of $T = (T_{s,L} - T_\infty)/2$

S: The spacing between plates.

L: Plate Length.

The terms q_{c-a} and q_{loss} can be evaluated as follows:

$$q_{c-a} = U_{c-a}(T_c - T_a) \quad \text{.......(3.12)}$$

$$q_{loss} = U_e(T_{pv} - T_a) \quad \text{.......(3.13)}$$

Where:

U_{c-a}: Total heat transfer coefficient for the heat lost through the glass cover.

T_c: Temperature of the glass cover.

U_e: Total heat transfer coefficient for the heat lost through the edges.

Those terms will be further discussed later in the simulation analysis.

The productivity of the still is defined as the amount of heat transferred by the vapor divided by the latent heat heat of evaporation as shown in the equation:

$$\dot{m}_c = \frac{q_e A_S}{h_{fg}} \quad (3.14)$$

Where:

$\dot{m}_c$: The condensate water productivity of the still in (kg/s)

h_{fg}: Latent heat of evaoparation for water.

q_e is obtained by re-arranging equation (3.1) to give:

$$q_e = (\tau\alpha)_e G - \dot{E}_{PV} - q_{pv-c} - q_{unevap} - q_{loss} \quad (3.15)$$

Substituting equation (3.14) in equation (3.13) we get:

$$\dot{m}_c = \frac{\left((\tau\alpha)_e G - \dot{E}_{PV} - q_{pv-c} - q_{unevap} - q_{loss}\right) A_S}{h_{fg}} \quad (3.16)$$

The instantaneous thermal efficiency of the system can be defined as the heat used to evaporate the water q_e divided by the incident radiation on the still G:

$$\eta_{th} = \frac{\left((\tau\alpha)_e G - q_{pv-c} - q_{unevap} - q_{loss}\right)}{G} \quad (3.17)$$

And the instantaneous total efficiency of the system into account the thermal and the PV module production:

$$\eta_{tot} = \frac{(\dot{m}_c \times h_{fg}) + \dot{E}_{PV}}{G \times A_S} \quad \text{......(3.18)}$$

The hourly total efficiency is:

$$\eta_{h,tot} = \frac{(\dot{m}_c \times h_{fg}) + \dot{E}_{PV} \times 3600}{3600 \times G \times A_S} \quad \text{......(3.19)}$$

And the daily total efficiency is:

$$\eta_d = \frac{\sum(\dot{m}_c \times h_{fg} + \dot{E}_{PV} \times 3600)}{\sum(3600 \times G \times A_S)} \quad \text{......(3.20)}$$

3.1.2 System Without Glass Cover Analysis:

Performing an energy balance on the system gives the following equation:

$$\alpha_e G - \dot{E}_{PV} = q_e + q_{pv-a} + q_{unevap} + q_{loss} \quad (3.21)$$

Where

q_{pv-a}: Heat loss from the PV to the ambient via convection and radiation.

$$\dot{E}_{PV} = GPF\eta_e\left[1 - \varphi_c(T_c - 25)\right] \quad (3.22)$$

With the exception of equations (3.4) and (3.12), equations (3.3) through (3.14) apply for the case of no glass cover as well. The other differences will be highlighted in the following sections.

q_e is obtained by re-arranging equation (3.18) to give:

$$q_e = \alpha_e G - \dot{E}_{PV} - q_{pv-a} - q_{unevap} - q_{loss} \quad (3.23)$$

Substituting equation (3.20) in equation (3.13) we get:

$$\dot{m}_c = \frac{(\alpha_e G - \dot{E}_{PV} - q_{pv-a} - q_{unevap} - q_{loss})A_S}{h_{fg}} \quad (3.24)$$

The instantaneous thermal efficiency of the system can be defined as the heat used to evaporate the water q_e divided by the incident radiation on the still G:

$$\eta_{th} = \frac{((\alpha_e G - q_{pv-a} - q_{unevap} - q_{loss})}{G} \ldots\ldots(3.25)$$

And the instantaneous total efficiency of the system into account the thermal and the PV module production:

$$\eta_{tot} = \frac{(\dot{m}_c \times h_{fg}) + \dot{E}_{PV}}{G \times A_S} \ldots\ldots(3.26)$$

The hourly total efficiency is:

$$\eta_{h,tot} = \frac{(\dot{m}_c \times h_{fg}) + \dot{E}_{PV} \times 3600}{3600 \times G \times A_S} \ldots\ldots(3.27)$$

And the daily total efficiency is:

$$\eta_d = \frac{\sum(\dot{m}_c \times h_{fg} + \dot{E}_{PV} \times 3600)}{\sum(3600 \times G \times A_S)} \ldots\ldots(3.28)$$

3.2 Simulation:

3.2.1 Introduction:

Following the method developed by Badran et al (2005), a modified computer simulation was performed to predict the performance of the still and the effect of various parameters on that performance. The simulation was done using MATLAB software. It was chosen because it has the ability to perform both calculations and plotting graphs.

3.2.2 Objectives of the Simulation:

The main objectives of this simulation are:

- To predict the productivity of the still under the effect of various parameters.
- To estimate the heat losses from the still.
- To predict the effect of using a PV panel to be the absorber plate versus using a black steel plate has a higher conductivity.

3.2.3 Theory:

Following the procedure illustrated by (Culp 1991). The normal beam radiation is calculated using the equation:

$$G_{DN} = A_s e^{\left(-B_s/\sin \beta_1\right)} \qquad (3.29)$$

Where:

A_s: The apparent extraterrestrial radiation.

B_s: The atmospheric extinction coefficient.

β_1: The altitude angle of the sun.

The total solar radiation is calculated using the equation:

$$G_{tot} = G_{DN} (\cos\theta + C_s F_{ss}) \qquad (3.30)$$

Where:

F_{ss}: The view factor between the surface and the sky and is calculated from:

$$F_{ss} = (1 + \cos(\beta_2))/2 \qquad (3.31)$$

The values of A_s, B_s, and C_s and the altitude angle β_1 were were all obtained from (Culp 1991).

$$\sin(\beta_1) = \cos(L)\cos(\delta)\cos(H) + \sin(L)\sin(\delta) \qquad (3.33)$$

Where:

The variables calculated in the following equations were illustrated by (Duffie and Beckman 2006)

L: The latitude angle (32° for Amman).

δ: The declination angle and can be calculated from:

$$\delta = 23.45 \times \sin[360(284 + n)/365] \qquad (3.34)$$

Where: n=day of the year; $1 \leq n \leq 365$

H: The hour angle and can be calculated from the following equation:

$$H = (AST - 720)/4 \qquad (3.35)$$

Where AST is the apparent solar time, and it can be calculated using the equation:

$$AST = MST + E \qquad (3.36)$$

Where MST is the mean solar time which can be calculated using the following equation:

$$MST = (\text{local solar time in minutes}) + 24 \qquad (3.37)$$

And E is the equation of time that can be calculated as follows:

$$E = 229.2[0.000075 + 0.001868\cos B - 0.032077\sin B - 0.014615\cos(2B)] \qquad (3.38)$$

$$B = (n - 1) \times (360/365) \qquad (3.39)$$

The incidence angle (θ) can be calculated from the following equation:

$$\cos(\theta) = \sin(\beta_1)\cos(\beta_2) + \cos(\beta_1)\sin(\beta_2)\cos(\alpha) \qquad (3.40)$$

Where:

α : Solar azimuth, which can be calculated from:

$\alpha = \cos(\delta)\sin(H)/\cos(\beta_1)$……………………………..………………………………..(3.41)

β_2: The tilt angle of the collector.

A typical value of the effective transmittance absorptance pdoduct $(\tau\alpha)_e$ was used as stipulated by (Duffie and Beckman 2006):

$(\tau\alpha)_e = 1.02 \times (\tau\alpha) = 1.02 \times 0.87 \times 0.8 = 0.70992$ ………………………………..(3.42)

Heat loss from the bottom was stated earlier in equation (3.8) where:

h_o: Outside film heat transfer coefficient.

T_w: Bottom condenser plate wall temperature.

T_a: Ambient temperature

$$h_o = \frac{k \times Nu}{L_c} \ldots\ldots\ldots (3.43)$$

Where $L_c = (4 \times \text{Plate Area})/\text{Perimeter}$

$Nu = 0.86Re^{1/2}Pr^{1/3}$ …….(Incropera et al 2007)

$Re = \frac{V \times L_c}{\upsilon}$ ……………….. (Crowe et al 2005)

Where:

k: Thermal conductivity of air.

Nu: Nusselt Number.

Re: Reynold’s Number.

Pr: Prantdle Number.

υ: Kinematic viscosity.

The values of Nu and Pr are variables that depend on the ambient temperature. Therefore, they are considered as inputs in the simulation.

Heat loss from the top:

$$q_{pv-c} = q_{c-a} = q_{pv-a} = U_T(T_{PVm} - T_a) \qquad (3.44)$$

Where U_T is the top loss coefficient that can be calculated from the following equation in the case of glass cover (Duffie and Beckman 2006)

$$U_T = \left\{ \frac{N}{\frac{C}{T_{PVm}}\left[\frac{T_{PVm} - T_a}{N + f}\right]^e} + \frac{1}{h_w} \right\}^{-1} + \frac{\sigma(T_{PVm} - T_a)(T_{PVm}{}^2 - T_a{}^2)}{(\varepsilon_{PV} + 0.00591Nh_o)^{-1} + \frac{2N + f - 1 + 0.133\varepsilon_{PVm}}{\varepsilon_g} - N} \qquad (3.45)$$

Where:

N: Number of glass covers (N=1 in this work).

$f = (1 + 0.089h_w - 0.1166h_w\varepsilon_{PVm})(1 + 0.07866N)$

$C = 520(1 - 0.000051(\beta_2)^2)$

$e = 0.43(1 - (100/T_{PVm}))$

β_2: Collector's tilt angle.

ε_g: Emittance of glass (0.88).

ε_{PV}: Emittance of PV panel which acts as the absorber plate (0.8) .

T_a: Ambient Temperature (K).

T_{PVm} : Mean PV panel temperature (K).

h_o: Wind heat transfer coefficient.

In the case of no glass cover, to calculate the top loss coefficient, equation 3.46 is used (Duffie and Beckman 2006)

$$U_T = h_o + h_{r,PV-a} \quad (3.46)$$

Where:

h_o: Outside, or wind heat transfer coefficient found in equation (3.43)

$h_{r,PV-a} = \sigma\varepsilon_{PV}(T_{PVm} + T_a)\left({T_{PVm}}^2 - {T_a}^2\right)$

Heat loss from the sides of the still:

$$q_{loss} = U_e(T_{PVm} - T_a) \quad (3.47)$$

Where U_e is the edge loss coefficient which can be calculated from the following equations:

$U_e = (U_{edge} \times A_{edge})/A_S$

$U_{edge} = k/t$

Where:

k: The thermal conductivity of the insulation.

t: The thickness of insulation.

$A_{edge} = \text{edge height} \times \text{perimeter}$

Chapter 4

Experimental Work

This chapeter deals with the design, building, and testing of the hybrid PV-T desalination system. It shows the componentes of the system, the operating principle and the way in which the variable parameters were measured.

4.1 System Description:

The PV-T collector system to be studied in this work has the following components:

1- Glazing:

A plate of 4mm thick glass of the same size as the PV panel (1655x990 mm) to work as glazing. The system is tested with the addition of this glass cover and without this glass cover to test the difference in system performance based on the presence of glazing and the lack of glazing.

This glass plate is installed in grooves in the wooden frame. The reason to use this glass is to allow solar radiation to enter the system reach the PV panel which works as an absorber plate, and to minimize the effect of forced convection cooling that occurs at the absorber plate preventing the heat from escaping the system creating a greenhouse effect.

2- Photovoltaic Panel:

The PV panel is mono-crystalline cells manufactured by Philadelphia-Solar. Its rated output is 250 Watt at a module efficiency of 15.3% (PS-M60H-250W Mono-Crystalline Solar Panel product sheet 2010). This panel is placed over an inverted trickle solar still and would work as the abosrber plate. Its color is dark as seen in Figure 4-1, so this would allow it to function properly as an absorber plate. The main function of this panel is to convert the solar radiation to electricity and to transfer the excess energy to the water flowing on its back.



Fig 4-1, The 250-Watt PV panel.

3- Jute:

A thin layer of jute is fixed to the back of the PV panel using an adhesive material to keep it connected to the back of the PV panel. The jute layer absorbs water and keeps it in contact with the back of the PV panel (absorber plate) and directs the flow of water downwards to make sure that the water stays in contact with the absorber plate long enough to evaporate by absorbing the heat energy falling on it. This serves a double purpose, on one hand, the water flowing at the back of the PV panel helps cool the panel which increases its efficiency, and at the same time produces desalinated water by heating the water flowing at the back of the PV panel till evaporation and then condensating it.

The jute layer also ensures uniform flow of water along the length of the absorber plate until it reaches the outlet header. Figure 4-2 shows this jute layer.

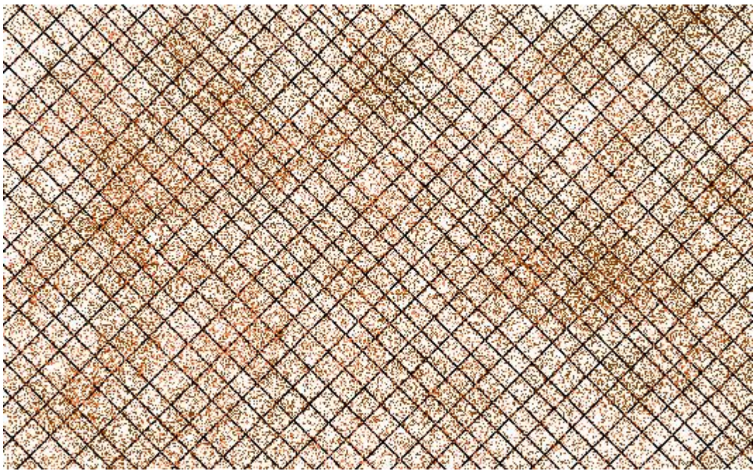


Fig 4-2, Thin Jute Layer.

4- Wire Screen:

A wire screen made of very thin stainless steel wires and its job is to keep the wet jute in contact with the backside of the absorber plate. It also helps direct the flow of water directly at the back of the PV panel. Figure 4-3 shows the wire screen.

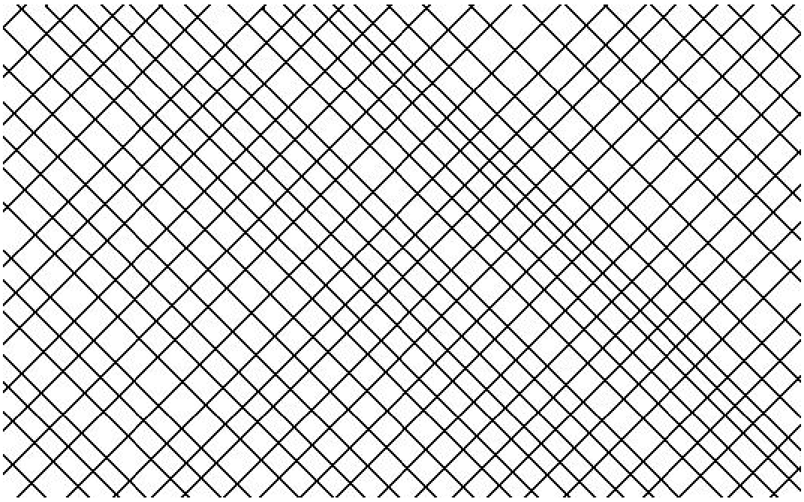


Fig 4-3, Wire Screen.

5- The Inlet Header and Water Holder:

The inlet header is made of galvanized steel of 90 cm length and it has holes of 1 mm diameter drilled in it with around 10 mm spacing between them. It is made in the shape of a prism and its function is to spread the water unifromly over the jute.

At the end of the inlet header is a curved galvanized steel plate that helps distribute the water on the jute uniformly and more importantly prevents the water from immediately dripping onto the insulation and in the space where the vapor moves to the condensing compartement. Figure 4-4 shows the inlet header and the water holder.

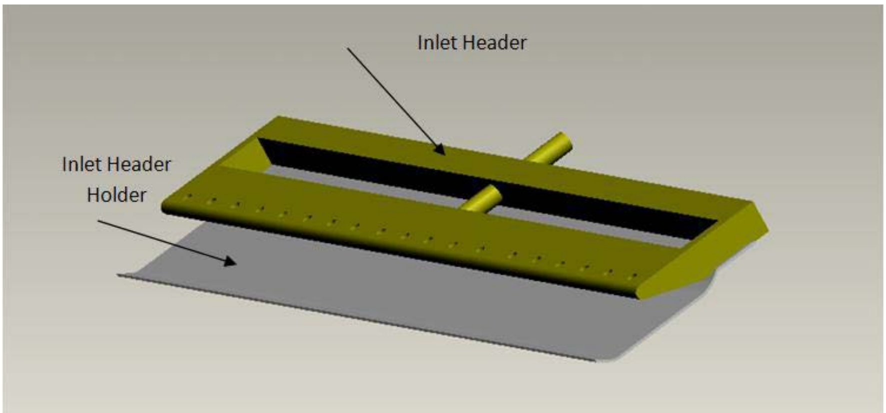


Fig 4-4, The Inlet Header and the Water Holder.

6- Insulation:

A Rigid Polyurethane Foam Board of 25 mm thickness with an aluminum foil of 0.2mm thickness on the top and the bottom of it. Its dimensions are 1400x980mm. This insulating material has an R value of around 7.1 to 8.7 W/m2.K.

The purpose of this insulation is to prevent heat exchange between the upper area of the collector where the solar radition is gathered and the lower area where the water condenses. Fig 4-5 shows the insulation panel.

After some time the low-conductivity gas in the foam escapes and air replaces it dropping the R value. This phenomenon is known as thermal drift. The aluminum foil present helps to keep the gases in, and prevents thermal drift. This reflective foil, if installed correctly, can also act as a radiant barrier. (Energy Savers, Polyurethane Insulation Material webage 2011)

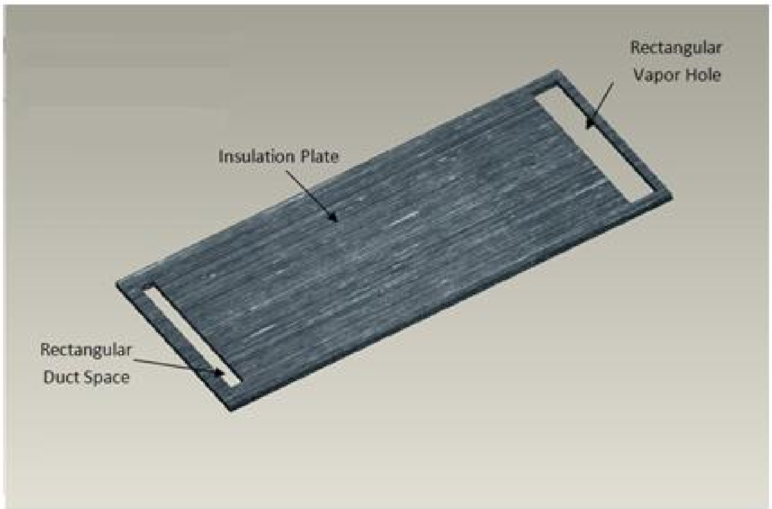


Fig 4-5, Insulation Plate.

7- Heat Exchanger:

A copper pipe with length of around 10 meters and an inner and outer diameters of 11 and 13 mm respectively. Its specific thermal conductivity is 385 W/m.K. This pipe is in the condensation compartment and is used as a form of heat recovery. The water vapor passing below the upper condenser plate moves through the heat exchanger heating the water passing through it. This water takes some of the energy carried by the vapor through the heat exchange between the water and the vapor.

This heat exchanger serves two purposes: The first one is to help cool the vapor to condensate as the desalinated water, and secondly it pre-heats the saline inlet water before entering the system through the inlet header. This would result in the water needing less energy to evaporate. Figures 4-6 and 4-7 show the heat exchanger.

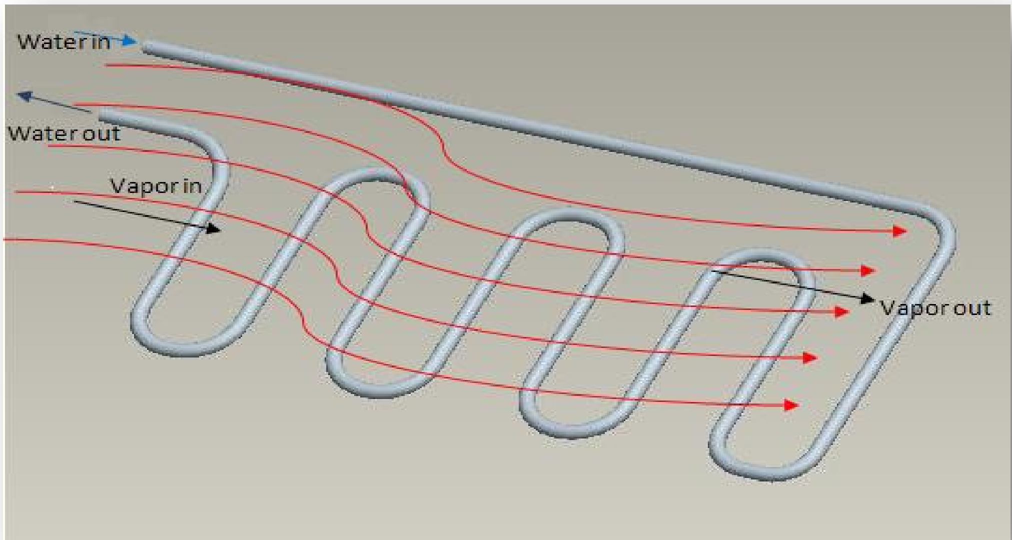


Fig 4-6, Heat Exchanger.



Fig 4-7, Heat Exchanger.

8- Condenser Plates:

The condensing area in the PV-T system consists of a galvanized steel plate of 1.1 mm thickness, the lower side of the insulation which is a 0.2 mm thick aluminum foil, and a heat exchanger. Figure 4-8 shows the condensation compartment.

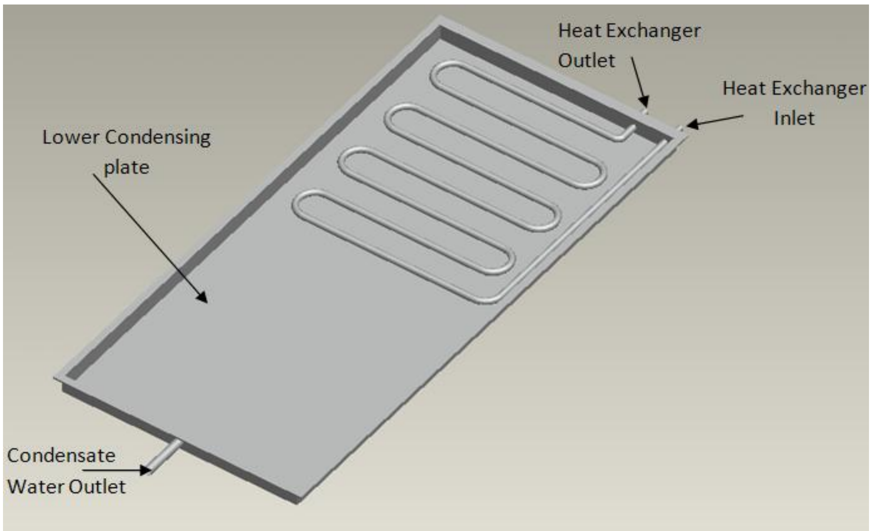


Fig 4-8, The Condensation Compartment.

9- Circulating Ducts (Air Ducts):

Three ducts that are made of galvanized steel with an opening of around 40x20mm each. The purpose of these ducts is to connect between the vapor compartment over the insulation plate and the condensation compartment under the insulation plate allowing the natural convection process to take place, and to allow the vapor that doesn’t condense to go around in a cycle and pass over the heat exchanger again to condensate.

10- The Outlet Header:

The outlet header consists of two outlet pipes, the first one is for the saline water that moves down the jute without evaporating and the second one is for the intermediate water which is the water that drips down from the jute and gets mixed with some of the vapor. Figure 4-9 shows this header.

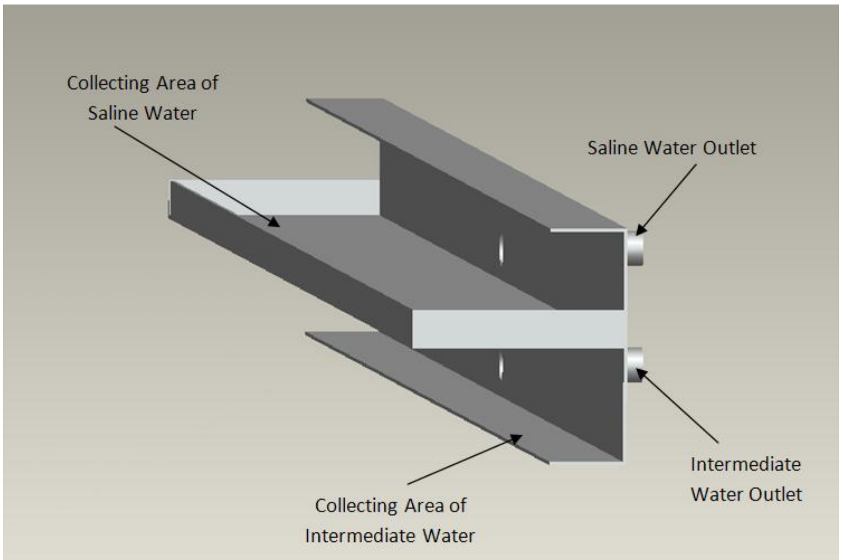


Fig 4-9, The Outlet Header.

11- Wooden Frame:

This frame is used to hold the upper part of the collector with the lower part and to prevent leakage. Another reason to use a wooden frame is to ensure that the upper and lower parts are totally insulated from each others.

12- Various Adhesives and Insulating Materials:

Around the corners of the collector and in between the wooden frame and the steel condensing plate and the PV panel, some adhesive insulation materials were used such as Silicon Sealant, Foam, and Rubber. Some adhesive materials were also used to keep the jute and wire screen connected to the back of the PV panel.

Figures 4-10 to 4-12 show the PV-T collector that was built to be investigated in this work as seen from the front, top and side views (Figures drawn using AutoCAD software).

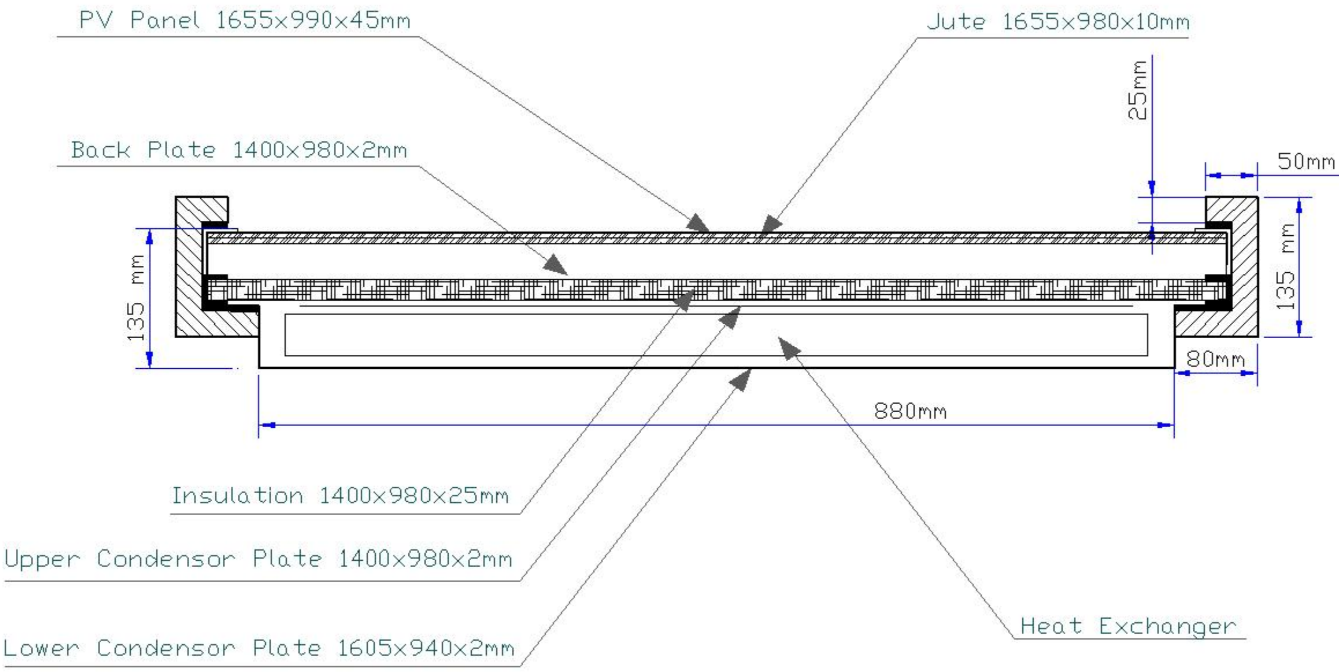


Fig 4-10, Transverse Cross-Section in the Hybrid PV-Desalination Device.

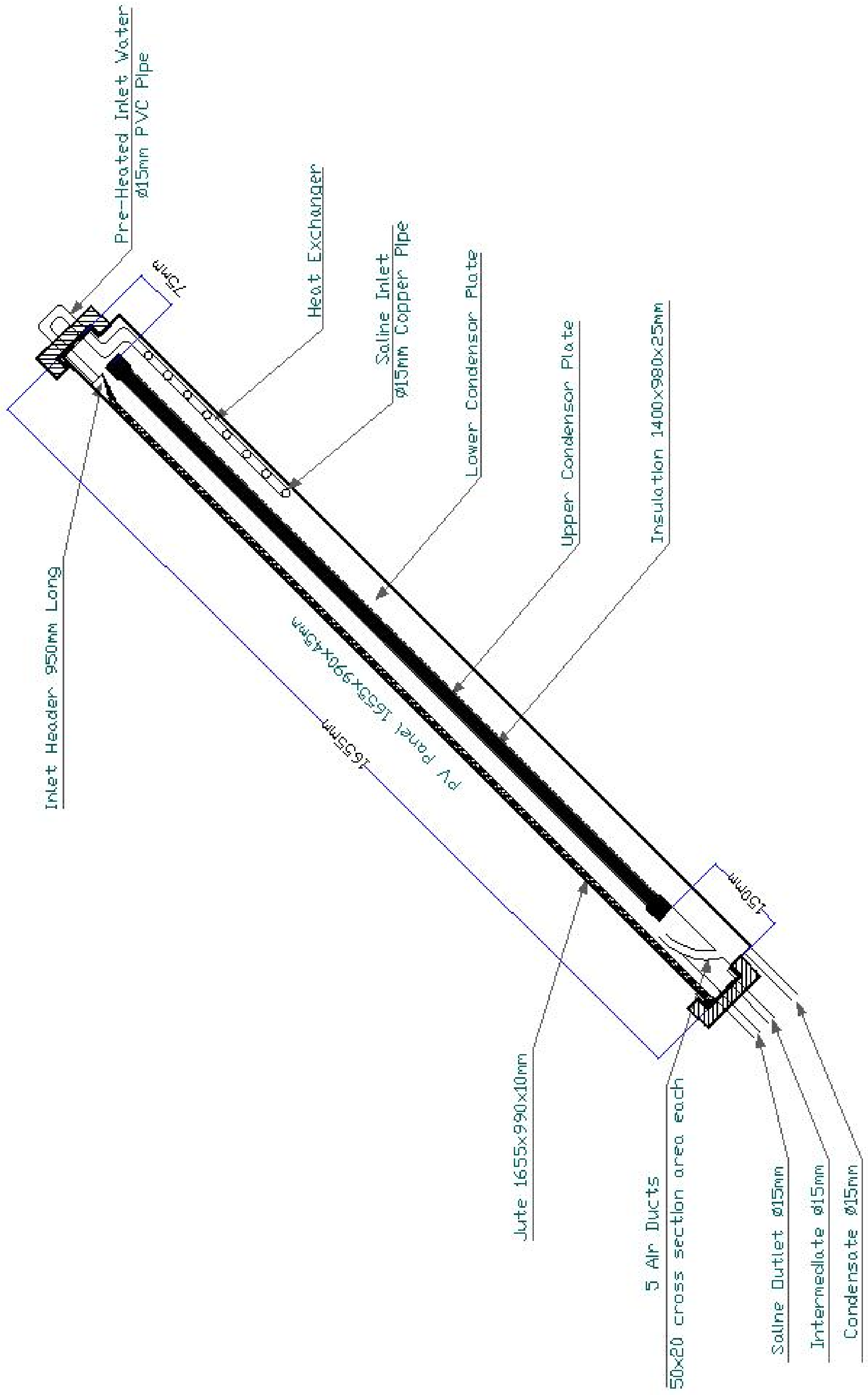


Fig 4-11, Longitudinal Section in the Hybrid PV-Desalination Device.

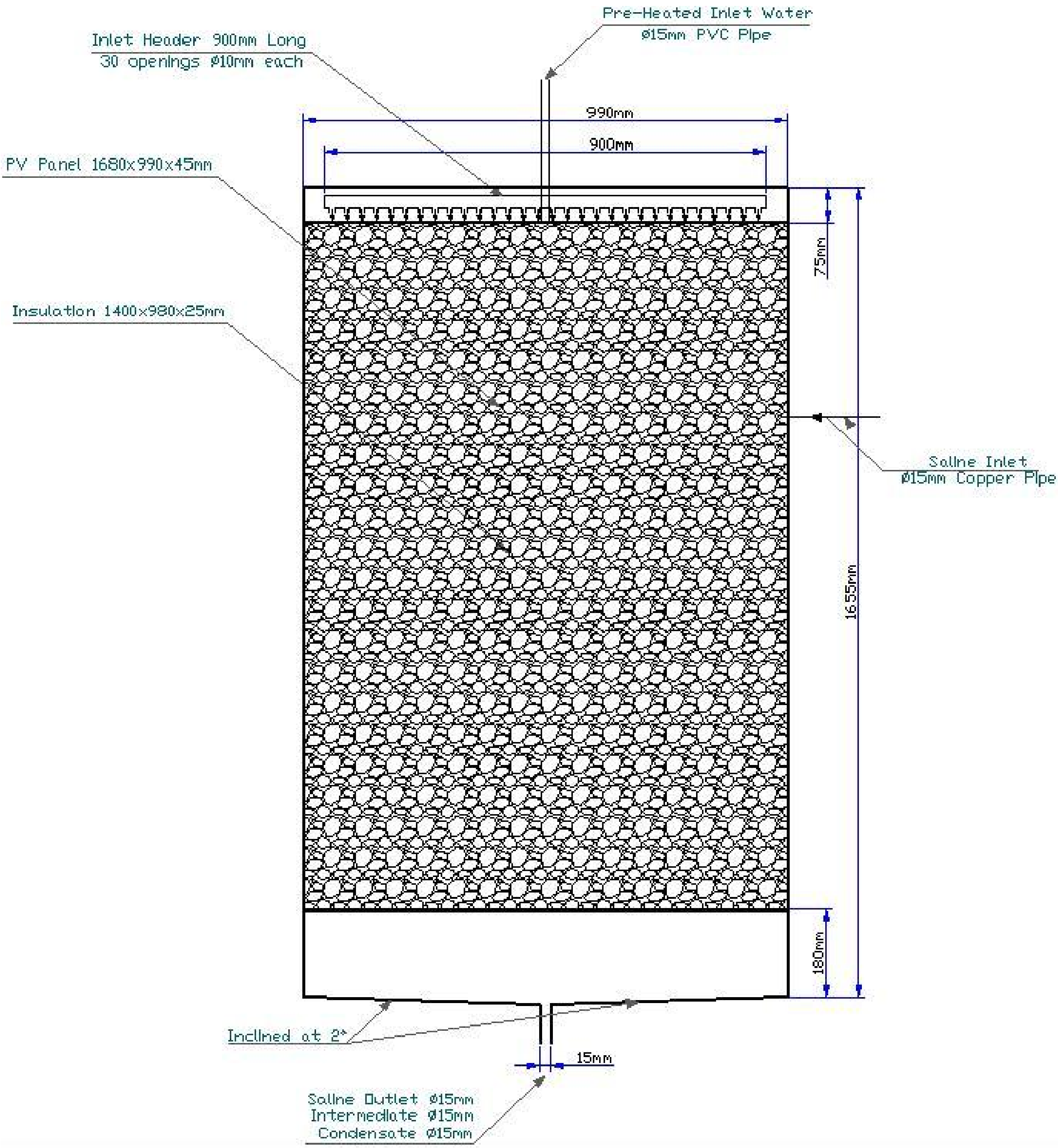


Fig 4-12, Frontal View of the Hybrid PV-Desalination Device.

4.2 Working Principle:

Solar energy has been used for a long time with the techniques to use it improving over time. In this work solar energy will be used to generate electricity and to desalinate water.

In this work the evaporation and condensation of water happens in separate areas unlike older methods were condensation used to happen on the glazing.

The process of evaporation and condensation in this solar trickle takes place under the absorber plate and in the condensation compartment respectively. Solar radiation is transmitted through the glazing to heat the PV Panel that works as an absorber plate as shown in Figure 4-12.

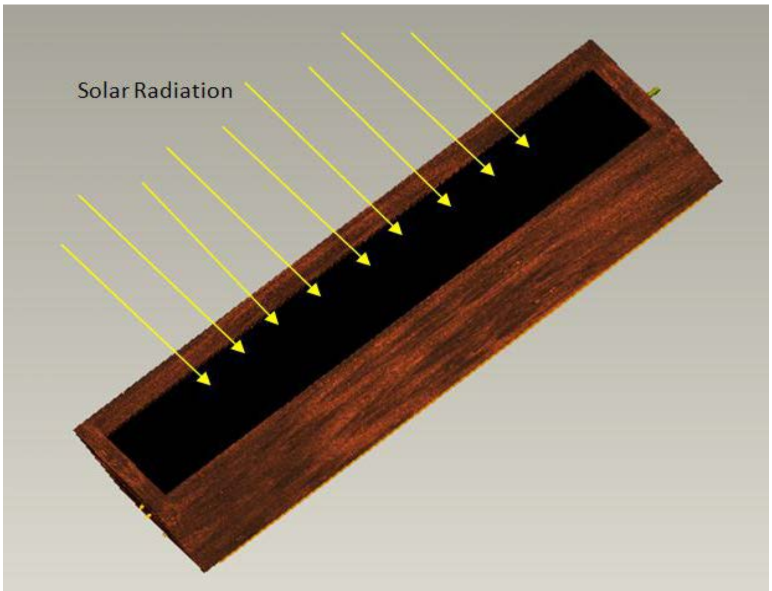


Fig 4-13, Solar Radiation Over the System.

Water first enters the system through a pipe that goes through the heat exchanger where a heat exchange happens between the entering water at ambient temperature, and the vapor coming from the upper area of the collector. This process is a heat recovery process to make

use of the energy carried by the water vapor into pre-heating the water before it enters the system. This energy added to the water reduces the amount of energy the water needs to take from the absorbing plate in order to evaporate.

The water exiting the heat exchanger at an elevated temperature re-enters the system as shown in Figure 4-14.

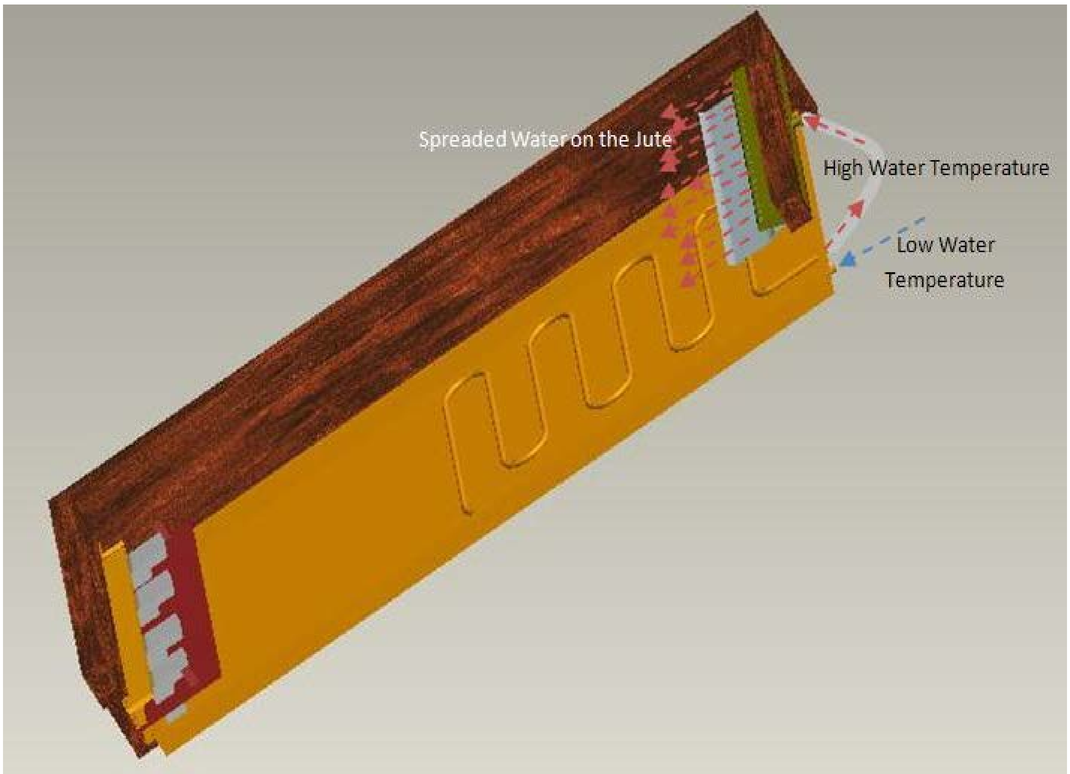


Fig 4-14, Heat Recovery.

The water exiting the heat exchanger after being preheated enters the inlet header and spreads through the holes to the jute which is in direct contact with the bottom of the PV panel (absorber plate) as seen in Figure 4-14.

Part of this water stays in contact with the back of the absorber plate and another part of the water goes into the jute until saturation. The last part slides down the wire screen.

All that water absorbes heat from the back of the PV panel, hence decreasing its temperature and increasing its efficiency, while that heat gained by the water increases its temperature to the point of evaporation. This water vapor goes upwards to the end of the insulation plate and to the heat exchanger where it starts to condense.

Some of the water evaporates and some of the unevaporated water keeps sliding down to the end of the absorber plate and the jute reaching the saline outlet header as water with high salinity due to some parts of it evaporating leaving the water with all its saline content.

Another part of the water drips from the jute to the insulation plate. Some of it mixes with the water vapor and reaches the intermediate outlet header as water with intermediate salinity as shown in Figure 4-15.

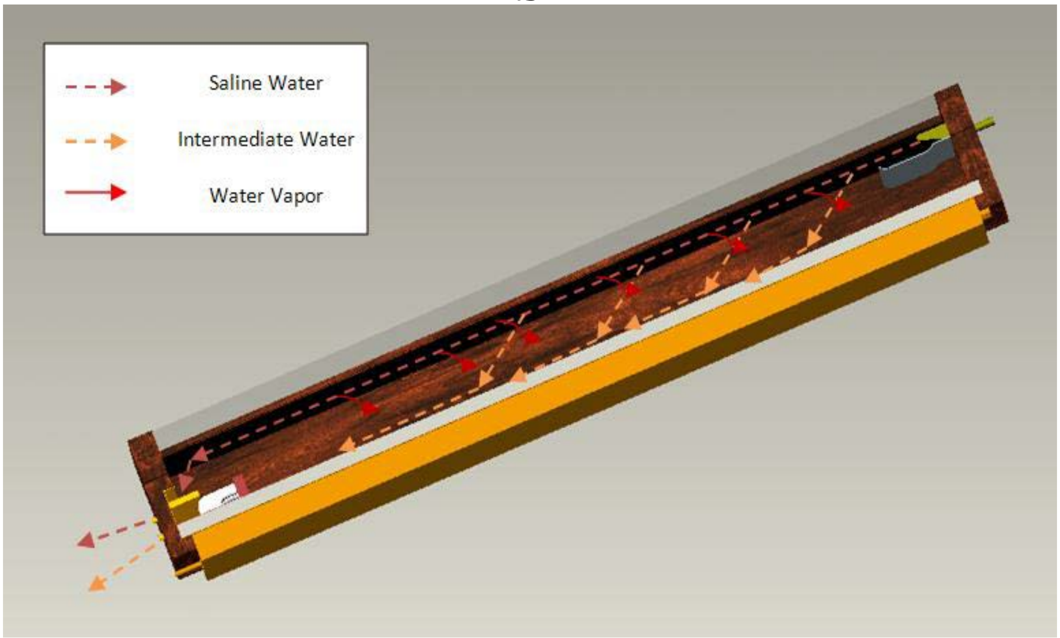


Fig 4-15, Water States in the Collector.

The water that reaches the point of evaporation moves upwards drived by the thermosyphonic process drived by the density differences of air as shown in the Figure 4-16.

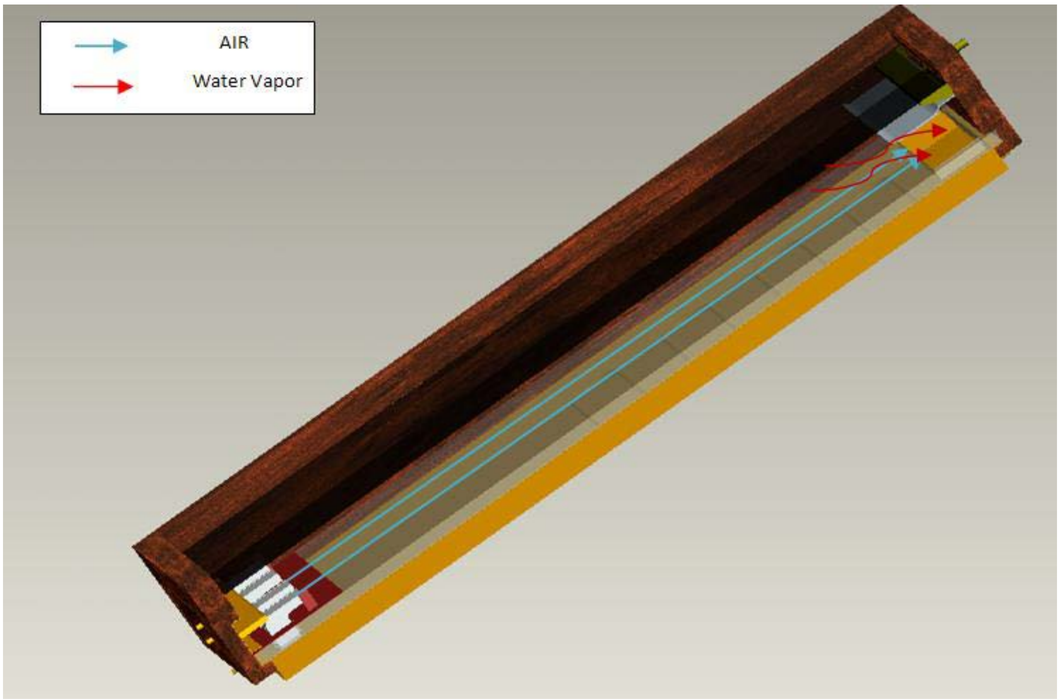


Fig 4-16, Thermosyphonic Process.

The vapor-air mixture reaches the hole at the end of the insulation plate and it goes through this hole reaching the condensation compartment where the vapour goes around the heat exchanger and condensates.

The water that condensated in the condensation compartment slides down the lower condenser plate all the way down to the bottom of the condensation compartment reaching the condensate water outlet as water with lowest salinity which is the desalinated water. This can be seen in Figure 4-17.

One last addition to the system was three small air ducts connecting the evaporation compartment and the condensation compartment. Those ducts allow natural convection. This is to improve the process by allowing the vapor that doesn't condensate in the lower compartment to go up again over the absorber plate to join the more recently evaporated water and then go back up to the heat exchanger to evaporate.

Figures 4-4 to 4-9, and Figures 4-13 to 4-17 were taken from (Sabra et al 2005).

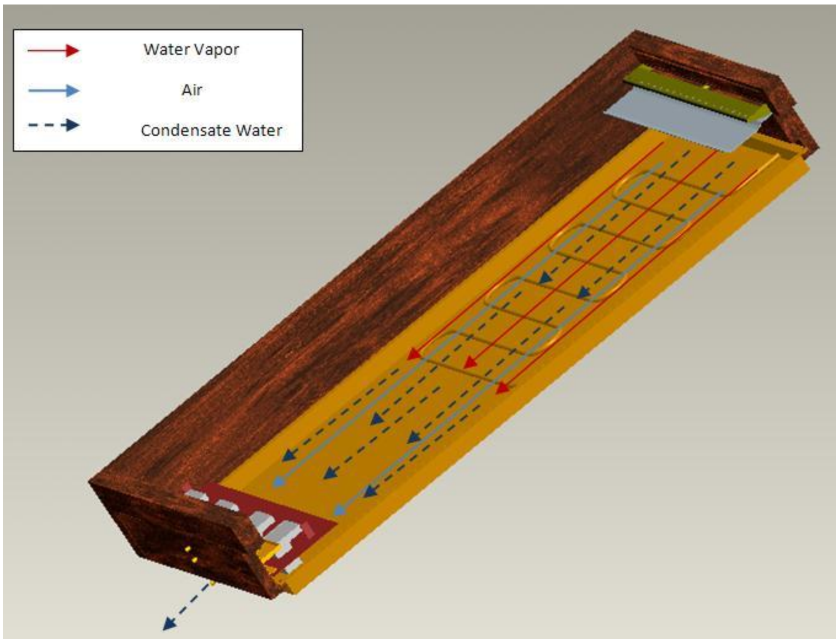


Fig 4-17, Condensation Process.

4.3 Design of Heat Exchanger for Solar Still:

The higher the temperature of water, the easier it becomes for this water to evaporate and the less energy it needs to reach evaporation. The water entering the system is at a temperature equal to or close to the ambient temperature. This means this water needs a lot of energy to evaporate and since water is flowing downward on the back of the PV module, then it might not get enough energy to evaporate before exiting through the outlet header.

To solve this problem, heat recovery was used in this work. This is done using a heat exchanger that is installed in the condensation compartement where the vapor condensates giving its energy to the water passing through the heat exchanger. The water passing through the heat exchanger gains significant energy raising its temperature considerably up to around 20 to 30°C over that of inlet water. This is achieved around solar noon. This heat recovery process serves two purposes; the water entering the system is pre-heated meaning that its easier for it to reach evaporation, and the addition of a heat exchanger makes the condensation process much more efficient by dropping the temperature of the condensation compartment.

There is an optimum size and length for the heat exchanger to do the required function which is to transfer all the heat in the vapor to the water. The length of the heat exhanger was determined and the detailed calculations for it are available in Appendix C.

4.4 Temperature, Salinity, Voltage, Current and Radiation measurements:

In this work the various parameters were measured using equipment detailed in Appendix E. Measurements were taken manually every hour from 8 in the morning till 5 in the afternoon. A data logger wasn’t used. The measurements taken are detailed in Appendix A, Tables A-1 though A-6.

The measurements included, the solar irradiation, the temperatures of various system components, the ambient temperature, the salinty of the three water outlets, the flow rate, the amount of water coming from the three outlet headers, the current, and the voltage.

The solar irradiation was measured using a pyranometer connected to a solar integrator. The pyranometer was placed on the inclined face of the device. The angle was 47°.

The various temperatures were measured using a thermocouple calibrator, and thermocouples used were Type T thermocouples. Various thermocouples were installed in the device; a thermocouple fixed to the upper face of the PV module using an adhesive material. This thermocouple measures the temperature of the absober plate (The PV module in this case). Another thermocouple was placed just over the heat exchanger where the water vapor passes. This thermocouple measures the temperature of the vapor at its peak value. A third thermocouple was placed inside the pipe that feeds water into the heat exchanger to measure the value of the temperature of the water entering the heat exchanger. A fourth thermocouple was placed inside the pipe that is the outlet of the heat exchanger and feeds water into the system via the inlet header. Similarly, thermocouples were added to the outlet pipes of saline,

intermediate and condensate water. Finally, a thermocouple was used to measure the ambient temperature.

Salinity was measured using a conductivity meter that was calibrated using a standard and then checked with a more accurate conducivity measuring device to make sure the calibration was done properly.

Water flow rate was measured using a flow meter that was fixed to the frame supporting the system. The flow meter measured the water input to the heat exchanger, which is the same as the water entering the system through the inlet header.

The amount of water obtained from each outlet header was measured using a calibrated cylinder.

The voltage and current were measured using an avometer and a variable resistance.

The system was left running during the night since susnet was at around 6 in the afternoon which means the system continues to generate condensate during that period and even after that since the system have stored energy throughout the day.

Figure 4-18 shows a general view of the device that was designed and studied in this work. Its area is 1.638 m^2.



Figure 4-18: General view of the device.

Chapter 5

Results and Discussion

5.1 Results:

This chapter shows the results of this work in four parts; the experimental results, the simulation results, a comparison between the experimental and simulation results, and finally a comparison with the previous work.

5.1.1 Experimental Results:

This section contains the experimental results obtained during the testing of the still over the course of six days during the period from the 12^{th} to the 20^{th} of April,2011. Experimental reusults are shown in Figures 5-1 to 5-9. The results are also shown in Appendix A, tables A-1 through A-6.

Figure 5-1 shows the electrical power output of the still with and without glazing.

Figures 5-2 and 5-3 represent the temperatures measured in various parts of the still over the working hours from 8:00 AM to 5:00 PM over the course of two days. The condensate productivity was directly obtained from the condensate output header and is shown in Figure 5-4 for various flow rates over the working hours of four days. The efficiency of the still was found using equations 3.19 and 3.27 and is plotted against time in Figure 5-5. Figure 5-6

shows the distribution of the incident solar radiation on the still at a tilt angle of 45° over the working hours of two days.

Figures 5-7 and 5-8 relate the productivity and efficiency of the still to the incident solar radiation for three different flow rates.

All the Figures listed above also compare the variables with regard to glazing being present and having no glazing.

Table 5-1 summarizes some of output parameters obtained experimentally.

Table5-1: Summary of the experimental results.

Date	Glazing	Flow Rate (g/s)	Condensate Productivity (ml/day)	Condensate Average Salinity (PPM)	Intermediate Productivty (ml/day)	Intermediate Average Salinity (PPM)	Daily Efficiency (%)	Average Power Output (Watt)
12/4	No Glazing	1.0	1775	113.5	572	767.6	24.400	167.32
14/4	No Glazing	1.0	2105	103.0	140	817.2	26.570	155.04
15/4	No Glazing	1.75	1965	57.52	170	530.0	25.480	163.40
16/4	No Glazing	0.7	2234	60.40	175	523.3	27.984	144.10
18/4	Glazed	1.0	3690	45.60	1490	562.0	33.132	128.21
20/4	Glazed	1.0	3855	20.44	165	545.0	34.355	134.22

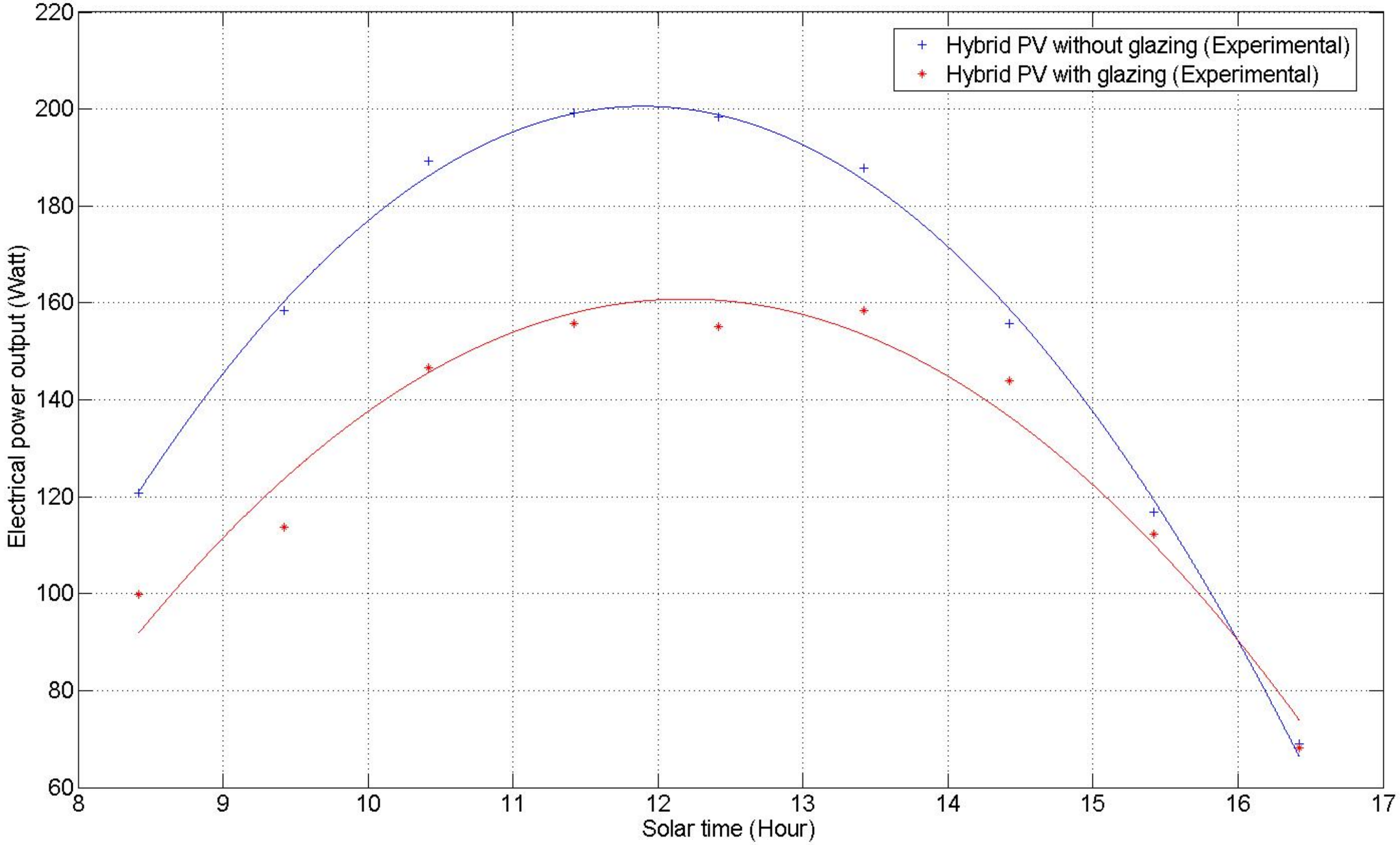


Figure 5-1: Electrical power output (Experimental)

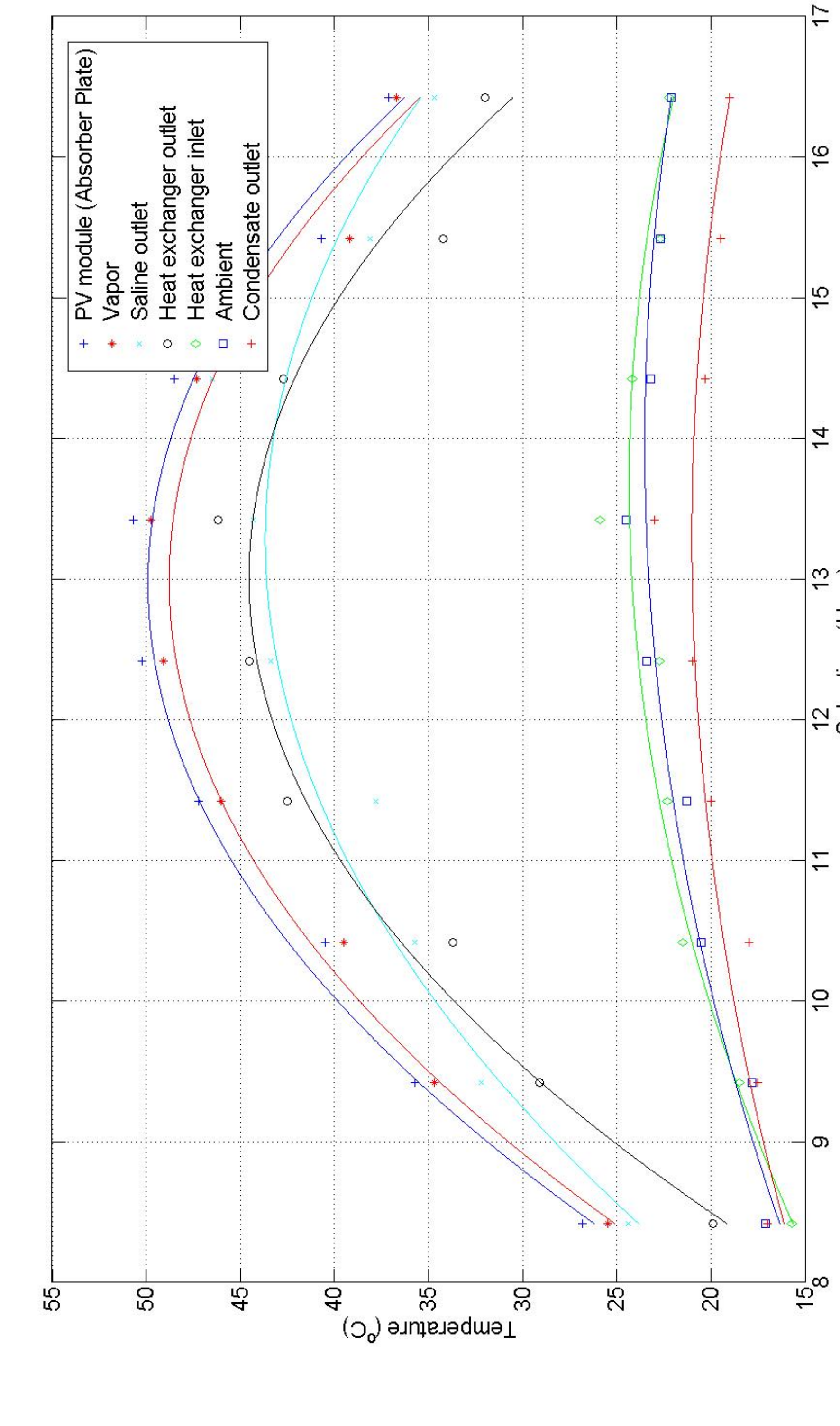


Figure 5-2: Temperature of still components without glazing versus time measured on 14/4/2011

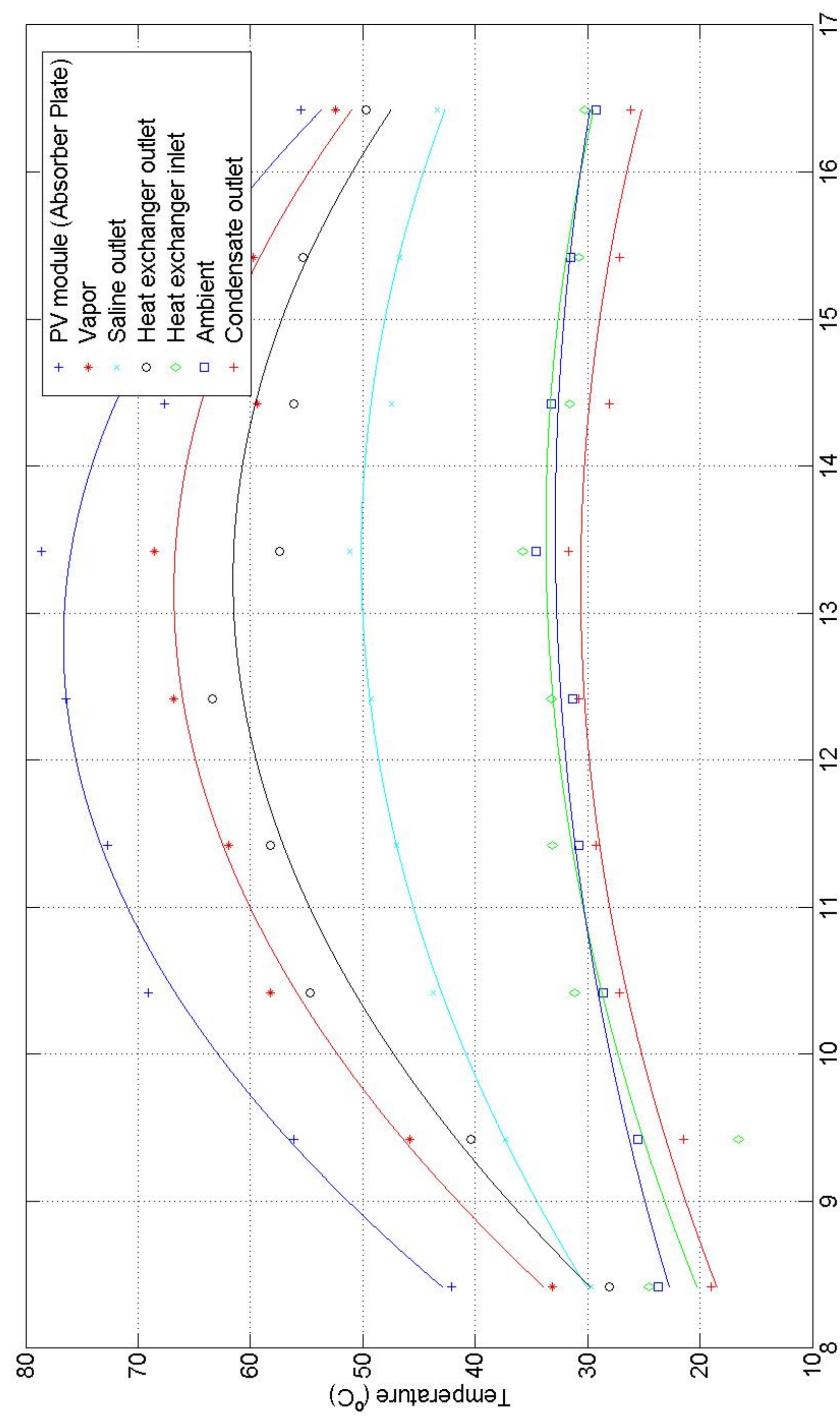


Figure 5-3: Temperature of still components with glazing versus time measured on 18/4/2011

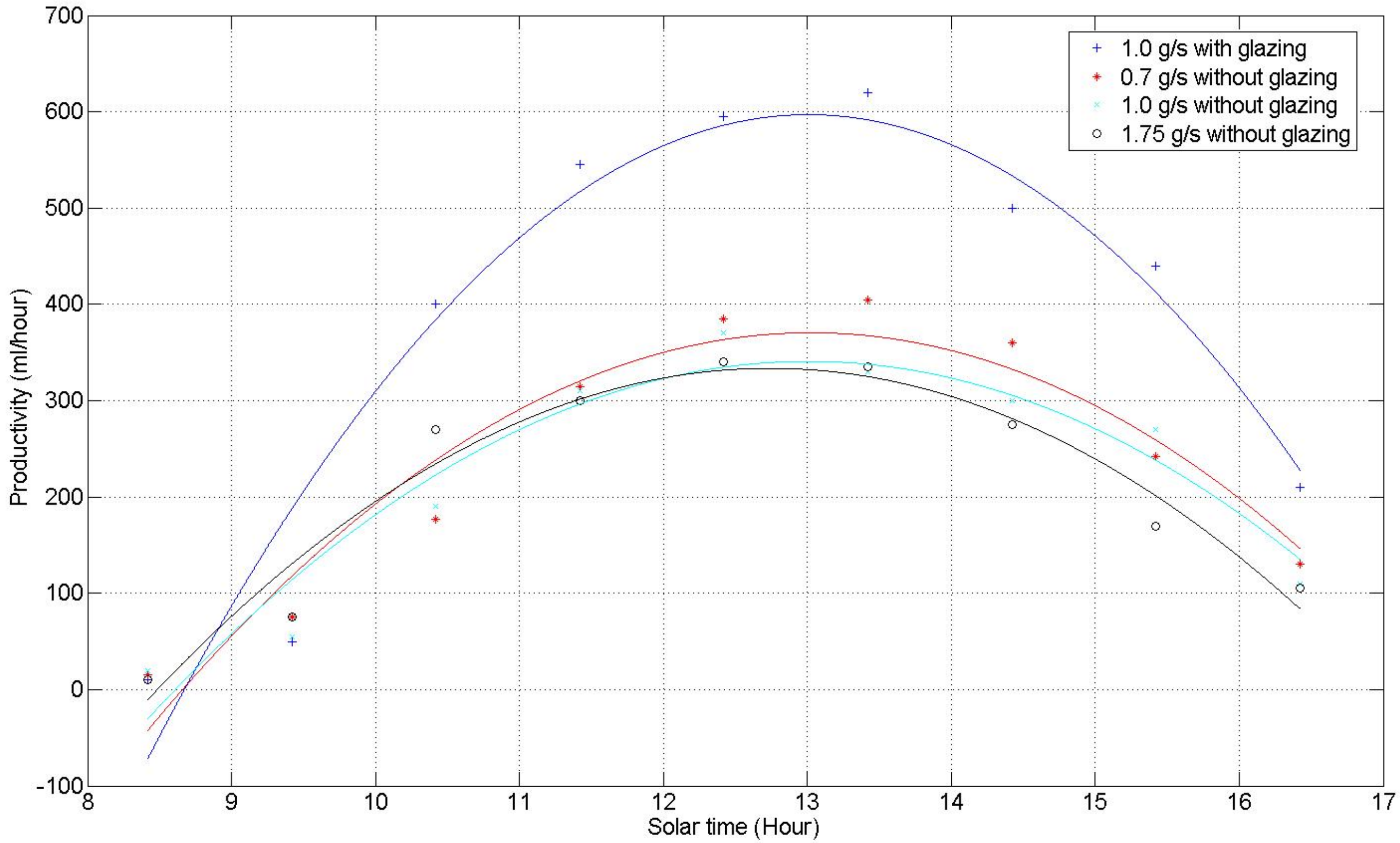


Figure 5-4: Productivity of still versus time over various flow rates

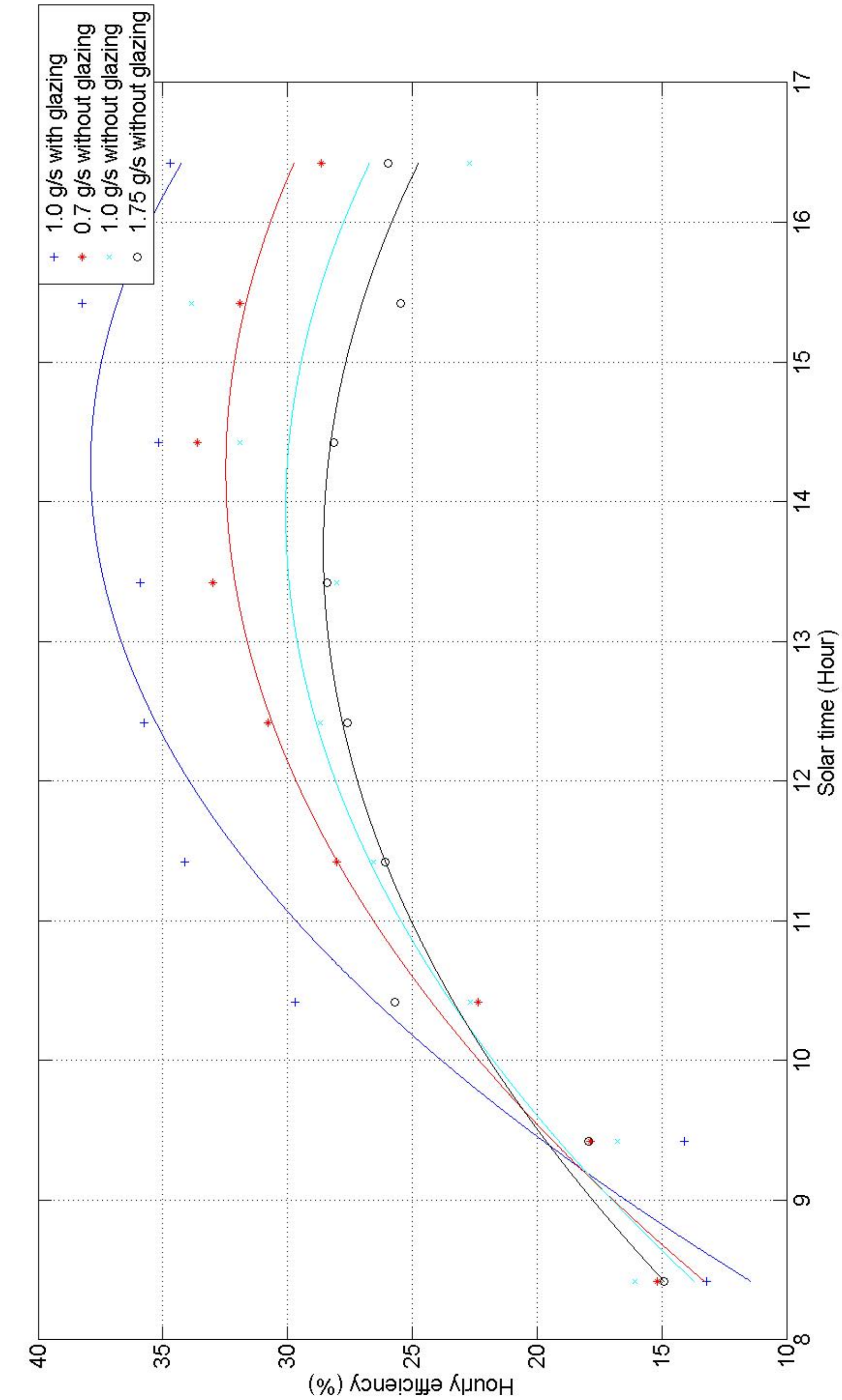


Figure 5-5: Efficiency of still versus time over various flow rates

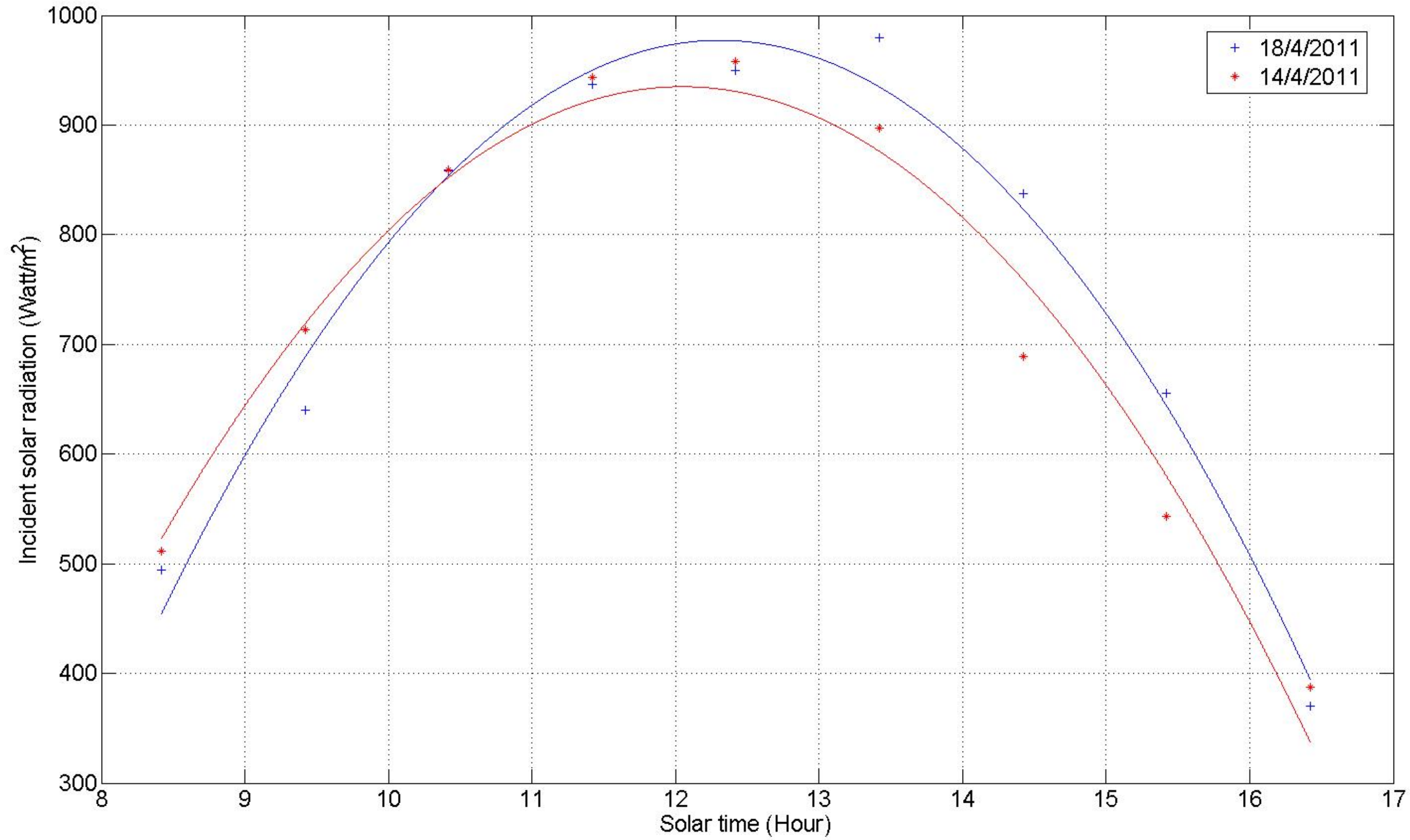


Figure 5-6: Solar radiation versus time over two days

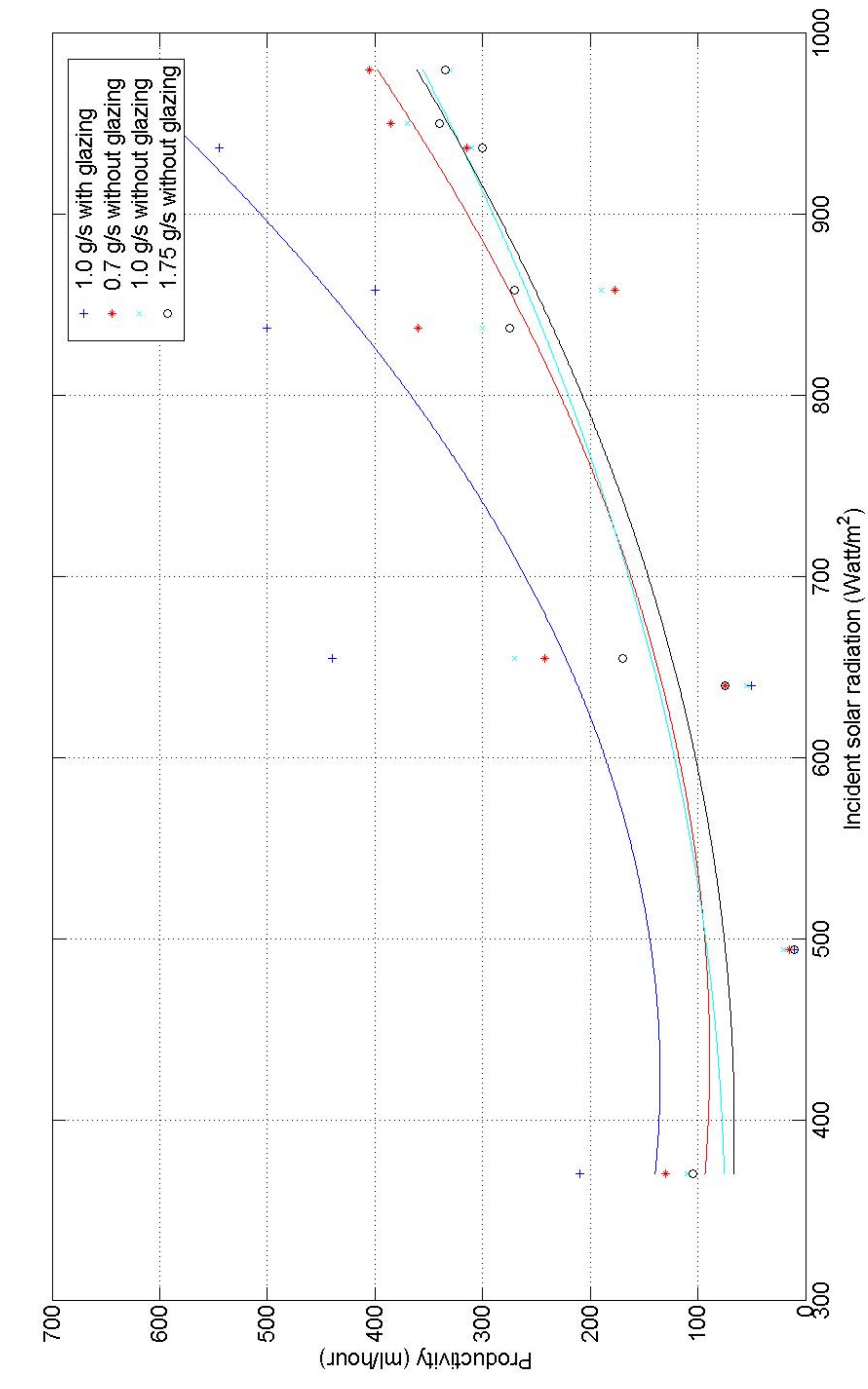


Figure 5-7: Productivity of still versus incident solar radiation over various flow rates

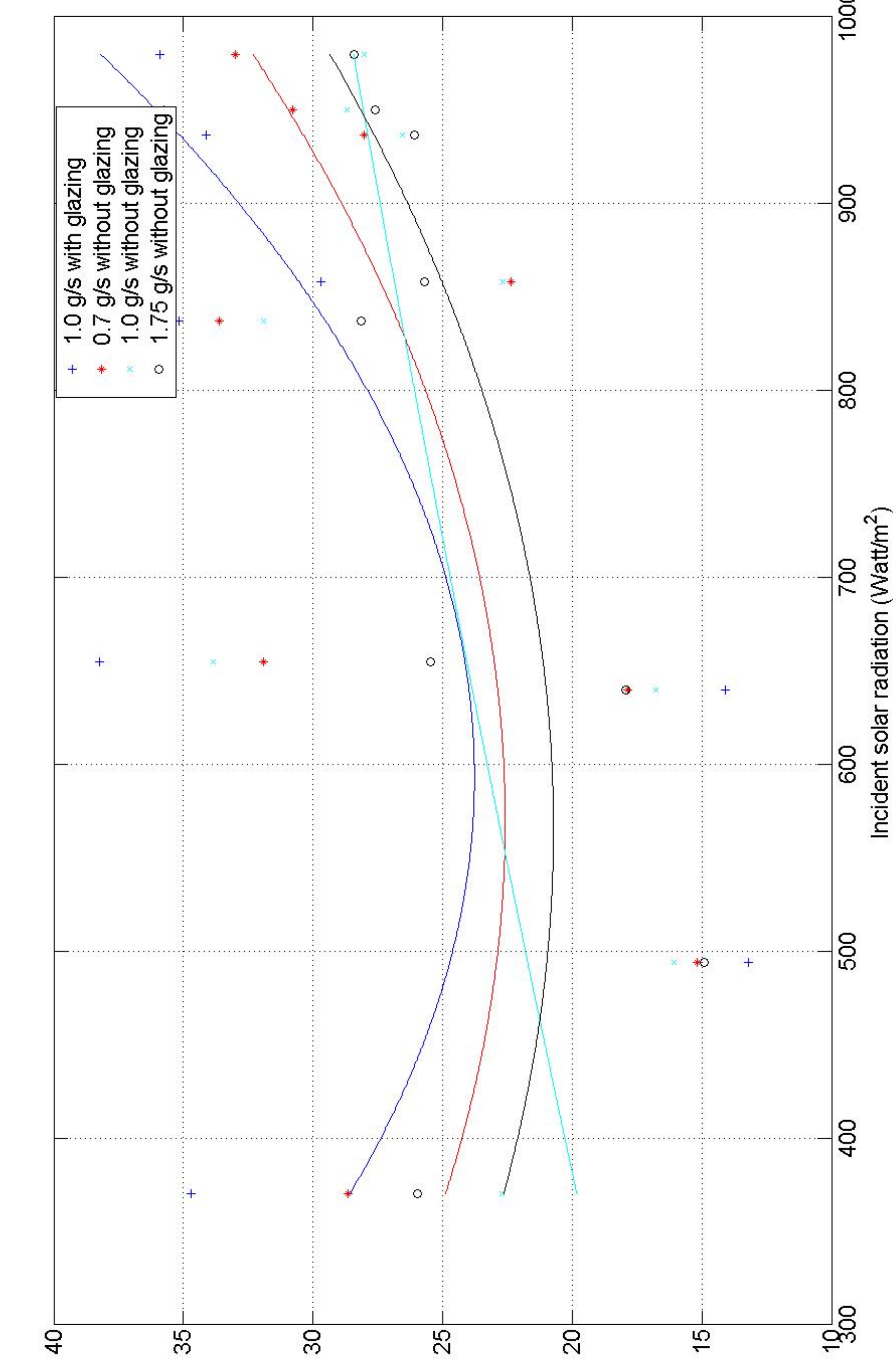


Figure 5-8: Efficiency of still versus incident solar radiation over various flow rates

5.1.2 Simulation Results:

The figures below were obtained after running the computer code written using MATLAB software. The simulation can predict the productivity while changing various input variables. The data obtained in the simulation is listed in the tables in Appendix B.

Figure 5-9 shows the electrical power output generated by the PV module with and without glazing.

Variables related to productivity:

1- Solar radiation:

   The productivity against radiation is shown in Figure 5-10 and the data obtained is listed in Appendix B. Also the efficiency against solar radiation is plotted in Figure 5-11.

2- Mass flow rate of the inlet saline water:

   The productivity and efficiency against time at different mass flow rates is shown in Figures 5-12 and 5-13 respectively and the data obtained is listed in table B-2.

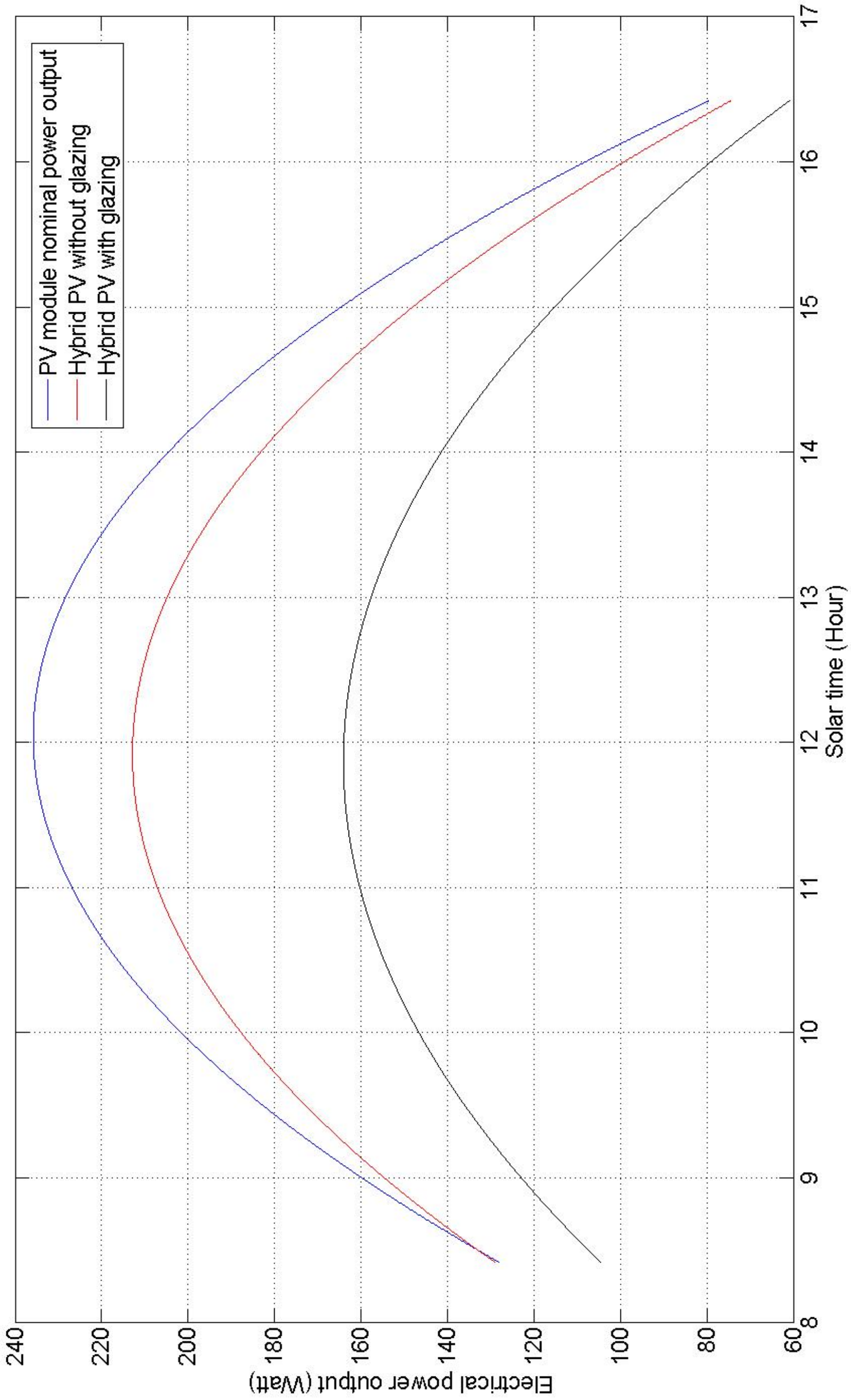


Figure 5-9: Electrical power output (Simulation)

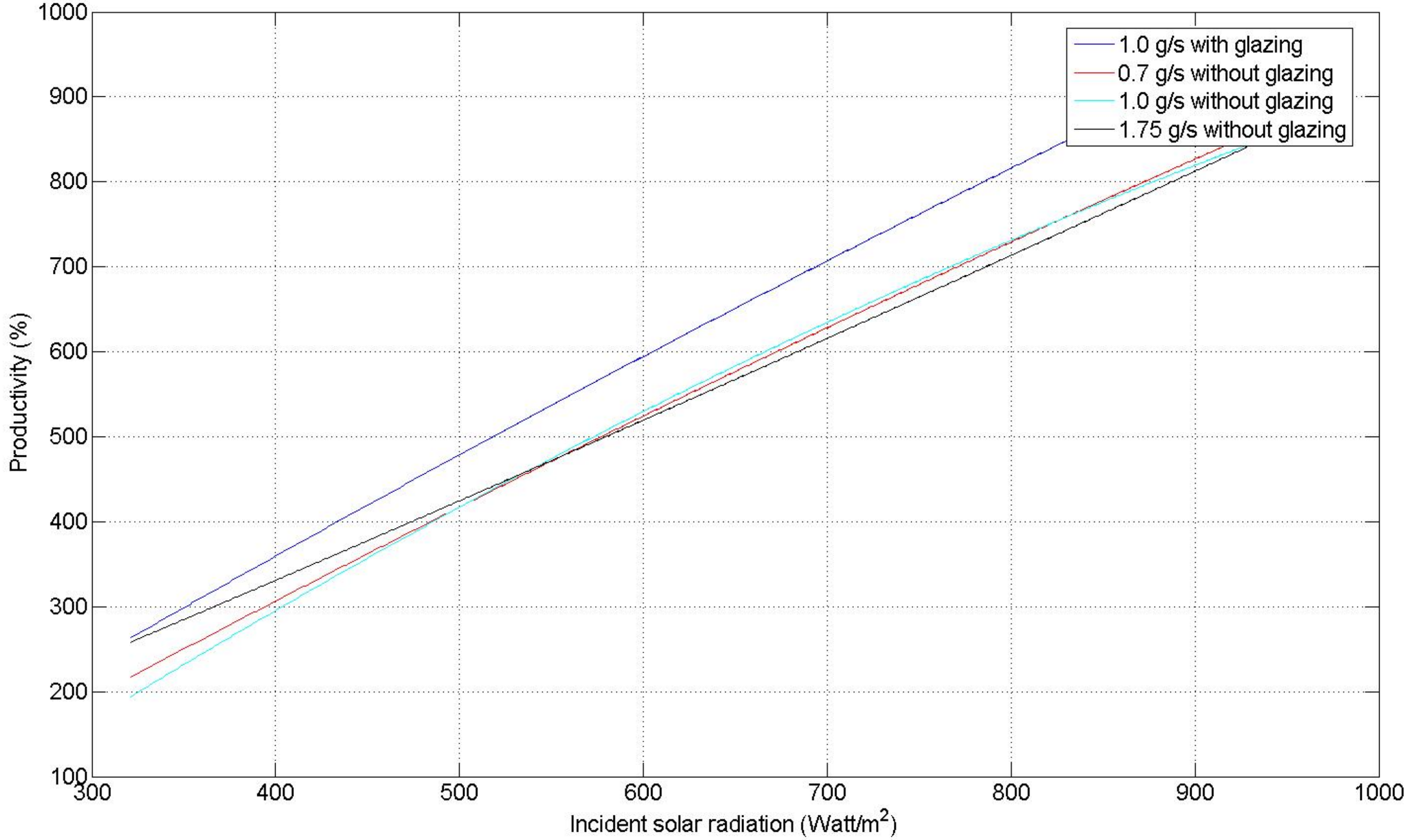


Figure 5-10: Productivity of still versus incident solar radiation over various flow rates

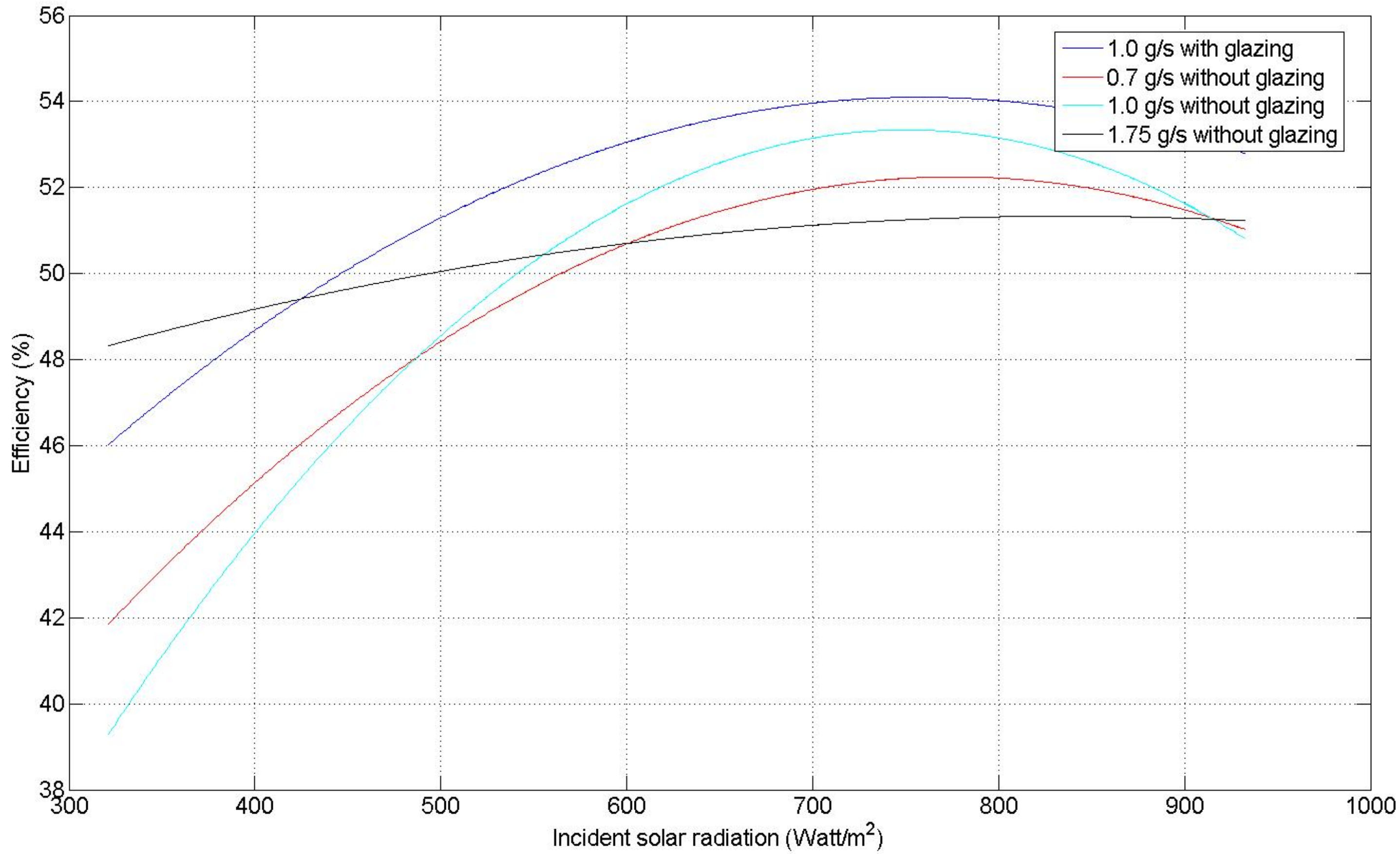


Figure 5-11: Efficiency of still versus incident solar radiation over various flow rates

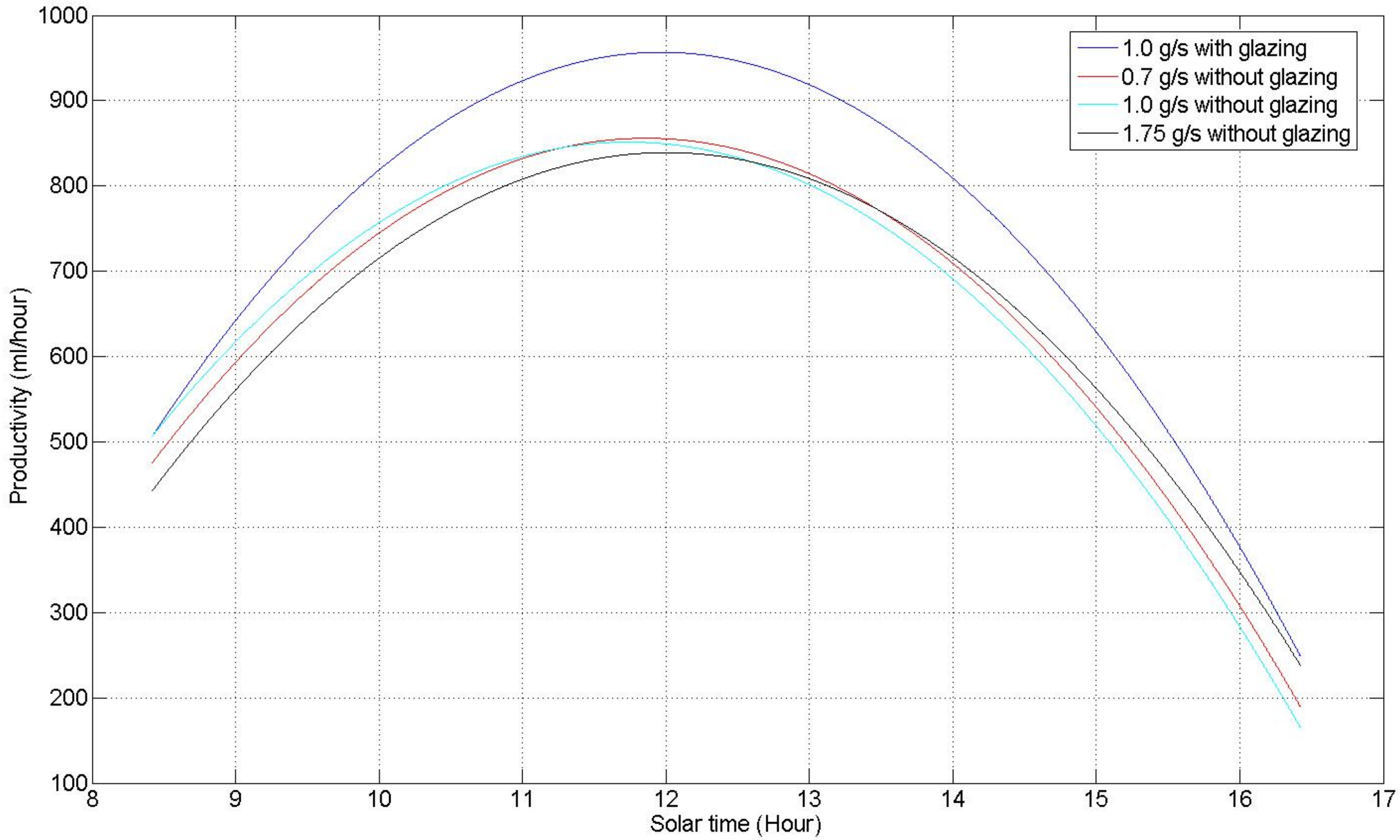


Figure 5-12: Productivity of still versus time over various flow rates

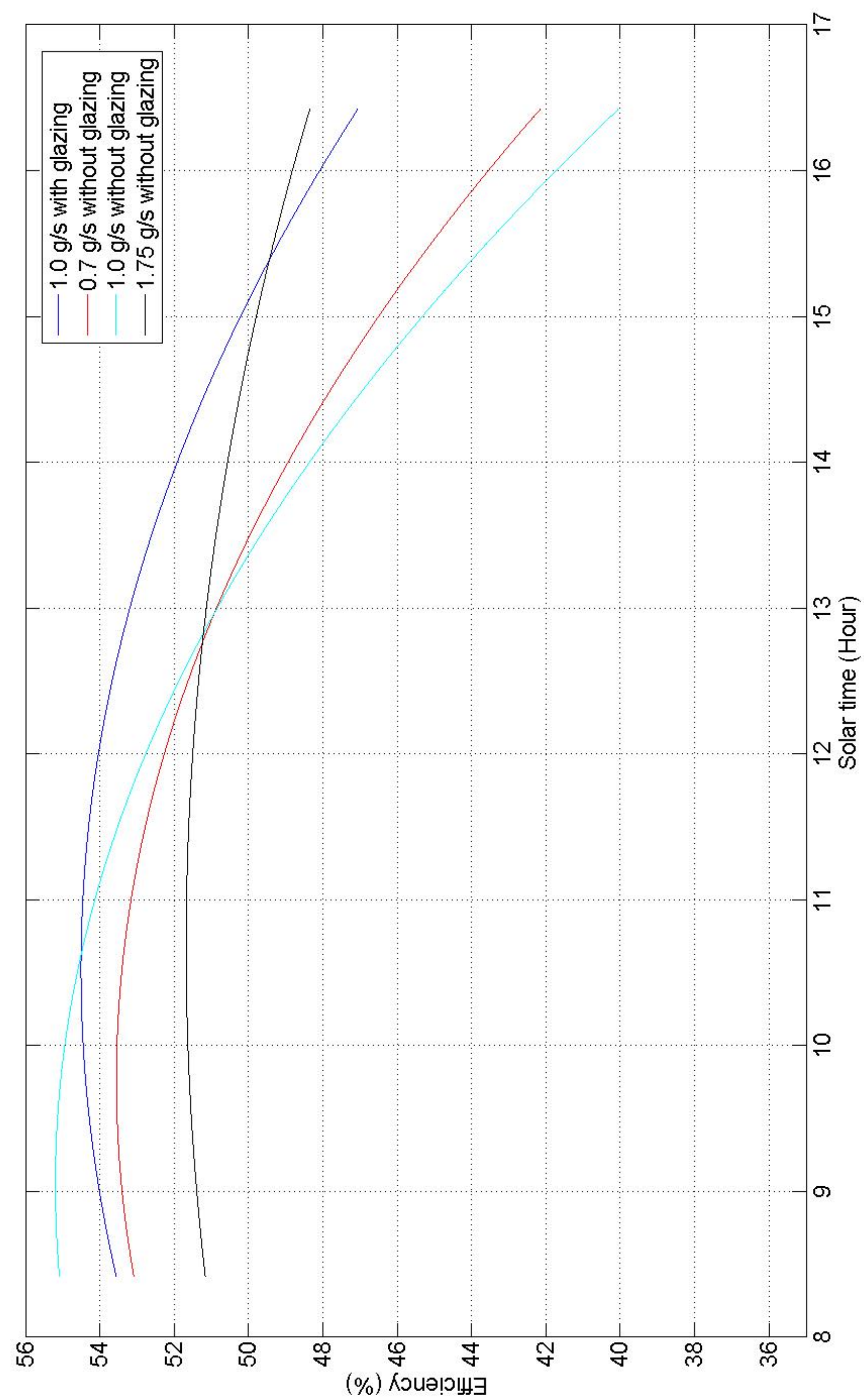


Figure 5-13: Efficiency of still versus time over various flow rates

5.1.3 Comparison Between Simulation and Experimental Results:

Simulation predicts the performance of the still by using some assumed temperatures. This makes it possible to compare the simulation and experimental results based on the following parameters:

- The electrical power output of the still.
- The condensate productivity of the still.
- The efficiency of the still.
- The instantaneous radiation on the still.

Temperatures measured on the 14th and the 18th of April were assumed in the simulation. On the 14th no galzing was used and on the 18th glazing was used. The results were listed in table B-. The experimental results for the same days were listed in Appendix A.

The electrical power output of the still was plotted in Figure 5-14 for both the experimental and simulation results and the nominal power output. The results were obtained by using glazing on the 18th and no glazing on the 14th.

The solar radiation against time is plotted in Figure 5-15 for both the experimental and theoretical values for the same day and under the same conditions.

The productivity against time is plotted in Figure 5-16 for the same days and under the same conditions.

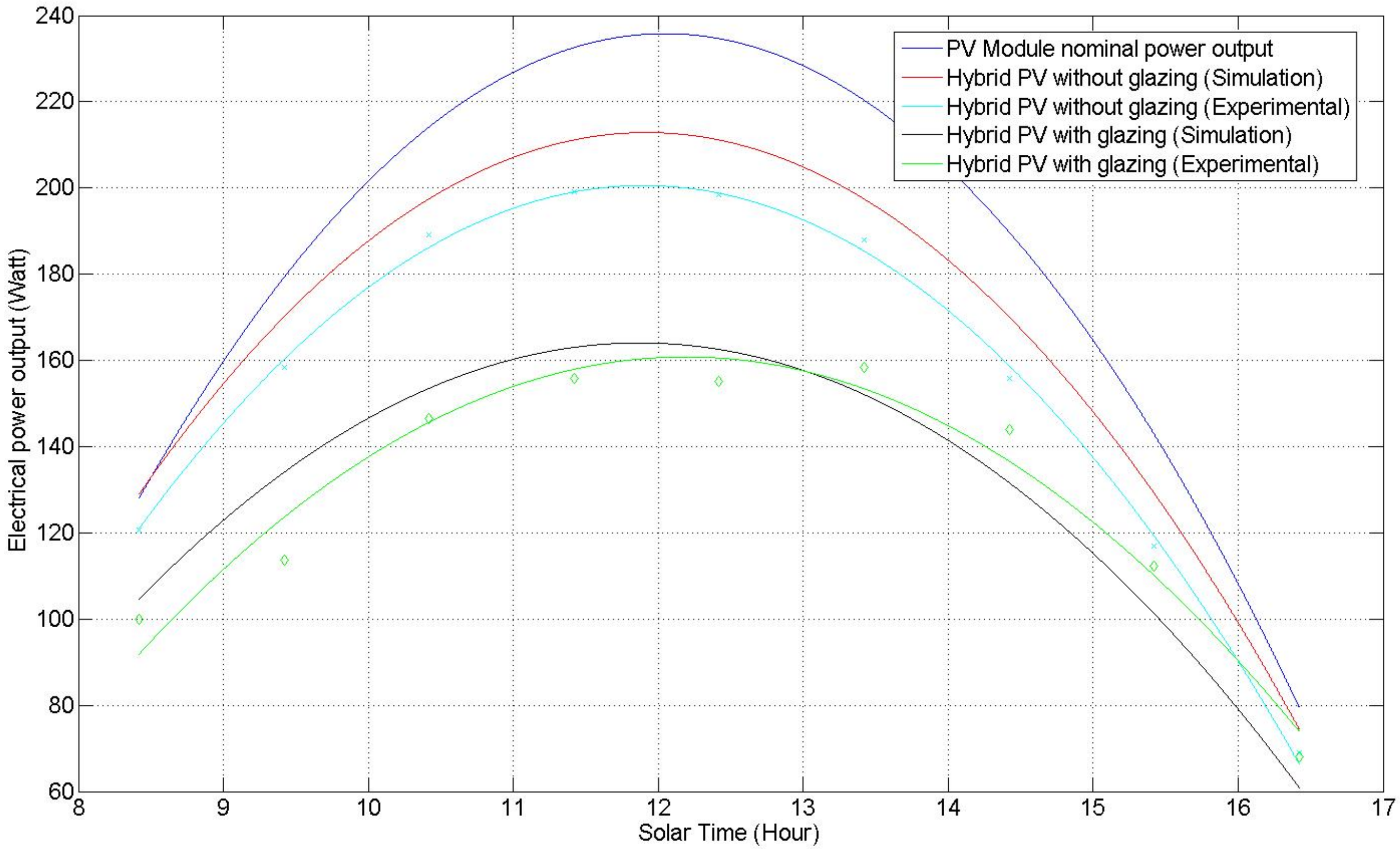


Figure 5-14: Electrical power output comparison (Simulation and Experimental)

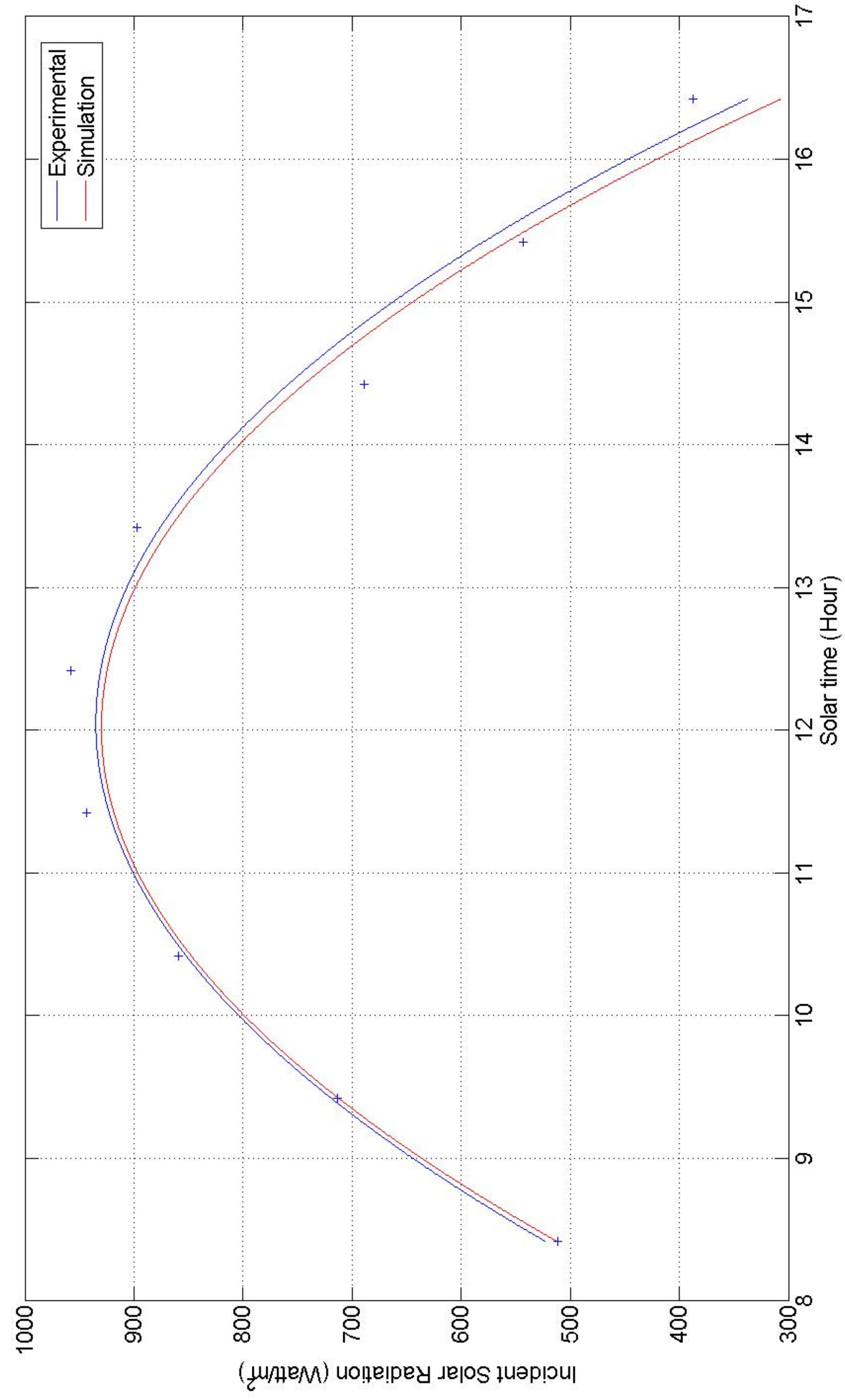


Figure 5-15: Solar radiation versus time comparison (Simulation and Experimental)

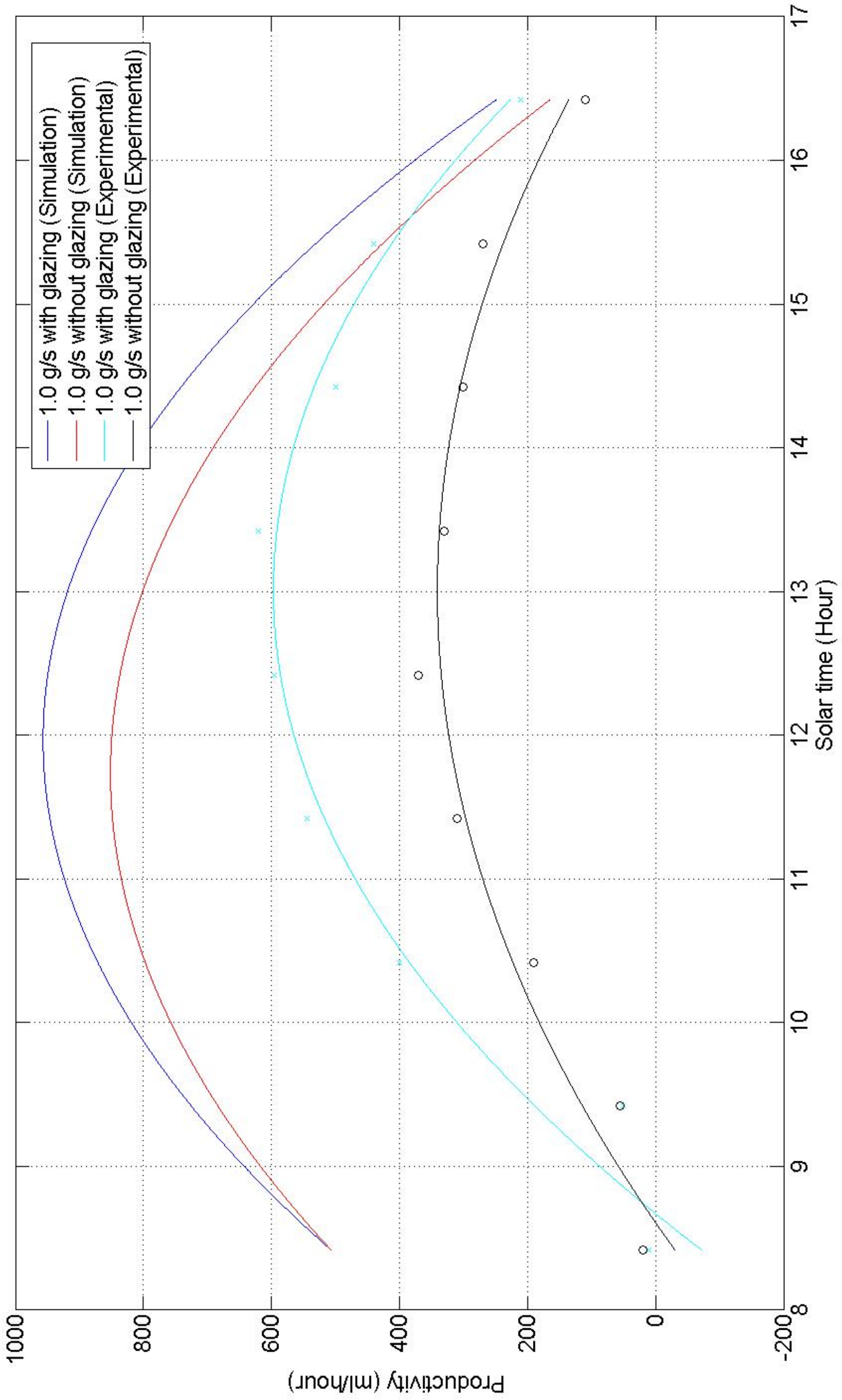


Figure 5-16: Productivity of still versus time for glazed and unglazed still (Simulation and Experimental)

5.2 Discussion:

5.2.1 Discussion of Experimental Results:

- Figure 5-1 shows that the power output is about 15% less when the still is covered with glazing. The reason is that a portion of the incident solar radiation is reflected by the glazing, another portion is absorbed by the glazing and later re-radiated to the environment. Another reason is that as the glazing is added to the device covering the PV module, the temperature of the module increases significantly and consequently its efficiency is dropped.

- Figures 5-2 and 5-3 show that the mean absorber plate temperature (The PV module) was the highest measured temperature followed by the vapor temperature, heat exchanger outlet temperature, saline outlet temperature, heat exchanger inlet temperaure, ambient temperature, and finally condensate temperature. This is due to the absorber plate being directly facing the incident solar radiation, so it gains a large amount of this energy. Among the output headers, the saline water has the highest temperature. This is due to this water flowing on the backside of the absorber plate, and thus it gains most of the energy. Due to the utilization of the latent heat of condensation in the heat exchanger, the condensate water has the lowest temperature among the output headers. All the temperatures were directly related to the incident solar radiation, so the maximum values of temperatures were obtained around solar noon. It is also clear that the temperatures were generally higher in the case of using glazing. This is due to the glazing preventing the loss of large quantities of energy.

- Figures 5-4 and 5-5 show the change in productivity and efficiency over the day for various flow rates. The higher values of productivity and efficiency were obtained at lower flow rates and with glazing present. This is due to the glazing preventing a lot of energy from escaping to the surroundings. Lower flow rates also help to increase the productivity and efficiency since with lower flow rates, water takes longer time to move down the back of the absorber plate and thus gives it more time to absorb energy and evaporate. Higher flow rates also help cool the absorber plate which decreases the amount of energy taken by the flowing water. The highest productivity was found to be 3.855 L/day in the presence of glazing and at a flow rate of 1 g/s. This is an improvement of 35% over the previous work. The peak efficiency was 34.35 % which was obtained at solar noon in the presence of glazing.

- The productivity and efficiency are directly related to the incident solar radiation as shown in Figures 5-7 and 5-8 . As the radiation increases, both the efficiency and the productivity increase since more solar radiation means more evaporation and thus the highest values of both parameters are obtained near solar noon.

- The salinity of the condensate water produced wasn’t affected much by the flow rate and the presence of glazing. The lowest salinty produced was 7.5 PPM (Part Per Million) around solar noon with glazing present at 1g/s flow rate.

- The losses from the solar still were minimized due to the use of the design and elaborate use of insulation and sealing materials to minimize the flow of energy from the still to the surroundings. The wooden frame, rubber, and silicon sealant prevent the loss of energy from the sides of the still. The high-resistance insulation material, rubber and silicon sealant prevent conduction heat transfer from the absorber plate to

the condensing compartment. The reason behind this design is essentially to maximize the temperature difference between the evaporation and condensation compartments.

5.2.2 Comparison With Previous Work:

Comparison between this work and the ones before it (Badran et al 2005) and (Sabra et al 2010) are listed in Tables 5-2 and 5-3 showing the concentrations, productivities, and efficiency. The PV-still function was not available in the previous work. It should also be noted that the area of the still used in this work is slightly larger than that in the previous work which helped raise the productivity, but should have no effect on the efficiency as the efficiency is calculated using equations 3.19 and 3.27 where the area is in the denominator which means its not a factor in that calculation.

Figures 5-17 through 5-19 represent a comparison between the current work and the previous work in 2005 and 2010 using three variables for the comparison. Figure 5-17 shows the salinity comparison between the current and the previous work while Figures 5-18 and 5-19 show the same comparison for productivity and efficiency respectively.

Table 5-2: Comparison between this work and previous work.

Water Type	Average Concentration, PPM			Average Productivty, L/Day		
	Previous work (2005)	Previous work (2010)	This work	Previous work (2005)	Previous work (2010)	This work
Intermediate water	3600	6330	550	5.12	16	0.5
Condensate water	257	50	40	1.8	2.45	2.75

Table 5-3: Comparison between this work and previous work at 1.0 g/s.

	Glazing	Condensate Productivity (ml/day)	Condensate Average Salinity (PPM)	Intermediate Productivty (ml/day)	Intermediate Average Salinity (PPM)	Daily Efficiency (%)	Average Power output (Watt)
Previous work (2005)	Glazed	2440	257	6120	3584	18.00	0
Previous work (2010)	Glazed	2728	50	10625	800.0	21.85	0
This Work	No Glazing	2105	57	140	817.0	26.57	155.0
This Work	Glazed	3855	20.44	165	545.0	34.35	134.2

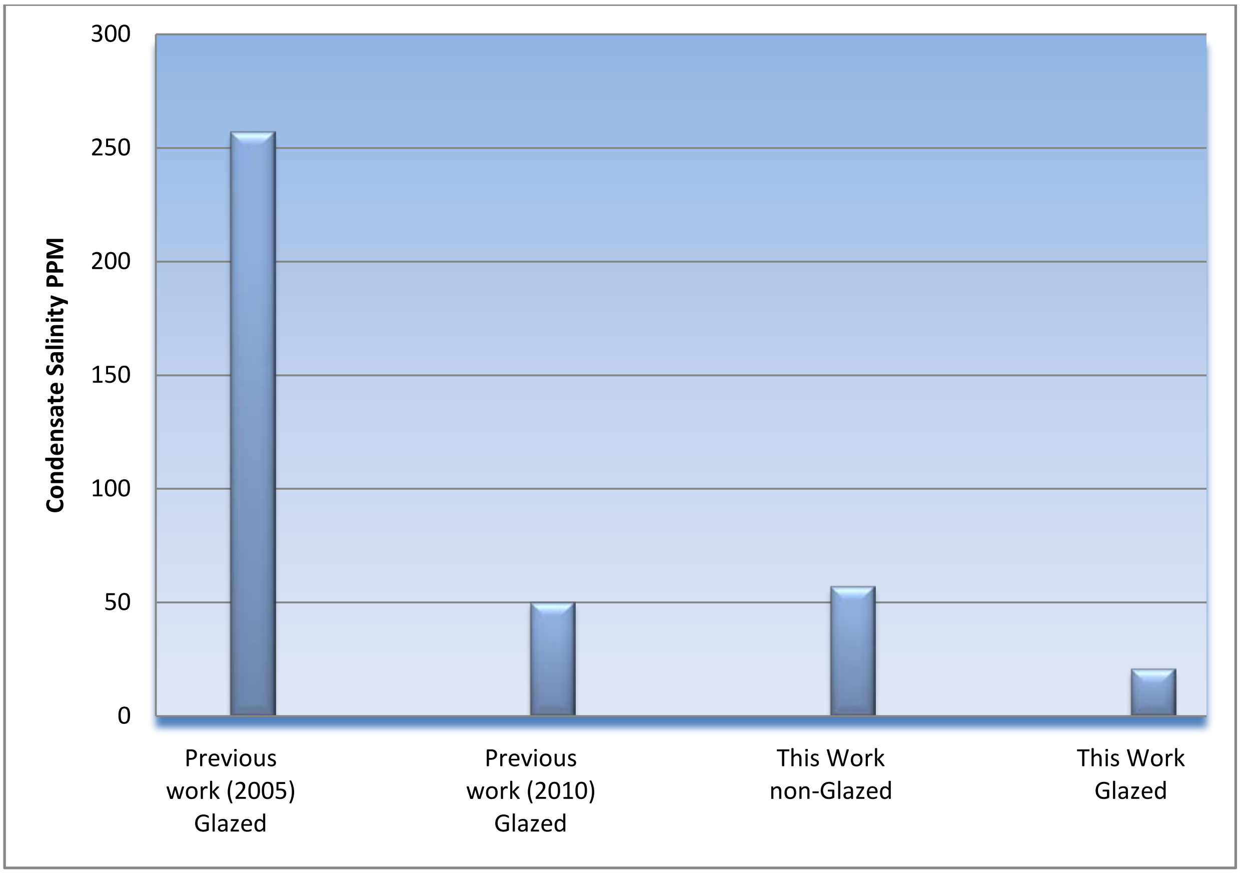


Figure 5-17: Salinity comparison with the previous work.

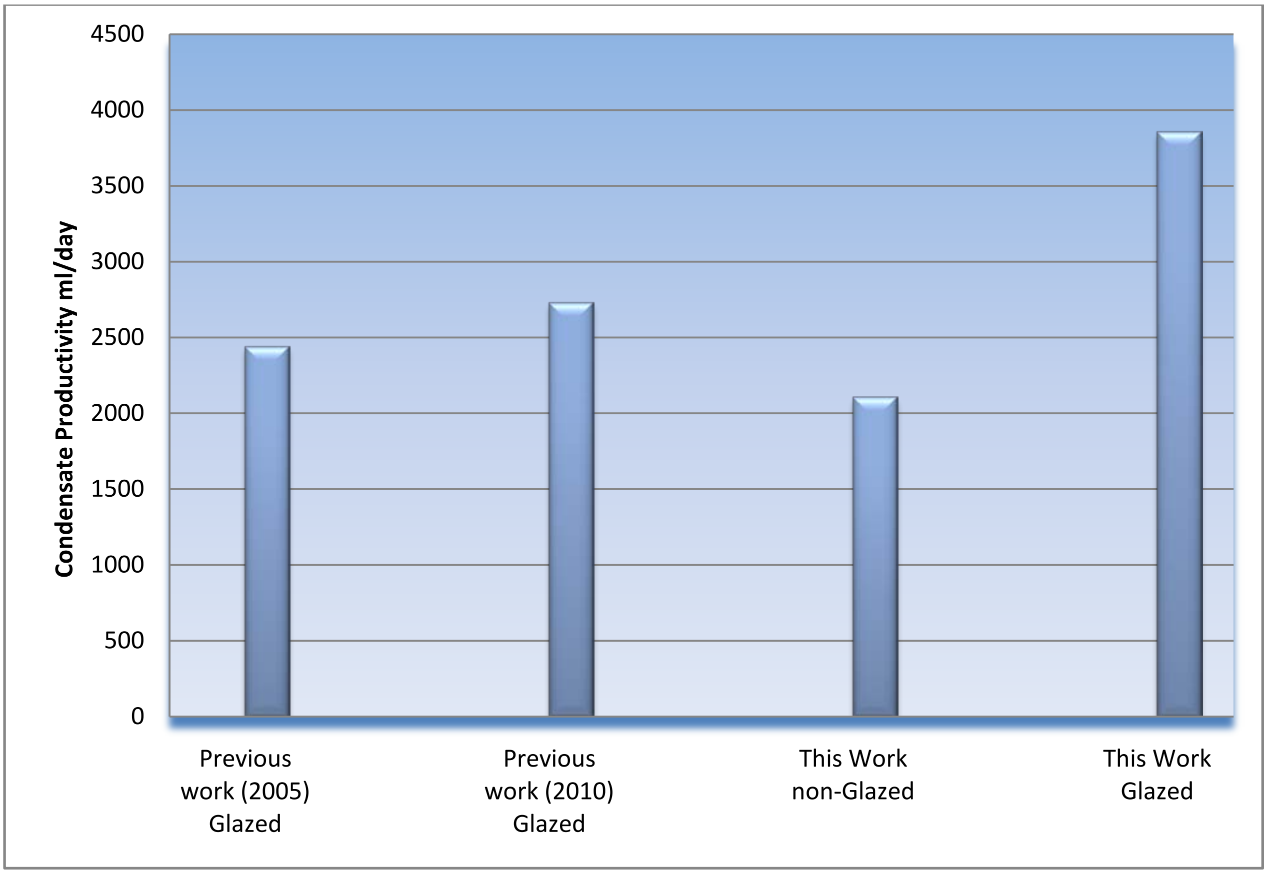


Figure 5-18: Productivity comparison with the previous work.

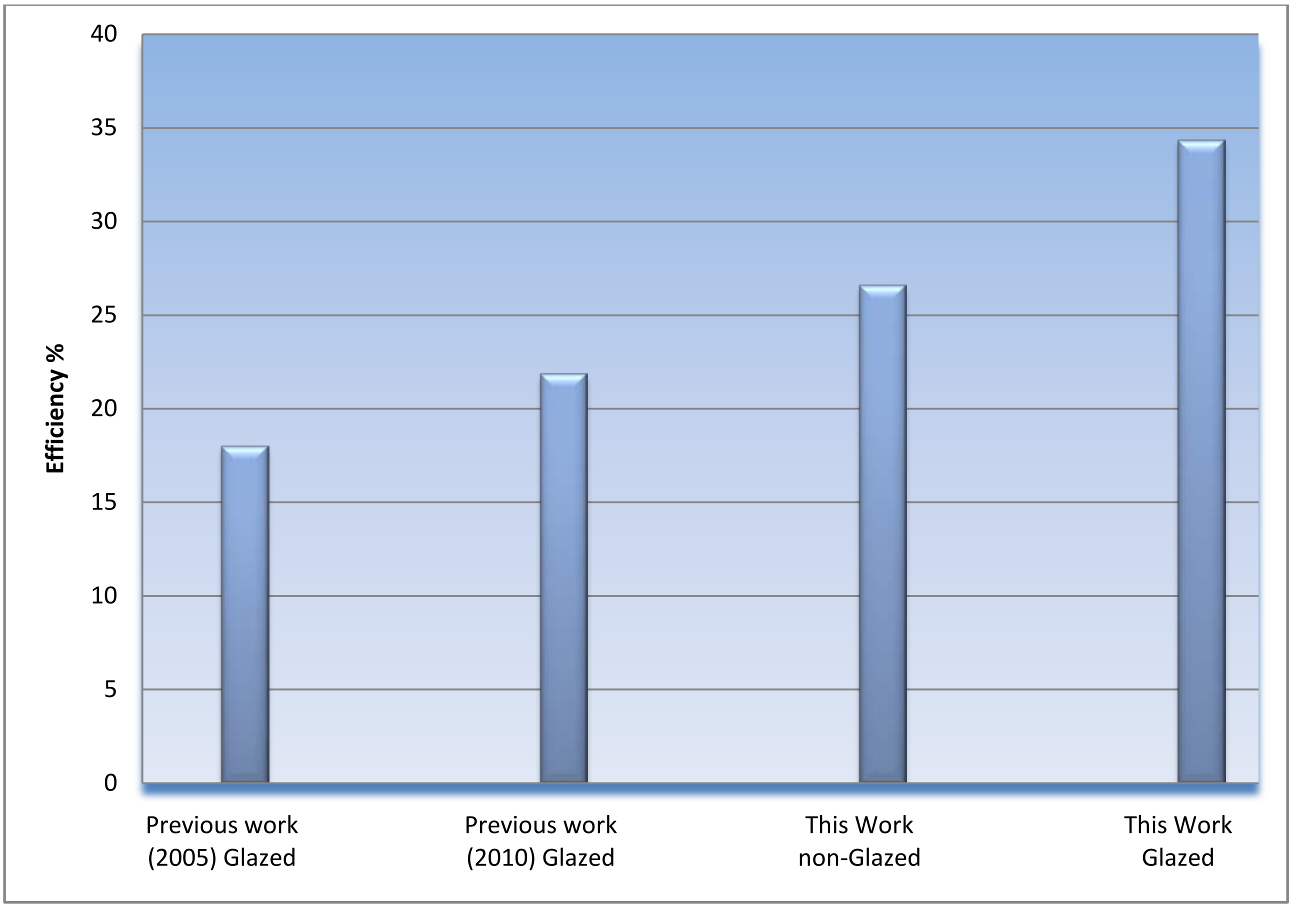


Figure 5-19: Efficiency comparison with the previous work.

5.2.3 Discussion of Simulation Results:

- Simulation results generally follow the same pattern of experimental results. This is due to assuming the temperature values obtained experimentally in the simulation. However, simulation results are generally higher than experimental results. This is due to some simplifications and assumptions used in the simulation such as; steady state operation, clear sky, constant solar irradiation over the time period within which the energy balance is made, and generally assuming perfect conditions. This is not the case for experimental results were dust, clouds, haze and non-steady state work to lower the performance from the predicted by simulation. Simulation predicts

performance of approximately 20 to 25% higher than the experimental results delivered which is to be expected when comparing theoretical work to experimental results.

- Figure 5-9 shows that there is a direct relationship between the incident solar radiation and the power output of the PV module as evidenced by the peak power obtained around solar noon when solar irradiation is maximum.

- Figures 5-10 and 5-11 show that there is a direct relationship between the productivty and efficiency against solar radiation. However, this relationship is not linear as solar irradiation has an effect on multiple parameters in the simulation including q_e and h_{fg}.

- Figures 5-12 and 5-13 show that better performance is achieved when the inlet water flow rate is lowered below 1g/s as this gives better productivity and efficiency. Also the highest productivity and efficiency achieved is at or around solar noon.

5.2.4 Comparison Between Simulation and Experimental Results:

- Figure 5-14 shows that the predicted electrical power output of the still was slightly higher than that of experimental results. This is due to the inability to measure the exact PV module temperature which was used to predict the power produced by the module as per equations 3.2 and 3.22. However, the experimental and simulation results both show that the addition of glazing drops the power output of the still by about 15 to 20%.

- Figure 5-15 shows that the solar radiation obtained from experimental results was slightly higher than that obtained from the simulation. This can be explained by the fact that the relationships used to predict the solar radiation assume clear sky model which is an ideal assumption. Those relationships do not take into account the altitude which can increase the incident solar radiation by about 15%. Also, experimental results express the actual weather, but simulation can't exactly do that. However, results obtained on a hot day with clear sky would result in slightly higher solar radiation than the simulation predicts.

- Referring to Figure 5-16, it can be seen that the productivity obtained from the simulation was higher than the experimental one. This is due to the fact that simulation follows perfect conditions, where during experimental work, there are many miscellaneaous losses that occur in the actual case that the simulation cannot follow or predict such as leakage. There is also the fact that the different variables under test experience small changes during an hour while the simulation assumes steady state operation. They were considered constants by taking their averages during the hour. This is close to the actual operation but not 100% accurate.

Chapter 6

Conclusions and Recommendations

6.1 Conclusions:

The idea of hybrid PV-Solar still combination was found reasonable. Utilizing the heat losses from a regular PV module to desalinate water was realized, simulated and experimented.

This combination probably could not have been possible without the use of the inverted trickle technique for water desalination. Using this technique, saline water trickle flows down the back of an absorber plater where it is heated up, evaporated and turned into three products: Saline outlet, Condensate, and a mixture of both, called intermediate.

Heat recovery was used to heat up the saline water feed by utilizing the heat given up by condensate.

- The maximum experimentally-obtained productivity of the still reached 3820 mL/day at 47° tilt angle at an inlet flow rate of 1g/s over the course of nine hours during the month of April. This represents an increase of 35% over previous work (Sabra et al 2010). The average productivity was around 2750 mL/day which is an increase of 12% over previous work and 53% over the one before it (Badran et al 2005).

- The maximum electric power produced while producing the maximum condensate production was 190 W, and the overall average power was 150 W. The maximum power obtained was 215 W, and the average power with glazing was 130 W. Without glazing the average power was 160 W.

- The productivity of the intermediate header decreased significantly from previous work dropping to around 0.5 L/day from 16 L/day, and 5.12 L/day from the previous work. This is due to the improved design of the solar trickle system that minimizes dripping for the sake of increasing the more-useful condensate productivity.

- The average daily efficiency of the still was increased to 30% compared to 20.8% in previous work (Sabra et al 2010). and 17.11% in a previous work (Badran et al 2005). This represents an increase of 44% and 75% respectively. This large increase in the efficiency is mainly due to adding a PV module to the design which gives electrical power output that raises the efficiency.

- The salinity of the condensate averages at around 40 PPM with the minimum value obtained being 7.5 PPM. This is significantly lower than in previous work with 257 PPM and 50 PPM average salinity of condensate. This is an improvement of 525% and 25% respectively. This water can be mixed with saline or intermediate water to produce drinking water of around 100 to 150 PPM (Badran et al 2005) and (Sabra et al 2010).

- The temperature difference between the condensation compartement and evaporation compartement was maximized by using highly insulating materials, including a low conductivity polyeurethane, silicon sealant, and thick rubber strips. This improved both the evaporation and condensation processes. The use of a wooden frame decreased the losses from the edges and thus increased the temperature in the evaporation compartment which increased the efficiency.

- To get optimum year-round performance in Amman, it is preferred to use a tilt angle of 32°. A 47° tilt angle is preferred during winter season and 17° for summer operation. In this work, winter operation was assumed and thus a tilt angle of 47° was used.

- The productivity and efficiency of the still decreases as the inlet flow rate increases.

- The uncertainty in evaluating the efficiency was ±0.16%.

6.2 Recommendations:

- Use different flow rates than the ones used in this work to get a more comprehensive study on the effect of flow rate on productivity and efficiency. This can be done by using flow rates higher than 1.75 g/s and lower than 0.75 g/s which were the upper and lower limits of flow rate used in this work.

- Obtain experimental results for various tilt angles during various seasons and during cloudy and hazy operation to see if the system performs well under little or no sun conditions.

- Use the output saline water, which is at a high temperature as an input to the system and study if this affects performance. This is done as a second heat recovery stage.

- Leakage and insulation were not a large problem during this work, but an improvement could be made by adding another insulation board and a thicker layer of insulation to the sides and study the difference this would make.

- Use double glazing instead of a single glazing and study the effect this second layer of glass has on the power output of the PV module and the condensate productivity.

- Employing a booster diffuse reflector to the system and studying the performance increase it would generate.

- Using a different design of the inlet header in order to allow for better distribution of water over the jute and wire screen. In this work, most of the water was flowing around the middle of the PV module's back. This is due to the very low flow rate which doesn't allow for better distribution of the flow, so a new design of the inlet header is needed to force the water to flow all over the jute

while still maintaining a low flow rate to make sure the thermal mass of the water is low to allow evaporation.

- Using different types of water as supply. In this work only tap water was used as supply. In future work, brackish and sea water can be used to study the performance of the system when using water with higher salinity.

- This work was mostly a study from an energy perspective. A more comprehensive study employing both energy and exergy analysis is needed.

References

Badran, A., Assaf L., Kayed k., Ghaith F., and Hammash M. (2005) "Simulation and experimental study for an inverted trickle solar still". **Desalination**, 164, 77-85.

Bakker, M., Zondag H., Elswijk M., Strootman K., and Jong, M. (2005) "Performance and costs of a roof-sized PV/thermal array combined with a ground coupled heat pump". **Solar Energy**, 78, 331–339.

Cengel, Y. and Boles, M. (2007), **Thermodynamics an Engineering Approach** (SI units), McGraw-Hill Inc, Sixth Edition.

Chow, T., He W., and Ji, J. (2006) "Hybrid photovoltaic-thermosyphon water heating system for residential application". **Solar Energy**, 80, 298–306.

Chow, T., Pei G., Fong K., Lin Z., Chan A., and Ji, J. (2009) "Energy and exergy analysis of photovoltaic–thermal collector with and without glass cover". **Applied Energy** 86 310–316.

Crowe, C., Elger, D., and Roberson, J. (2005), **Engineering Fluid Mechanics**, John Wiley and sons, Inc, Eighth edition.

Culp, Archie, W. (1991), **Principles of Energy Conversion**, McGraw-Hill Inc, Second edition.

Duffie, J., Beckman, W. (2006), **Solar Engineering of Thermal Processes**, John Wiley and sons Inc, Third edition.

Energy Savers, Polyurethane Insulation Material webage, link [**http://www.energysavers.gov/your_home/insulation_airsealing/index.cfm/mytopic=11600**]. Last accessed on April 24th, 2011.

Fraisse, G., Menezo, C., and Johannes, K. (2007) "Energy performance of water hybrid PV/T collectors applied to combisystems of Direct Solar Floor type" **Solar Energy**, 81, 1426–1438.

Garg, H., and Agarwal, K. (1995) "Some aspects of a PV/T collector/forced circulation flat plate solar water heater with solar cells". **Energy Convers. Mgmt** 36, No. 2, pp. 87-99.

Incropera, F., Dewitt, D., Bergman, T., and Lavine, A. (2007), **Fundamentals of Heat and Mass Transfer**. John Wiley and sons Inc, Sixth edition.

PS-M60H-250W Mono-Crystalline Solar Panel product sheet, published by Philadelphia Solar, Jordan. Available online via link [**http://www.philadelphia-solar.com/datasheets/PS-M60H%20-%20250watt.pdf**], Last accessed on April 24th, 2011.

Press Releases, SunPower Announces New World Record Solar Cell Efficiency webpage, link [**http://us.sunpowercorp.com/about/newsroom/press-releases/?relID=482133**] Last accessed on April 24th, 2011.

Sabra, Ma., Sabra, Mo., Barkawi, A., Abdullah, K. (2011), **Effect of Heat Transfer Enhancement on Solar Desalination**, BSc. Graduation project, Faculty of Engineering and Technology, Mechanical Engineering Department, University of Jordan.

Saitoh, H., Hamada, Y., Kubota, H., Nakamura, M., Ochifuji, K., Yokoyama, S., and Nagano, K. (2003) "Field experiments and analysis on a hybrid solar collector" **Applied Thermal Engineering**, 23, 2089–2105.

Tiwari, A., and Sodha, M.S. (2006) "Performance evaluation of solar PV/T system:An experimental validation" **Solar Energy**, 80, 751–759.

Tripanagnostopoulos, Y., Nousia, Th., Souliotis, M., and Yianoulis, P., (2002) "Hybrid Photovoltaic/Solar Thermal Systems". **Solar Energy**, 72, 217-234.

UD-led team sets solar cell record, joins DuPont on $100 million project webpage, link [**http://www.udel.edu/PR/UDaily/2008/jul/solar072307.html**], Last accessed on April 24th, 2011.

Wolf, M. (1976) "Performance analysis of combined heating and photovoltaic power systems for residences". **Energy Convers**, 16, 79–90.

Zakharchenko, R., Licea-Jimenez, L., Perez-Garcia, S.A., Vorobievb, P., Dehesa-Carrascoc, U., Perez-Roblesa, J.F., Gonzalez-Hernandeza, J., and Vorobieva, Yu. (2004) "Photovoltaic solar panel for a hybrid PV/thermal system". **Solar Energy Materials & Solar Cells**, 82, 253–261.

Zondag, H., Vries D., Helden W., Zolingen R., and Steenhoven A., (2003) "The Thermal and Electrical yield of a PV-Thermal Collector". **Solar Energy**, 72, 113–128.

Zondag, H., Vries D., Helden W., Zolingen R., and Steenhoven A., (2003) "The yield of different combined PV-thermal collector designs". **Solar Energy**, 74, 253–269.

Zondag, H. (2008) "Flat-plate PV-Thermal collectors and systems: A review". **Renewable and Sustainable Energy Reviews**, 12, 891–959.

Appendix A: Experimental Results

Date: 12/4/2010
Flow Rate: 1.0mL/sec
Without glazing and with Natural Convection

Tap Water
Slope=45°
Condition: Clear Sky

Table A.1: Tap Water, 1.0mL/sec, with natural convection without glazing.

Time	**8-9**	**9-10**	**10-11**	**11-12**	**12-13**	**13-14**	**14-15**	**15-16**	**16-17**	**Sum**
$\dot{m}_c$, ml/hr	20	125	245	310	280	245	190	140	120	1775
$\dot{m}_s$, ml/hr	3390	3305	3345	3245	3290	3328	3375	3420	3455	30153
$\dot{m}_I$, ml/hr	190	170	10	45	30	27	35	40	25	572
G, W/m^2	523	733	871	947	972	935	830	603	377	
V, Volt	35.05	33.82	33.47	33.3	33.22	33.54	33.7	34.16	34.37	
I, mA	3.53	4.88	5.85	6.3	6.49	5.94	5.4	3.83	2.44	
P, Watt	123.73	165.04	195.80	209.79	215.60	199.23	181.98	130.83	83.86	
T_p, C°	25.5	37.2	40.6	40.8	40.9	49.1	45.3	42.3	35.4	
T_a, C°	17.2	17.5	20.3	21.4	23.6	23.8	22.9	22.6	21.6	
T_v, C°	24.3	35.8	45.5	47.2	48.3	48.5	48.3	40.1	35.2	
T_{Cond}, C°	19	20	21.5	22	21	21.2	21	20	20	
T_{Inter}, C°	21	20	25	24	25	22	22	21	21	
T_s, C°	23.2	31	34	36.1	39.7	40.4	40.3	37.6	32.3	
$T_{ex,i}$, C°	14.3	15.1	20.5	23.1	22.2	24.9	23.7	22.3	20	
$T_{ex,o}$, C°	21.7	25.5	39.7	40.4	42.6	43.5	39.3	37.3	30.5	
Saline, PPM	870	786	825	861	864	840	840	780	750	
Inter, PPM	723	729	756	753	825	819	813	729	723	
Cond, PPM	285	243	156	111	72	50	41.7	28.5	33.9	
Feed, PPM	750	750	750	750	750	750	750	750	750	
h_{fg}, kJ/kg	2456.2	2453.8	2450.2	2449	2451.4	2450.9	2451.4	2453.8	2453.8	
$\eta_{Hourly,Total}$ (%)	16.03	20.84	25.41	27.11	25.51	23.89	22.90	22.90	26.82	
η_{Daily} (%)	**24.397**									

Date: 14/4/2010
Flow Rate: 1mL/sec
Without glazing and with Natural Convection

Tap Water
Slope=45°
Condition: Clear Sky

Table A.2: Tap Water, 1.0mL/sec, with natural convection without glazing.

Time	8-9	9-10	10-11	11-12	12-13	13-14	14-15	15-16	16-17	Sum
$\dot{m}_c$, ml/hr	20	55	190	310	370	330	300	270	110	2105
$\dot{m}_s$, ml/hr	3570	3540	3400	3265	3210	3250	3275	3315	3480	30305
$\dot{m}_I$, ml/hr	10	5	10	25	20	20	25	15	10	140
G, W/m^2	511	713	859	943	958	897	689	543	387	
V, Volt	34.7	33.71	33.02	32.8	32.2	32	32.6	33.2	33.64	
I, mA	3.48	4.7	5.73	6.07	6.16	5.87	4.78	3.52	2.05	
P, Watt	120.76	158.44	189.20	199.10	198.35	187.84	155.83	116.86	68.96	
T_p, C°	26.8	35.7	40.5	47.2	50.2	50.7	48.5	40.7	37.1	
T_a, C°	17.1	17.8	20.5	21.3	23.4	24.5	23.2	22.7	22.1	
T_v, C°	25.5	34.7	39.5	46	49.1	49.77	47.3	39.2	36.7	
T_{Cond}, C°	17	17.5	18	20	21	23	20.3	19.5	19	
T_{Inter}, C°	21	22	22.6	23	23.4	24	22	21	20	
T_s, C°	24.4	32.2	35.7	37.8	43.4	44.3	46.5	38.1	34.7	
$T_{ex,i}$, C°	15.7	18.5	21.5	22.3	22.75	25.9	24.2	22.7	22.2	
$T_{ex,o}$, C°	19.9	29.1	33.7	42.5	44.5	46.2	42.7	34.2	32	
Saline, PPM	890	921	1052	1077	1167	950	930	780	770	
Inter, PPM	780	850	950	960	965	800	780	650	620	
Cond, PPM	300	240	88	61	49	35	37	45	72	
Feed, PPM	860	850	850	850	780	742	730	705	700	
h_{fg}, kJ/kg	2461	2459.8	2458.6	2453.8	2451.4	2446.8	2453.1	2455	2456.2	
$\eta_{Hourly,Total}$ (%)	16.06	16.78	22.66	26.56	28.69	28.04	31.91	33.83	22.71	
η_{Daily} (%)	26.571									

Date: 15/4/2010
Flow Rate: 1.75mL/sec
Without glazing and with Natural Convection

Tap Water
Slope=45°
Condition: Clear Sky

Table A.3: Tap Water, 1.75mL/sec, with natural convection without glazing.

Time	8-9	9-10	10-11	11-12	12-13	13-14	14-15	15-16	16-17	Sum
$\dot{m}_c$, ml/hr	10	75	270	300	340	335	275	170	105	1965
$\dot{m}_s$, ml/hr	6275	6210	6010	5980	5935	5945	6005	6115	6175	54650
$\dot{m}_I$, ml/hr	15	15	20	20	25	20	20	15	20	170
G, W/m^2	543	737	903	951	971	901	773	584	357	
V, Volt	34.02	33.32	32.66	32.2	31.2	32.98	33.4	33.8	34.14	
I, mA	3.70	4.97	6.03	6.31	6.69	5.84	5.07	3.79	2.35	
P, Watt	125.87	165.60	196.94	203.18	208.73	192.60	169.34	128.10	80.23	
T_p, C°	31.47	39.1	47.9	48.7	49.2	49.7	44.1	39.2	30.5	
T_a, C°	19.7	20.5	22.1	24.5	24.3	25.3	24.5	23.4	22.1	
T_v, C°	28.8	37.3	43.5	45.1	46.3	45.7	40.7	37.7	31.1	
T_{Cond}, C°	19.1	20	23	25	27	25.7	23	21.5	17	
T_{Inter}, C°	20	21	25	30	31	29	27	25	24	
T_s, C°	26.7	34.3	44.5	43.7	44.5	45.2	41.3	37.2	31.1	
$T_{ex,i}$, C°	18.72	19.1	20.9	22.2	21.7	24.1	24.8	24.5	22.2	
$T_{ex,o}$, C°	22.8	29.8	35.9	37.9	40.1	38.7	34.2	31.5	26	
Saline, PPM	595	655	630	655	625	590	570	557	570	
Inter, PPM	500	635	600	550	520	510	500	480	475	
Cond, PPM	107	157	43	37	32.5	37.2	33.5	27.5	43	
Feed, PPM	575	650	640	640	600	600	600	600	600	
h_{fg}, kJ/kg	2456	2453.8	2446.8	2442.4	2438	2440.9	2446.8	2450.2	2461	
$\eta_{Hourly,Total}$ (%)	14.92	17.95	25.71	26.1	27.59	28.43	28.13	25.48	25.99	
η_{Daily} (%)	25.48									

Date: 16/4/2010
Flow Rate: 0.75mL/sec
Without glazing and with Natural Convection

Tap Water
Slope=45°
Condition: Clear Sky

Table A.4: Tap Water, 0.75mL/sec, with natural convection without glazing.

Time	8-9	9-10	10-11	11-12	12-13	13-14	14-15	15-16	16-17	Sum
$\dot{m}_c$, ml/hr	15	75	177	315	385	405	360	242	130	2234
$\dot{m}_s$, ml/hr	2675	2615	2488	2370	2295	2275	2315	2433	2555	22021
$\dot{m}_I$, ml/hr	10	10	35	15	20	20	25	25	15	175
G, W/m^2	534	687	787	857	872	811	710	521	347	
V, Volt	33.63	33.07	32.75	32.41	31.93	31.82	31.86	32.23	32.79	
I, mA	3.65	4.53	5.14	5.56	5.62	5.19	4.64	3.37	2.28	
P, Watt	122.75	149.81	168.34	180.20	179.45	165.15	147.83	108.62	74.76	
T_p, C°	33.7	43.9	50.7	51.5	56.7	58.1	55.4	49.3	42.1	
T_a, C°	22.5	23.7	25	26.2	30.2	30.7	32.5	29.7	28	
T_v, C°	31.1	42.2	48.3	51.5	56.7	57.5	55.3	50.5	43.2	
T_{Cond}, C°	20	22	24.2	25.7	27.7	31.1	30.1	27.5	25.3	
T_{Inter}, C°	23	24	27	28	29	33	30.5	29	27	
T_s, C°	27.5	37.1	41.2	43.7	46.1	48.7	49.1	45.7	41.1	
$T_{ex,i}$, C°	22.5	24.9	27.5	29.5	33.9	36.3	36	33.5	30.7	
$T_{ex,o}$, C°	26.9	38.7	44.5	47.8	53.6	54.9	52	47.7	41.7	
Saline, PPM	555	570	545	555	593	590	572	560	560	
Inter, PPM	520	520	530	520	525	530	525	520	520	
Cond, PPM	150	125	55	39	40	34.7	30.3	37	33	
Feed, PPM	550	550	520	550	550	550	550	550	550	
h_{fg}, kJ/kg	2453.8	2449	2444.2	2440.9	2436.2	2428.2	2430.6	2436.8	2441.7	
$\eta_{Hourly,Total}$ (%)	15.2	17.84	22.38	28.04	30.79	32.99	33.6	31.91	28.66	
η_{Daily} (%)	27.984									

Date: 18/4/2010
Flow Rate: 1.0mL/sec
With glazing and with Natural Convection

Tap Water
Slope=45°
Condition: Clear Sky

Table A.5: Tap Water, 1.0mL/sec, with natural convection with glazing.

Time	8-9	9-10	10-11	11-12	12-13	13-14	14-15	15-16	16-17	Sum
$\dot{m}_c$, ml/hr	10	50	400	545	595	620	500	440	210	3690
$\dot{m}_s$, ml/hr	3540	3475	3100	2755	2805	2680	2900	2960	3325	27540
$\dot{m}_I$, ml/hr	50	75	100	300	200	300	200	200	65	1490
G, W/m^2	494	640	858	937	950	980	837	655	370	
V, Volt	32.34	30.82	30.1	29.89	29.45	29.88	30.23	29.8	30.81	
I, mA	3.09	3.69	4.87	5.21	5.27	5.3	4.76	3.77	2.21	
P, Watt	99.90	113.73	146.59	155.73	155.20	158.37	143.89	112.35	68.09	
T_p, C°	42.1	56.1	69.1	72.7	76.4	78.6	67.6	64.2	55.5	
T_a, C°	23.7	25.5	28.6	30.8	31.3	34.6	33.2	31.5	29.2	
T_v, C°	33.1	45.8	58.2	61.9	66.8	68.5	59.4	59.8	52.4	
T_{Cond}, C°	19	21.5	27.2	29.2	30.8	31.7	28.1	27.2	26.2	
T_{Inter}, C°	20	23	30.4	31.6	32.7	33	30.5	28.3	26.7	
T_s, C°	29.7	37.3	43.7	47	49.3	51.2	47.4	46.7	43.4	
$T_{ex,i}$, C°	24.5	16.6	31.1	33.1	33.2	35.8	31.6	30.8	30.2	
$T_{ex,o}$, C°	28.1	40.4	54.7	58.2	63.4	57.4	56.1	55.3	49.7	
Saline, PPM	575	580	603	610	605	600	589	610	575	
Inter, PPM	550	550	590	600	590	560	550	540	530	
Cond, PPM	100	70	39.4	25.7	29.2	25.4	29.6	46.1	45	
Feed, PPM	550	550	520	550	550	550	550	550	550	
h_{fg}, kJ/kg	2456.2	2450.2	2437.5	2432.7	2428.9	2426.7	2435.4	2437.5	2439.8	
$\eta_{Hourly,Total}$ (%)	13.19	14.09	29.69	34.13	35.76	35.89	35.16	38.23	34.71	
η_{Daily} (%)	33.132									

Date: 20/4/2010
Flow Rate: 1.0mL/sec
With glazing and with Natural Convection

Tap Water
Slope=45°
Condition: Clear Sky

Table A.6: Tap Water, 1.0mL/sec, with natural convection with glazing.

Time	8-9	9-10	10-11	11-12	12-13	13-14	14-15	15-16	16-17	Sum
$\dot{m}_c$, ml/hr	10	110	440	510	650	670	480	410	275	3855
$\dot{m}_s$, ml/hr	3580	3480	3145	3075	2920	2895	3095	3180	3310	28680
$\dot{m}_I$, ml/hr	10	10	15	15	30	35	25	10	15	165
G, W/m^2	312	570	927	1011	1098	950	855	621	465	
V, Volt	32.34	31.81	31.02	30.7	30.5	30.31	31.39	31.56	31.86	
I, mA	1.77	3.15	5.31	5.7	6.22	5.27	4.89	3.49	2.71	
P, Watt	57.24	111.65	164.72	174.99	189.71	159.73	153.50	110.14	86.34	
T_p, C°	42.1	56.1	61.7	64.8	66.4	69.7	58.2	55.4	47.9	
T_a, C°	15.7	16.2	16.8	17.2	19.4	21.7	21.5	19.7	17.5	
T_v, C°	28.3	40.8	50.3	53.2	56.8	60.6	49.5	45.3	41.6	
T_{Cond}, C°	18.7	19.2	19.5	20.5	21.4	23.5	24.2	20.5	18.6	
T_{Inter}, C°	20	23	30.4	31.6	32.7	33	30.5	28.3	26.7	
T_s, C°	27.3	37.1	43.4	46.6	47.3	47.6	42.7	40.3	38.1	
$T_{ex,i}$, C°	15.5	16.3	17.6	17.7	23.2	26.7	20.5	20.1	19.6	
$T_{ex,o}$, C°	22.3	32.4	41.6	45.5	51.7	57.1	43.8	39.6	36.3	
Saline, PPM	550	550	550	580	580	578	597	596	593	
Inter, PPM	530	520	535	570	570	560	550	540	530	
Cond, PPM	40	25	27	24	15	8.5	7.9	15	21.6	
Feed, PPM	550	550	520	550	550	550	550	550	550	
h_{fg}, kJ/kg	2456.9	2455.7	2455	2452.6	2450.4	2445.7	2444.2	2452.6	2457.2	
$\eta_{Hourly,Total}$ (%)	12.53	19.99	30.6	31.54	35.14	39.51	34.22	38.28	35.97	
η_{Daily} (%)	34.355									

Appendix B: Simulation Results

Date: 14/4/2010
Flow Rate: 1.0mL/sec
Without glazing and with Natural Convection

Slope=45°
Condition: Clear Sky

Table B.1: 1.0mL/sec, with natural convection without glazing.

Time	G W/m^2	P, Watt	Condensate Productivity ml/hour	Efficiency %
8-9	511	127	510	56
9-10	707	169	655	53
10-11	849	200	826	54
11-12	926	212	847	52
12-13	932	211	847	51
13-14	866	195	766	50
14-15	733	167	588	47
15-16	545	128	439	47
16-17	320	76	172	37
			5654	**Daily Efficiency = 51%**

Date: 15/4/2010
Flow Rate: 1.75mL/sec
Without glazing and with Natural Convection

Slope=45°
Condition: Clear Sky

Table B.2: 1.75mL/sec, with natural convection without glazing.

Time	G W/m^2	P, Watt	Condensate Productivity ml/hour	Efficiency %
8-9	510	124	459	52
9-10	705	167	625	51
10-11	848	194	718	49
11-12	925	210	843	51
12-13	930	211	858	52
13-14	864	197	788	51
14-15	732	170	657	51
15-16	544	129	450	48
16-17	320	78	252	47
			5655	**Daily Efficiency = 50.9%**

Date: 16/4/2010
Flow Rate: 0.75ml/sec
Without glazing and with Natural Convection

Slope=45°
Condition: Clear Sky

Table B.3: 0.75mL/sec, with natural convection without glazing.

Time	G W/m^2	P, Watt	Condensate Productivity ml/hour	Efficiency %
8-9	509	123	500	55
9-10	704	163	636	51
10-11	846	191	754	50
11-12	923	208	875	52
12-13	929	204	874	52
13-14	863	189	768	50
14-15	731	162	651	50
15-16	543	123	430	46
16-17	319	74	198	40
			5690	**Daily Efficiency = 50.7%**

Date: 18/4/2010
Flow Rate: 1.0mL/sec Slope=45°
With glazing and with Natural Convection Condition: Clear Sky

Table B.4: 1.0mL/sec, with natural convection with glazing.

Time	**G W/m^2**	**P, Watt**	**Condensate Productivity ml/hour**	**Efficiency %**
8-9	508	103	516	54
9-10	702	135	712	53
10-11	844	153	860	53
11-12	920	164	959	53
12-13	926	162	955	53
13-14	860	149	880	52
14-15	728	133	747	53
15-16	541	100	514	50
16-17	318	61	257	45
			6403	**Daily Efficiency =52.8%**

Appendix C: Heat Exchanger Design

The mean diameter of the heat exchanger piper is asssumed to be 12 mm and the heat exhanger is made of copper of 385 W/mK (Incropera et al 2007).

To find the overall heat transfer coefficient for the heat exchanger:

$$U_{ov} = \frac{1}{R_{Total}} = \frac{1}{\frac{1}{h_i} + \frac{r_1}{K}\ln\left(\frac{r_2}{r_1}\right) + \frac{1}{h_o}\frac{r_1}{r_2}} \ldots\ldots\ldots\ldots\ldots\ldots\ldots\ldots\ldots\ldots\ldots\ldots\ldots\ldots\ldots\ldots\ldots\ldots\ldots\ldots.(C.1)$$

Where:

U_{ov}: The overall heat transfer coefficient.

h_i: The inside convection heat transfer coefficient for the pipe.

h_o: The outside convection heat transfer coefficient for the pipe.

k: The thermal conductivity of the pipe.

r_1 and r_1: The inner and outer radii of the pipe equal to 11 and 13 mm respectively.

The inside convection heat transfer coefficient of the heat exchanger can be calculated by following raltionship:

$$h_i = \frac{Nu_x . k}{D} \ldots\ldots\ldots\ldots\ldots\ldots\ldots\ldots\ldots\ldots\ldots\ldots\ldots\ldots\ldots\ldots\ldots\ldots\ldots\ldots\ldots\ldots\ldots\ldots\ldots\ldots\ldots\ldots\ldots\ldots\ldots\ldots.(C.2)$$

Where:

Nu: The dimensionless Nusselt number.

k: The thermal conductvity of the water inside the heat exchanger.

D: The mean diameter of the pipe of the heat exchanger.

The heat exchanger was assumed to be ten meters long according to previous work where it was stated that the optimum heat exchanger size is ten passes (Badran et al 2005). In this section, analysis of the heat exchanger is done to verify that assumption.

Taking a set of results from operating on April 14th,2011 at solar noon (Results shown in table A.2) temperature of the water entering the heat exchanger ($T_{ex,i}$) was 22.75°C and the water temperature leaving the heat exchanger ($T_{ex,o}$) was 44.5°C, thus the mean temperature (T_{mean}) is 33.625°C.

At T_{mean}=33.625°C and from (Cengel and Boles 2007) k=622.6x10^{-3} W/mK, the dynamic viscosity is 745.05x10^{-6} N.s/m^2, and C_p = 4178 J/kg.K.

To find the appropriate equation for the Nusselt number, the Reynold's number inside the heat exchanger must be determined.

For a flow rate of 1 g/s:

$$\mathrm{Re} = \frac{4\dot{\mathrm{m}}}{\pi \mathrm{D} \mu_\mathrm{f}} \ldots\ldots\ldots\ldots\ldots\ldots\ldots\ldots\ldots\ldots\ldots\ldots\ldots\ldots\ldots\ldots\ldots\ldots\ldots\ldots . (C.3)$$

Substituting in equation 4.3:

$$\mathrm{Re} = \frac{4 \times 1 \times 10^{-3}}{\pi \times 12 \times 10^{-3} \times 745.05 \times 10^{-6}} = 142.4$$

This is less than 2300, so the flow inside the heat exchanger is laminar. Nusselt number can be obtained from the equation (Incropera et al 2007)

Nu=4.36 (For laminar fully developed flow) $\dots\dots\dots\dots\dots\dots\dots\dots\dots\dots\dots\dots\dots\dots\dots\dots\dots\dots.(C.4)$

Substituting in equation (4.2):

$$\mathrm{h_i} = \frac{4.36 \times 622.6 \times 10^{-3}}{12 \times 10^{-3}} = 226.2\ \frac{W}{m^2K}$$

The outside convection heat transfer coefficient can be determined experimentally (Incropera et al 2007).

$$\mathrm{h_o} = 8.555 \frac{W}{m^2K} \dots\dots\dots\dots\dots\dots\dots\dots\dots\dots\dots\dots\dots\dots\dots\dots\dots\dots\dots\dots\dots\dots\dots\dots\dots\dots\dots\dots\dots\dots\dots\dots\dots\dots.(C.5)$$

Substituting in equation (4.1):

$$\mathrm{U_{ov}} = \frac{1}{\frac{1}{226.2} + \frac{11 \times 10^{-3}}{385}\ln\left(\frac{13}{11}\right) + \frac{1}{8.555}\frac{11}{13}} = 9.7\frac{W}{m^2K}$$

The total energy gain by the water can be given as follows:

$$\mathrm{Q} = \dot{\mathrm{m}}C_p\Delta T_{Water} \dots\dots\dots\dots\dots\dots\dots\dots\dots\dots\dots\dots\dots\dots\dots\dots\dots\dots\dots\dots\dots\dots\dots\dots\dots\dots\dots\dots\dots\dots\dots\dots\dots.(C.6)$$

$\dot{m}$=1g/s, C_p=4178J/kg.K, ΔT_{Water}=44.5-22.75=21.71°C

Substituting in equation (4.6):

$$Q = 1 \times 10^{-3} \times 4178 \times 21.75 = 90.87\,W$$

And

$$Q = U_{OV} \times A \times \Delta T_{lm} = \dot{m} C_p \Delta T_{Water} = 90.87W$$

Where: ΔT_{lm} is the logarithmic mean temperature, and A is the surface area of the heat exchanger.

$$\Delta T_{lm} = \frac{\Delta T_{max} - \Delta T_{min}}{ln\left(\frac{\Delta T_{max}}{\Delta T_{min}}\right)} \ldots\ldots\ldots\ldots\ldots\ldots\ldots\ldots\ldots\ldots\ldots\ldots\ldots\ldots\ldots\ldots\ldots\ldots\ldots.(C.7)$$

Where: $\Delta T_{max} = T_{hi} - T_{ex,o}$ and $\Delta T_{min} = T_{ho} - T_{ex,i}$

T_{hi}: The vapor temperature entering the shell of the heat exchanger which is 49.1°C

T_{ho}: The vapor temperature leaving the shell of the heat exchanger which is 45.05°C

$\Delta T_{max} = 49.1 - 44.5 = 4.6°C$ $\Delta T_{min} = 45.05 - 22.75 = 22.3°C$

Substituting in eqution (4.7):

$$\Delta T_{lm} = \frac{4.6 - 22.3}{ln\left(\frac{4.6}{22.3}\right)} = 11.2\text{ °C}$$

$$A = \frac{Q}{U_{OV} \times \Delta T_{lm}} = \pi \times D \times L \ldots\ldots\ldots\ldots.\ldots\ldots\ldots\ldots\ldots\ldots\ldots\ldots\ldots\ldots\ldots\ldots.\ldots(C.8)$$

$$L = \frac{Q}{\mathrm{U_{OV}} \times \Delta T_{lm} \times \pi \times D} \ldots\ldots\ldots\ldots\ldots\ldots\ldots\ldots\ldots\ldots\ldots\ldots\ldots\ldots\ldots\ldots\ldots\ldots\ldots\ldots\ldots\ldots\ldots\ldots\ldots\ldots\ldots\ldots\ldots\ldots.. (C.9)$$

Substituting in equation (4.9):

$$L = \frac{90.81}{9.7 \times 11.2 \times \pi \times 12 \times 10^{-3}} = 11.1m$$

According to this result the heat exchanger used of ten meters length was sufficient.

Appendix D: Uncertainty Analysis

The method used for estimating uncertainty in experimental results has been presented by Kline and Mc Clintock. The method is based on careful specification of uncertainties in the various primary experimental measurements.

The uncertainty of each device is taken as one-half the smallest scale interval reading and its recorded in the table below:

Table D-1: The Uncertainty of the Measurement Devices.

Measuring Device	Uncertainty
Metric Scale	± 0.005 m
Flow Meter	± 0.25 g/sec
Temperature Processor	± 0.05°C
Radiation Processor (Pyranometer)	± 0.5 W/m^2
Graduating Cylinder	± 1 mm
Avometer	± 0.005 V, ± 0.005 A

The analysis was made using results obtained on April, 18th on 13:00 PM which gave the following readings:

G = 980 W/m2

$\dot{m}_c$ = 620 ml

h_{fg} = 2426.7 kJ/kg.K

η_h = 35.89

V = 29.88 Volt

I = 5.3 Ampere

From these readings, the uncertainty of the still hourly efficiency can be found from equation 3.19;

$$\eta_h = \frac{(\dot{m}_c \times h_{fg}) + \dot{E}_{PV} \times 3600}{3600 \times G \times A_c}$$

The uncertainty in efficiency can found as follows:

- Uncertainty in Area:

$$A_s = L \times W$$

Where:

A_s: Still Area.

L: Still Length.

W: Still Width.

Thus,

$L = L \pm \omega_L = 1.65 \pm 0.005$ m

$W = W \pm \omega_W = 0.99 \pm 0.005$ m

$$\omega_{A_s} = \pm\sqrt{\left(\left(\frac{\partial A_s}{\partial L}\right)\omega_L\right)^2 + \left(\left(\frac{\partial A_s}{\partial W}\right)\omega_W\right)^2}$$

$$\omega_{A_s} = \pm\sqrt{(W \times \omega_L)^2 + (L \times \omega_W)^2}$$

Substituting the values, then:

$$\omega_{A_s} = \pm\sqrt{(0.99 \times 0.005)^2 + (1.65 \times 0.005)^2}$$

$$\omega_{A_s} = \pm 0.00962\ m^2$$

- Uncertainty in Electrical Power:

$$\dot{E}_{PV} = I \times V$$

Where:

$\dot{E}_{PV}$: PV Power output.

I: PV Current.

V: PV Voltage.

Thus,

$I = I \pm \omega_I$

$V = V \pm \omega_V$

$$\omega_{\dot{E}_{PV}} = \pm\sqrt{\left(\left(\frac{\partial \dot{E}_{PV}}{\partial I}\right)\omega_I\right)^2 + \left(\left(\frac{\partial \dot{E}_{PV}}{\partial V}\right)\omega_V\right)^2}$$

$$\omega_{\dot{E}_{PV}} = \pm\sqrt{(V \times \omega_I)^2 + (I \times \omega_V)^2}$$

Substituting the values, then:

$$\omega_{\dot{E}_{PV}} = \pm\sqrt{(29.88 \times 0.005)^2 + (5.3 \times 0.005)^2}$$

$$\omega_{\dot{E}_{PV}} = \pm 0.1517\, W$$

- Uncertainty in Efficiency:

$$\eta_h = \frac{(\dot{m}_c \times h_{fg}) + \dot{E}_{PV} \times 3600}{3600 \times G \times A_c}$$

Where:

$G = 980 \pm 0.5\ W/m^2$.

$\dot{m}_c = 620 \pm 1$ mL

$A_s = 1.6335 \pm 0.00962\ m^2$

$h_{fg} = 2426700$ J/kg (As obtained from the tables)

$\dot{E}_{PV} = 158.364 \pm 0.1517$ W

Uncertainty in hourly efficiency is:

$$\eta_h = \pm\sqrt{\left(\left(\frac{\partial\eta}{\partial\dot{m}_c}\right)\omega_{\dot{m}_c}\right)^2 + \left(\left(\frac{\partial\eta}{\partial A_s}\right)\omega_{A_s}\right)^2 + \left(\left(\frac{\partial\eta}{\partial G}\right)\omega_G\right)^2 + \left(\left(\frac{\partial\eta}{\partial\dot{E}_{PV}}\right)\omega_{\dot{E}_{PV}}\right)^2}$$

Where:

$$\frac{\partial\eta}{\partial\dot{m}_c} = \frac{h_{fg}}{3600 \times G \times A_s}$$

$$\frac{\partial\eta}{\partial A_s} = \frac{-\dot{m}_c \times h_{fg}}{3600 \times G \times {A_s}^2}$$

$$\frac{\partial\eta}{\partial G} = \frac{-\dot{m}_c \times h_{fg}}{3600 \times G^2 \times A_s}$$

$$\frac{\partial\eta}{\partial\dot{E}_{PV}} = \frac{1}{G \times A_s}$$

Then,

$$\eta_h = \pm\sqrt{\begin{array}{c}\left(\left(\frac{2426700}{3600 \times 980 \times 1.6335}\right)0.001\right)^2 + \left(\left(\frac{-0.62 \times 2426700}{3600 \times 980 \times 1.6335^2}\right)0.00962\right)^2 + \\ \left(\left(\frac{-0.62 \times 2426700}{3600 \times 980^2 \times A_s}\right)0.5\right)^2 + \left(\left(\frac{1}{980 \times 1.6335}\right)0.1517\right)^2\end{array}}$$

$$\eta_h = \pm\sqrt{\begin{array}{c}(0.000421)^2 + (0.0015375)^2 + \\ (0.0001332)^2 + (0.0000947)^2\end{array}} = \pm 0.0016 = \pm 0.16\%$$

Thus the efficiency is $\eta_h = 35.89\% \pm 0.16\%$

Appendix E: Measurement Toools

E.1 Thermocouple Calibrator

Martel Electronics Thermocouple calibrator model TC-100

It has the following features:

- 0.01 degree resolution.
- Built in °C °F select button on the front panel.
- Built in thermocouple type button on the front panel.



E.2 Salinity measuring device

Mettler Toledo Seven Go Portable Meter

It has the following features:

- Single-channel insturment for measuring conductivity, TDS (Total Dissolved Solids), salinity, specific resistance, and temperature.
- Predifined conductivity standard: 84 µS/cm, 1413 µS/cm, 12.88 mS/cm. The one used to calibrate the device for this work was the 12.88 mS/cm standard.
- Linear temperature compensation.
- Device specifications:

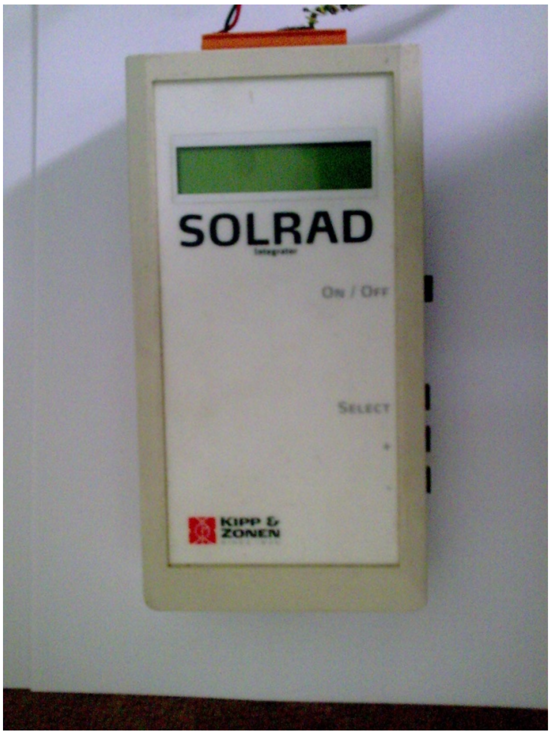
	Measuring range	Resolution	Accuracy
Conductivity	0.01 µS/cm to 500 mS/cm	0.01 to 1	± 0.5%
Temperature	-5.0 to 105°C	0.1°C	± 0.2°C
TDS	0.01 mg/L to 300 g/L	0.01 to 1	± 0.5%
Spec. resistance	0.00 to 100.0 MΩcm	0.01 to 0.1	± 0.5%
Salinity	0.00 to 80.0 ppt	0.01 to 0.1	± 0.5%



E.3 Pyranometer and solar integrator

The pyranometer is designed for outdoor use. Due to its flat spectral sensitivity from 300 to 3000 nm, it can be used in natural sunlight.

This pyranometer consisits of a thermopile sensor, housing, dome, and cable. The thermopile is coated with a black absorbent coating. The paint absorbs the radiation and converts it to heat. The resultant temperature difference is converted to voltage by copper-constantan thermopile. The thermopile is encapsulated in the housing in such a way that it has a field of vision of 180 degrees and the angular characteristics needed to fullfil the cosine response requirement. The type of solar integrator is Kipp and Zonen.



Pyranometer specification:

- Response time 95%: 18 seconds.
- Zero offset due to 200 W/m^2: < $15W/m^2$.
- Non-stability (% change per year): < ±1%.
- Non linearity (0 to 1000 W/m^2): < ±2.5%.
- Directional error (at 80° with 1000 W/m^2 beam): < ±20 W/m^2.



E.4 Flow meter

This device was used to regulate the water mass flow rate delivered to the still.



E.5 Avometer

Unit-T portable Avometer modet UT 33A. This device was used to measure the voltage and current generated by the PV module with specifications:

- Voltage, Current and Resistance measuring ability.
- Voltage range: max 500 Volt.
- Current range: max 10 Ampere.
- Resolution 0.1 μAmpere, 0.1 mVolt



Appendix F: Computer Simulation Code

```
x=[1 11 21 31 32 42 52 59 60 70 80 90 91 101 111 120 121 131 141 151 152 162 172 181
182 192 202 212 213 223 233 243 244 254 264 273 274 284 294 304 305 315 325 334 335
345 355 365];
As=[1231 1230 1229 1224 1223 1218 1213 1206 1205 1195 1185 1169 1167 1151 1135
1126 1125 1114 1103 1098 1097 1092 1087 1086 1086 1085 1084 1091 1092 1099 1106
1120 1122 1136 1150 1162 1164 1177 1191 1200 1201 1211 1220 1224 1224 1228 1232
1231];
Bs=[0.142 0.142 0.142 0.142 0.143 0.143 0.144 0.147 0.148 0.152 0.156 0.164 0.165 0.172
0.180 0.185 0.186 0.191 0.196 0.199 0.199 0.202 0.205 0.206 0.206 0.206 0.207 0.205 0.205
0.203 0.201 0.193 0.192 0.185 0.177 0.172 0.171 0.166 0.160 0.157 0.156 0.153 0.149 0.147
0.147 0.144 0.142 0.142];
Cs=[0.057 0.058 0.058 0.058 0.059 0.059 0.06 0.063 0.063 0.067 0.071 0.079 0.080 0.088
0.096 0.104 0.105 0.113 0.121 0.125 0.126 0.130 0.134 0.135 0.135 0.135 0.136 0.132 0.132
0.126 0.122 0.113 0.112 0.097 0.092 0.086 0.086 0.079 0.073 0.070 0.069 0.066 0.063 0.061
0.061 0.059 0.057 0.057];
size(x);
size(As);
size(Bs);
size(Cs);
L=32
T=input('Enter the time in minutes:');
y=input('Enter the day of the year, assuming February is 28 days:');
B2=input('Enter the tilt angle of the still in degrees:');
Tak=input('Enter the ambient temperature in K:');
Tsi=input('Enter the temperature of the saline water inlet to the still in C:');
Tse=input('Enter the temperature of the saline water outlet from the heat exchanger to the still
in C:');
Tso=input('Enter the temperature of the saline water outlet from the still in C:');
Tio=input('Enter the temperature of the intermediate water outlet from the still in C:');
Tpmk=input('Enter the mean aborber plate temperature in K:');
Tpv=input('Enter the PV temperature in C:');
mass=input('Enter the value of the saline water intet mass flow rate in kg/sec:');
ms=input('Enter the value of the saline outlet mass flow rate in kg/sec:');
mi=input('Enter the value of the Intermediate outlet mass flow rate in kg/sec:');
'The area of the still:'
Area=1.63845
'The thickness of insulation in m:'
t=0.025
Vwind=2
'The value of the perimeter in m:'
Per1=5.29
'The value of the perimeter including the sides in m:'
Per2=5.49
'The height of the sides in m:'
hsides=0.135
v=0.000018538
kair=0.026118
'The value of the thermal conductivity of the insulation:'
```

```
kins=0.03
Pr=0.71429
hfg=input('Enter the value of enthalpy:');
'The emittance of PV:'
epv=0.8
'The emittance of glass:'
eg=0.88
'The value of Boltzmans constant:'
sigma=0.0000000567
'The PV temperature coefficient:'
Phi=-0.0038
'The Packing Factor:'
PF=1
'Glazing transmissivity:'
tg=0.87
'The PV electrical conversion efficiency:'
PVeff=0.153
Glass=input('Enter 1 if there is glazing and 0 if there is no glazing')

for n=1:48
   if x(n)==y
      AS=As(n)
      BS=Bs(n)
      CS=Cs(n)
      'B in Degree'
      B=((y-1)*360)/365
      'Equation of time'
      E=229.2.*(0.000075+0.001868.*cosd(B)-0.032077.*sind(B)-0.014615.*cosd(2.*B)-
0.04089.*sind(2.*B))
      'Mean solar time'
      MST=T+24
      'The apparent solar time'
      AST=MST+E
      'The hour angle in degree'
      H=(AST-720)/4
      'The declination angle in degree'
      dec=23.45*sind(360*(284+y)/365)
      'B1 in radian'
      B1=asin((cosd(L).*cosd(dec).*cosd(H))+(sind(L).*sind(dec)))
      'The direct normal beam radiation is:'
      Gnormal=AS.*exp(-BS./sin(B1))
      Fss=(1+cosd(B2))/2
      'A in radian'
      A=asin(cosd(dec).*sind(H)./cos(B1))
      'The angle of incidence in radian'
      theta=acos((sin(B1).*cosd(B2))+(cos(B1).*sind(B2).*cos(A)))
      'The total solar radiation is:'
      Gtot=Gnormal.*(cos(theta)+CS.*Fss)
      'The heat delivered to the heat exchanger is:'
      Qex=(mass./Area).*4180.*(Tse-Tsi)
```

```
Epvn=Gtot.*PVeff.*Area
if Glass==1
'The Electrical Output Power:'
Epvg=(Area.*Gtot.*tg.*PF.*PVeff.*(1+(Phi.*(Tpv-25))))
'The heat lost with unevaporated water is:'
Qunevap=(4180./Area).*(ms.*(Tso-Tse)+mi.*(Tio-Tse))
length=(4*Area)/Per1
'The value of Reynolds number is:'
Re=(Vwind.*length)./v
'The value of the outside film heat transfer coefficient is:'
ho=(0.86.*kair.*Re.^0.5.*Pr.^0.3333333)./length
f=1.07866.*(1+0.089.*ho-0.1166.*ho.*epv)
C=520.*(1-0.000051.*(B2.^2))
e=0.43.*(1-(100./Tpmk))
'The top loss coefficient:'
Ut=(((C./Tpmk).*((Tpmk-Tak)./(1+f)).^(-1.*e))+(1/ho)).^-1+((sigma.*(Tpmk-
Tak).*(Tpmk.^2-Tak.^2))./((epv+0.00591.*ho).^-1+((1+f+0.133.*epv)./eg)-1))
'The heat losses to the ambient'
Qpvc=Ut.*(Tpmk-Tak)
Uedge=(kins/t)
Aedge=hsides.*Per2
'The loss coefficient from edges is:'
Ue=(Uedge.*Aedge)./Area
'The heat losses from the sides of the still:'
Qloss=Ue.*(Tpmk-Tak)
'The heat used to evaporate water in the presence of a heat exchanger is:'
Qe=(0.70992.*Gtot)-Qpvc-Epvg-Qloss-Qunevap
'The instantaneous productivity of the still:'
mc=Qe.*Area./hfg
'The hourly production of the still:'
mch=3600.*mc
'The thermal efficiency of the still:'
effth=((0.70992.*Gtot)-Qpvc-Qloss-Qunevap)./Gtot
'The instantaneous efficiency of the still:'
eff=((mch.*hfg)+Epvg.*3600).*100./(Gtot.*3600.*Area)
effd=sum(((mch.*hfg)+Epvg.*3600).*100)/sum(3600*Gtot.*Area)
elseif Glass==0
'The Electrical Output Power:'
Epv=Area.*Gtot.*PF.*PVeff.*(1+Phi.*(Tpv-25))
    'The heat lost with unevaporated water is:'
Qunevap=(4.180./Area).*(ms.*(Tso-Tse)+mi.*(Tio-Tse))
length=(4*Area)/Per1
'The value of Reynolds number is:'
Re=(Vwind.*length)./v
'The value of the outside film heat transfer coefficient is:'
ho=(0.86.*kair.*Re.^0.5.*Pr.^0.3333333)./length
f=1.07866.*(1+0.089.*ho-0.1166.*ho.*epv)
C=520.*(1-0.000051.*(B2.^2))
e=0.43.*(1-(100./Tpmk))
'The top loss coefficient:'
```

```
        hr=sigma*epv.*(Tpmk+Tak).*(Tpmk.^2-Tak.^2)
        Ut=ho+hr
        'The heat losses to the ambient'
        Qpvc=Ut.*(Tpmk-Tak)
        Uedge=(kins/t)
        Aedge=hsides.*Per2
        'The loss coefficient from edges is:'
        Ue=(Uedge.*Aedge)./Area
        'The heat losses from the sides of the still:'
        Qloss=Ue.*(Tpmk-Tak)
        'The heat used to evaporate water in the presence of a heat exchanger is:'
        Qe=(0.816.*Gtot)-Qpvc-Epv-Qloss-Qunevap
        'The instantaneous productivity of the still:'
        mc=Qe.*Area./hfg
        'The hourly production of the still:'
        mch=3600.*mc
        'The thermal efficiency of the still:'
        effth=((0.816.*Gtot)-Qpvc-Qloss-Qunevap)./Gtot
        'The instantaneous efficiency of the still:'
        eff=((mch.*hfg)+Epv.*3600).*100./(Gtot.*3600.*Area)
        effd=sum(((mch.*hfg)+Epv.*3600).*100)/sum(3600*Gtot.*Area)
        end
    else
AS=interp1(x,As,y)
BS=interp1(x,Bs,y)
CS=interp1(x,Cs,y)

 'B in Degree'
        B=((y-1)*360)/365
        'Equation of time'
        E=229.2.*(0.000075+0.001868.*cosd(B)-0.032077.*sind(B)-0.014615.*cosd(2.*B)-
0.04089.*sind(2.*B))
        'Mean solar time'
        MST=T+24
        'The apparent solar time'
        AST=MST+E
        'The hour angle in degree'
        H=(AST-720)/4
        'The declination angle in degree'
        dec=23.45*sind(360*(284+y)/365)
        'B1 in radian'
        B1=asin((cosd(L).*cosd(dec).*cosd(H))+(sind(L).*sind(dec)))
        'The direct normal beam radiation is:'
        Gnormal=AS.*exp(-BS./sin(B1))
        Fss=(1+cosd(B2))/2
        'A in radian'
        A=asin(cosd(dec).*sind(H)./cos(B1))
        'The angle of incidence in radian'
        theta=acos((sin(B1).*cosd(B2))+(cos(B1).*sind(B2).*cos(A)))
        'The total solar radiation is:'
```

```
Gtot=Gnormal.*(cos(theta)+CS.*Fss)
'The heat delivered to the heat exchanger is:'
Qex=(mass./Area).*4180.*(Tse-Tsi)
Epvn=Gtot.*PVeff
if Glass==1
'The Electrical Output Power:'
Epvg=(Gtot.*tg.*PF.*PVeff.*(1+(Phi.*(Tpv-25))))
'The heat lost with unevaporated water is:'
Qunevap=(4.180./Area).*(ms.*(Tso-Tse)+mi.*(Tio-Tse))
length=(4*Area)/Per1
'The value of Reynolds number is:'
Re=(Vwind.*length)./v
'The value of the outside film heat transfer coefficient is:'
ho=(0.86.*kair.*Re.^0.5.*Pr.^0.3333333)./length
f=1.07866.*(1+0.089.*ho-0.1166.*ho.*epv)
C=520.*(1-0.000051.*(B2.^2))
e=0.43.*(1-(100./Tpmk))
'The top loss coefficient:'
Ut=(((C./Tpmk).*((Tpmk-Tak)./(1+f)).^(-1.*e))+(1/ho)).^-1+((sigma.*(Tpmk-
Tak).*(Tpmk.^2-Tak.^2))./((epv+0.00591.*ho).^-1+((1+f+0.133.*epv)./eg)-1))
'The heat losses to the ambient'
Qpvc=Ut.*(Tpmk-Tak)
Uedge=(kins/t)
Aedge=hsides.*Per2
'The loss coefficient from edges is:'
Ue=(Uedge.*Aedge)./Area
'The heat losses from the sides of the still:'
Qloss=Ue.*(Tpmk-Tak)
'The heat used to evaporate water in the presence of a heat exchanger is:'
Qe=(0.70992.*Gtot)-Qpvc-Epvg-Qloss-Qunevap
'The instantaneous productivity of the still:'
mc=Qe.*Area./hfg
'The hourly production of the still:'
mch=3600.*mc
'The thermal efficiency of the still:'
effth=((0.70992.*Gtot)-Qpvc-Qloss-Qunevap)./Gtot
'The instantaneous efficiency of the still:'
eff=((mch.*hfg)+Epvg.*3600).*100/(Gtot.*3600.*Area)
effd=sum(((mch.*hfg)+Epvg.*3600).*100)/sum(3600*Gtot.*Area))
elseif Glass==0
'The Electrical Output Power:'
Epv=Gtot.*PF.*PVeff.*(1+Phi.*(Tpv-25))
    'The heat lost with unevaporated water is:'
Qunevap=(4.180./Area).*(ms.*(Tso-Tse)+mi.*(Tio-Tse))
length=(4*Area)/Per1
'The value of Reynolds number is:'
Re=(Vwind.*length)./v
'The value of the outside film heat transfer coefficient is:'
ho=(0.86.*kair.*Re.^0.5.*Pr.^0.3333333)./length
f=1.07866.*(1+0.089.*ho-0.1166.*ho.*epv)
```

```
        C=520.*(1-0.000051.*(B2.^2))
        e=0.43.*(1-(100./Tpmk))
        'The top loss coefficient:'
        hr=sigma*epv.*(Tpmk+Tak).*(Tpmk.^2-Tak.^2)
        Ut=ho+hr
        'The heat losses to the ambient'
        Qpvc=Ut.*(Tpmk-Tak)
        Uedge=(kins/t)
        Aedge=hsides.*Per2
        'The loss coefficient from edges is:'
        Ue=(Uedge.*Aedge)./Area
        'The heat losses from the sides of the still:'
        Qloss=Ue.*(Tpmk-Tak)
        'The heat used to evaporate water in the presence of a heat exchanger is:'
        Qe=(0.816.*Gtot)-Qpvc-Epv-Qloss-Qunevap
        'The instantaneous productivity of the still:'
        mc=Qe.*Area./hfg
        'The hourly production of the still:'
        mch=3600.*mc
        'The thermal efficiency of the still:'
        effth=((0.816.*Gtot)-Qpvc-Qloss-Qunevap)./Gtot
        'The instantaneous efficiency of the still:'
        eff=((mc.*hfg)+Epv)./(Gtot.*Area)
        effd=sum(((mc.*hfg)+Epv.*3600).*100)/sum(3600*Gtot.*Area)
        end
    end
end
```

تحليل نظام هجين لخلية كهرضوئية ولاقط شمسي حراري مدمج مع تحلية الماء.

إعداد
مراد محمود

المشرف
الأستاذ الدكتور علي بدران

ملخص

في هذه الدراسة، تم تصميم وبناء واختبار جهاز هجين لخلية كهرضوئية ولاقط شمسي حراري مدمج. مساحة الجهاز 1.63 م^2. هدف الدراسة هو دراسة أداء الجهاز حيث أن الحرارة المفقودة من الخلية الكهرضوئية تستعمل لتسخين المياه وتحليتها في نفس الوقت. الجهاز يتكون من خلية كهرضوئية تقوم بمهمة لوح امتصاص. على ظهر هذا اللوح يوجد مادة مسامية تمر خلالها المياه المالحة عن طريق الخاصية الشعرية والجاذبية. العديد من الأمور تم ادخالها إلى الجهاز ومنها المبادل الحراري بحجم مناسب، إطار خشبي، لوح عازل من مادة البوليوريثين لتخفيف الفقد الحراري إلى الخارج ولتحسين عمليتي التبخر والتكثف.

تمت دراسة قياس المبادل الحراري لإعطاء الأداء الأفضل من خلال استغلال حرارة التكثف في تسخين المياه المالحة الداخلة إلى الجهاز. تم تصميم الإطار الخشبي بحيث يؤمن سهولة التركيب والصيانة ولفصل حجرتي التبخر والتكثف. تم تركيب مادة ذات عزل حراري عالي بين حجرتي التبخر والتكثف، هذه المادة مكونة من لوح عازل من مادة البوليوريثين الموجودة بين طبقتي ألمنيوم رقيقتين. الهدف من تركيب هذه المادة هو رفع فرق درجة الحرارة بين حجرتي التبخر والتكثف إلى الحد الأقصى.

تمت دراسة الجهاز عملياً وتمت كتابة برنامج لمحاكاة أداء الجهاز باستخدام برنامج MATLAB. الجانب العملي ركز على قياس الأداء لمجموعة من مكونات الجهاز، الملوحة للمياه الداخلة والناتجة، الفولتية، التيار، والإشعاع الشمسي.

وُجد من خلال الدراسة ارتفاع ملحوظ في الإنتاجية والكفاءة مقارنة مع الدراسات السابقة. الإنتاجية القصوى بلغت 3.85 لتر مياه محلية في اليوم بمعدل ملوحة 40 جزء بالمليون وأقل ملوحة تم الحصول عليها كانت 7.5 جزء بالمليون. الكفاءة القسوى بلغت 34%. تم اختبار الجهاز بحالة عدم تغطية الخلية الكهرضوئية بالزجاج ثم عند تغطيتها بالزجاج. أنتجت الخلية طاقة كهربائية بمعدل 160 واط بدون وجود الزجاج و 130 واط بوجود الزجاج و كانت الإنتاجية القصوى 215 واط بدون وجود الزجاج و 190 واط بوجود الزجاج. القدرة الإسمية للخلية الكهرضوئية هي 250 واط.